

SIZE-RESOLVED PARTICULATE MATTER (PM) IN URBAN AREAS:
TOXICO-CHEMICAL CHARACTERISTICS, SOURCES, TRENDS
AND HEALTH IMPLICATIONS

by

Nancy Daher

A dissertation presented to the
FACULTY OF THE USC GRADUATE SCHOOL
UNIVERSITY OF SOUTHERN CALIFORNIA
In Partial Fulfillment of the
Requirements for the Degree
DOCTOR OF PHILOSOPHY
(ENVIRONMENTAL ENGINEERING)

December 2013

Dedication

À Tony

Acknowledgements

The successful completion of this dissertation would not have been possible without the contribution of many great people.

I am deeply grateful to my advisor, Professor Constantinos Sioutas, for his guidance and support throughout my doctoral work. I thank him for providing me with the invaluable opportunity of being part of his group. His keen scientific vision, creative discussions and enthusiasm have been and remain a great motivation and inspiration to engage in research.

I would like to thank all members of my guidance committee, Professor Caleb Finch, Professor Scott Fruin and Professor Ronald C. Henry, for taking the time to review this dissertation and for their valuable comments.

Many collaborators contributed to this research work. I am very thankful to Professor James J. Schauer and Dr. Martin M. Shafer for their insightful and constructive feedback. I also wish to thank Professor Alan L. Shihadeh for his continuous support.

Moreover, this dissertation would not have been possible without the collective effort of former and current colleagues at USC. I wish to thank Dr. Zhi Ning, Dr. Kalam Cheung, Dr. Winnie Kam, Dr. Payam Pakbin, Dr. Vishal Verma, Dr. Neelakshi Hudda, James Liacos, Dongbin Wang, Sina Hasheminassab and Arian Saffari. It was a great pleasure to work with you.

I also would like to express my sincerest gratitude to my family who never failed to support and encourage me.

My sincerest appreciation is also due to my fiancé Tony Saad. Tony has immeasurably helped me in many aspects of my life and academic career. I thank him for many inspiring scientific discussions and for providing me with helpful tips on writing. I am also truthfully thankful for his unwavering support, encouragement and above all patience.

Lastly, I wish to acknowledge the support of USC Provost's Ph.D. fellowship.

Table of Contents

Dedication	i
Acknowledgements	ii
List of Figures	viii
List of Tables.....	xi
Abstract	xii
Chapter 1 Introduction.....	1
1.1 Background.....	1
1.2 PM Characteristics: Particle-Size	2
1.3 PM Exposure and Health Effects.....	3
1.4 Rationale of Current Work.....	4
1.4.1 Motivation	4
1.4.2 Objectives	6
1.5 Dissertation Layout.....	7
Chapter 2 Chemical Composition of PM and its Seasonal and Spatial Variability: A Case Study of Ambient Quasi-Ultrafine PM (PM _{0.25}) in the Megacity of Los Angeles	10
2.1 Introduction.....	10
2.2 Methodology	13
2.2.1 Sampling sites.....	13
2.2.2 Sample Collection.....	15
2.3 Meteorology.....	16
2.4 Results and Discussion	17
2.4.1 Particulate Mass.....	19
2.4.2 Mass Reconstruction.....	21
2.4.3 Chemical Composition	25
2.4.3.1 Carbonaceous Species	25
2.4.3.2 Secondary Ions	30
2.4.3.3 Metals and Elements.....	32
2.4.4 Spatial Variability.....	38
2.5 Summary and Conclusions	40
2.6 Acknowledgements.....	41

Chapter 3	Chemical Composition of PM and its Relation to Sources: A Case Study of Ambient Fine and Coarse PM in Milan	43
3.1	Introduction.....	43
3.2	Methodology	45
3.2.1	Sample Collection.....	45
3.2.2	Chemical Analyses	45
3.2.3	Source Apportionment.....	46
3.3	Results and Discussion	49
3.3.1	Particulate Mass and Composition	49
3.3.1.1	Crustal Material and Trace Elements	50
3.3.1.2	Carbonaceous Compounds	54
3.3.1.3	Inorganic Ions	55
3.3.2	Mass Closure	57
3.3.3	Organic Species and Source Identification.....	58
3.3.4	MM-CMB results	63
3.3.4.1	Source Apportionment of Fine OC.....	63
3.3.4.2	Source Apportionment of Total PM _{2.5}	67
3.4	Summary and Conclusions	68
3.5	Acknowledgements.....	69
Chapter 4	Chemical Composition of PM and its Relation to Particle-Size: A Case Study of Size-Resolved PM at Near-Freeway and Urban Background Sites in the Greater Beirut Area ...	70
4.1	Introduction.....	70
4.2	Methodology	71
4.2.1	Sampling Sites	71
4.2.2	Sample Collection.....	73
4.2.3	Sample Analysis	74
4.3	Results and Discussion	75
4.3.1	Size-Resolved Particle Mass Concentration.....	75
4.3.2	Size-Resolved Particle Mass Composition.....	76
4.3.2.1	Carbonaceous Species	78
4.3.2.2	Secondary Ions	80
4.3.2.3	Sea-Salt.....	84

4.3.2.4	Crustal Material and Trace Elements	84
4.3.2.5	Chemical Mass Closure	85
4.3.3	Organic Compounds Characterization.....	86
4.3.3.1	Polycyclic Aromatic Hydrocarbons (PAHs)	86
4.3.3.2	Hopanes and Steranes	89
4.3.3.3	N-Alkanes	90
4.3.3.4	Dicarboxylic Acids	92
4.4	Summary and Conclusions	93
4.5	Acknowledgements.....	95
Chapter 5 A Comparative Assessment of the Oxidative Potential of PM: The Role of Particle-Size and Chemical Composition		
96		
1.	Oxidative Potential of Fine PM (PM _{2.5}) at an Urban Site in Milan, Italy.....	97
5.1.1.	Introduction	97
5.1.2.	Methodology.....	98
5.1.2.1	Sample Collection.....	98
5.1.2.2	Chemical Analyses	98
5.1.2.3	Reactive Oxygen Species (ROS) assay	99
5.1.3.	Monthly Variation of ROS-Activity.....	100
5.1.4.	Association with PM _{2.5} Species	102
5.1.5.	Summary and Conclusions	104
5.1.6.	Acknowledgements	104
2.	Oxidative Potential and Chemical Speciation of Size-Resolved PM at Near-Freeway and Urban Background Sites in the Greater Beirut Area.....	106
5.2.1.	Introduction	106
5.2.2.	Methodology.....	107
5.2.2.1	Sampling Sites	107
5.2.2.2	Sample Collection.....	108
5.2.2.3	Sample Analyses.....	109
5.2.3.	Results and Discussion	110
5.2.3.1	Size-Resolved Particle Mass and Composition	110
5.2.3.2	Metals and Trace Elements.....	113
5.2.3.3	Size-Resolved Reactive Oxygen Species (ROS)-activity	121

5.2.3.4	Association of (ROS)-activity with PM components	123
5.2.4.	Summary and Conclusions	125
5.2.5.	Acknowledgements	126
3.	ROS-Activity: Comparison of Urban Areas	127
5.3.1.	Comparison of Intrinsic ROS-Activity	127
5.3.2.	Summary and Conclusions	128
Chapter 6	Synthesis, Broader Implications and Recommendations.....	131
6.1	Conclusions and Broader Implications	131
6.2	Limitations	135
6.3	Recommendations.....	137
6.3.1	Health Effects Community	137
6.3.2	Regulatory Community	138
6.3.3	Atmospheric Community	139
Bibliography	142

List of Figures

Figure 2.1 Location of the sampling sites.	13
Figure 2.2 Mean peak levels of ozone in Riverside, central and eastern LA as well as western LA. Data acquired from the online database of the California Air Resources Board.	20
Figure 2.3a-d Chemical composition and gravimetric mass concentration of quasi-UFP ($d_p < 0.25 \mu\text{m}$) by site in a) spring; b) summer, c) fall and d) winter. Error bars correspond to one standard error.	22
Figure 2.4a-d Linear regression plot of monthly reconstructed and gravimetric mass concentrations in a) spring, b) summer, c) fall and d) winter.	24
Figure 2.5a-d Average concentration of organic carbon (OC) and elemental carbon (EC) in quasi-UFP ($d_p < 0.25 \mu\text{m}$) by site in a) spring, b) summer, c) fall and d) winter. Error bars correspond to one standard error.	29
Figure 2.6a-d Average concentration of sulfate, nitrate and ammonium in quasi-UFP ($d_p < 0.25 \mu\text{m}$) by site in a) spring, b) summer, c) fall and d) winter. Error bars correspond to one standard error.	33
Figure 2.7a-d. Average molar concentration ratio of measured ammonium to theoretical ammonium required for complete neutralization of nitrate and sulfate ions in a) spring, b) summer, c) fall and d) winter. Error bars represent one standard error.	34
Figure 2.8a-d Average concentration of total metals and elements in quasi-UFP ($d_p < 0.25 \mu\text{m}$) by sites' cluster in a) spring, b) summer, c) fall and d) winter. Error bars represent one standard error.	37
Figure 2.9 Coefficient of divergence (COD) between sites pairs across the year. Box plots show the minimum, first quartile, median, third quartile and maximum observed values.	38
Figure 3.1a-b Monthly bulk composition and average gravimetric mass (standard error) of ambient a) $\text{PM}_{2.5}$ and b) $\text{PM}_{10-2.5}$ in Milan. * indicates coarse ions sample for March was lost during chemical analysis.	50
Figure 3.2 Yearly average (standard deviation) crustal enrichment factor (CEF) of select total elements in ambient $\text{PM}_{2.5}$ and $\text{PM}_{10-2.5}$ in Milan.	52
Figure 3.3 Monthly variation in the concentration ($\mu\text{g}/\text{m}^3$) of $\text{PM}_{2.5}$ water-insoluble organic carbon (WIOC), water-soluble organic carbon (WSOC) and elemental carbon (EC) as well as in the concentration ratio of fine organic carbon-to-EC (OC/EC).	55
Figure 3.4 Monthly concentration ratio of measured ammonium to required ammonium for complete neutralization of nitrate and sulfate ions in ambient $\text{PM}_{2.5}$ in Milan. Error bars represent the uncertainty of analytical measurement.	57
Figure 3.5a-f Monthly concentration of a) levoglucosan, b) picene, c) polycyclic aromatic hydrocarbons, d) hopanes, e) n-alkanes along with the variation in their carbon preference index (CPI) and f) secondary organic aerosol tracers in ambient $\text{PM}_{2.5}$ in Milan.	61
Figure 3.6a-b contribution to ambient a) $\text{PM}_{2.5}$ organic carbon (OC) and b) $\text{PM}_{2.5}$ mass estimated using a molecular marker chemical mass balance (MM-CMB) model.	65

Figure 3.7a-d GC/MS chromatograms of ambient PM _{2.5} in Milan in: a) December, b) January, c) July and d) August monthly samples.	66
Figure 4.1. Map of the urban background (A) and near-freeway sites (B).....	72
Figure 4.2 a-b. Chemical composition and gravimetric mass concentration of PM _{10-2.5} , PM _{2.5-0.25} and PM _{0.25} at the a) near-freeway and b) urban background sites. Error bars correspond to one standard error.	76
Figure 4.3a-b. Average concentration of water-soluble organic carbon (WSOC), organic carbon (OC) and elemental carbon (EC) in PM _{10-2.5} , PM _{2.5-0.25} and PM _{0.25} at the a) near-freeway and b) urban background sites. Error bars correspond to one standard error.	78
Figure 4.4a-b. Comparison of size-resolved a) organic carbon (OC) and b) elemental carbon (EC) concentrations (current study) with data from I-710 freeway and an urban background site in the Los Angeles (LA) area (Kam et al., 2012).	80
Figure 4.5a-b. Average concentration of nitrate, non-sea-salt sulfate and ammonium in PM _{10-2.5} , PM _{2.5-0.25} and PM _{0.25} at the a) near-freeway and b) urban background sites. Error bars correspond to one standard error.....	81
Figure 4.6. Average charge balance ratio of cations (Na ⁺ , NH ₄ ⁺ , ssCa ²⁺ , Mg ²⁺) to anions (Cl ⁻ , NO ₃ ⁻ , SO ₄ ²⁻). Error bars represent one standard error.	83
Figure 4.7. Backward air mass trajectories for the entire sampling campaign (July-August 2012), simulated using HYSPLIT model from NOAA. For each sampling day, four 48-hour trajectories were modeled every six hours at 500 m-agl using vertical wind velocity field from the meteorological data.	83
Figure 4.8a-c. Average n-alkanes concentration (C ₁₉ -C ₃₄) in a) PM _{10-2.5} , b) PM _{2.5-0.25} and c) PM _{0.25} at the near-freeway and urban background sites. Only values above the limit of detection (LOD) are shown. Error bars correspond to one analytical or standard error.....	91
Figure 4.9a-b Average concentration of dicarboxylic acids in PM _{10-2.5} , PM _{2.5-0.25} and PM _{0.25} at the a) near-freeway and b) background sites. Only values above the limit of detection (LOD) are shown. Error bars correspond to one standard or analytical error.	93
Figure 5.1 Monthly a) mass concentration (µg/m ³) (secondary axis) as well as air volume-based (µg Zymosan/m ³) and b) PM mass-based (intrinsic) (µg Zymosan/mg PM) water-soluble reactive oxygen species (ROS)-activity of ambient PM _{2.5} in Milan. Error bars represent one-sigma propagated uncertainty.	101
Figure 5.2 Map of the urban background (A) and near-freeway sites (B).....	107
Figure 5.3a-b Average total concentration of metals and elements in PM _{10-2.5} , PM _{2.5-0.25} and PM _{0.25} at the a) near-freeway and b) urban background sites. Error bars represent one standard error.	114
Figure 5.4a-b Average crustal enrichment factors (CEF) in PM _{10-2.5} and PM _{2.5} at the a) near-freeway and b) urban background sites. Error bars represent one standard error.....	115
Figure 5.5 Water-solubility of metals and elements in PM _{10-2.5} , PM _{2.5-0.25} and PM _{0.25} , averaged across the sampling sites. Error bars represent one standard error.	120

Figure 5.6 Water-soluble elemental composition of PM_{10-2.5}, PM_{2.5-0.25} and PM_{0.25}, averaged across the sampling sites. Error bars represent one standard error. 121

Figure 5.7 Average a) air volume-based (μg Zymosan/m³) and b) PM mass-based (intrinsic) (μg Zymosan/mg PM) reactive oxygen species (ROS)-activity of PM_{10-2.5}, PM_{2.5-0.25} and PM_{0.25} at the near-freeway and urban background sites. Error bars represent one standard error. 122

Figure 5.8 Comparison of average intrinsic reactive oxygen species (ROS)-activity (μg Zymosan/mg PM) of PM_{10-2.5}, PM_{2.5} and PM_{0.25} in Beirut (current study) with data from Los Angeles (LA) (Saffari et al., 2013a; Verma et al., 2009b), Milan (Daher et al., 2012) and Lahore (Shafer et al., 2010) during July-August. Error bars represent one standard error. *ROS-activity of ambient PM_{2.5} in LA corresponds to that of samples collected in October-November 2007 during and after wildfires (Verma et al., 2009b)..... 127

List of Tables

Table 2.1 Select meteorological parameters at sites clusters during spring (March-May), summer (June-August), fall (September-November) and winter (December-February). *Data corresponds to December.....	18
Table 2.2 Seasonal mass concentration (average \pm standard error) of quasi-UFP ($dp < 0.25 \mu\text{m}$) at the 10 sampling sites.....	18
Table 2.3 Yearly-average (\pm standard error) percent fraction of quasi-UFP ($dp < 0.25 \mu\text{m}$) components.....	23
Table 2.4 Average ratio (\pm standard error) of organic carbon (OC) to elemental carbon (EC) and Pearson correlation coefficient between OC and EC at the 10 sampling sites. Missing value indicates that EC concentrations were mostly below detection limit.....	28
Table 3.1a-b Average source contribution estimates (SCE) to ambient: a) fine organic carbon, b) $\text{PM}_{2.5}$ in Milan and associated standard errors (SE). Statistically significant sources ($> 2 \times \text{SE}$) are shown in bold. *uncertainty of analytical measurement.....	47
Table 3.2 Monthly concentration of total metals and elements in ambient $\text{PM}_{2.5}$ and $\text{PM}_{10-2.5}$ in Milan.....	53
Table 3.3 Monthly concentration of secondary organic aerosol tracers in ambient $\text{PM}_{2.5}$ in Milan. n.d. indicates that compound was not detected.....	62
Table 4.1. Average (\pm standard error) size-resolved particle mass levels at the near-freeway and urban background sites.....	75
Table 4.2. Average (\pm standard error) concentration and limit of detection (LOD) of PAHs, hopanes and steranes in $\text{PM}_{10-2.5}$, $\text{PM}_{2.5-0.25}$ and $\text{PM}_{0.25}$ at the near-freeway and urban background sites.....	88
Table 4.3 Limit of detection (LOD) of n-alkanes and dicarboxylic acids.....	92
Table 5.1 Spearman correlation coefficient (R) between monthly ROS-activity and select species of ambient $\text{PM}_{2.5}$ in Milan. Bold indicates significant correlation at a 0.05 level and $R \geq 0.7$. Italic indicates significant correlation at a 0.05 level.....	103
Table 5.2 Average (\pm standard error) mass concentration and chemical composition of $\text{PM}_{10-2.5}$, $\text{PM}_{2.5-0.25}$ and $\text{PM}_{0.25}$ at the near-freeway and urban background sites.....	111
Table 5.3 Spearman correlation coefficients (R) between ROS-activity (μg Zymosan/mg PM) and select species (ng/ μg PM) in $\text{PM}_{10-2.5}$, $\text{PM}_{2.5-0.25}$ and $\text{PM}_{0.25}$. Bold indicates $R \geq 0.70$ and significant at a 0.05 level.....	125
Table 5.4 Summary of studies that examined $\text{PM}_{0.25-}$, $\text{PM}_{2.5-}$, and $\text{PM}_{2.5-10}$ -associated oxidative potential using the <i>in vitro</i> macrophage-based ROS assay.....	130

Abstract

Compelling epidemiological and toxicological evidence indicates consistent associations between exposure to particulate matter (PM) and increased risk of adverse health outcomes. Many of these health effects may result, at least in part, from cellular oxidative stress. However, although an association between PM and health endpoints has been observed, the contribution of specific particle components to aerosol toxicity remains unknown. Most of the evidence is based on mass measures of PM albeit aerosol mass is probably only a surrogate for the real causative particle components. An accurate identification of specific agents of aerosol toxicity, with subsequent targeted emission controls, necessitates an improved characterization of PM composition (chemical and physical), variability (temporal and spatial), sources and their relation to particle oxidative potential.

This dissertation focused on determining the chemical and oxidative properties of size-resolved PM ($PM_{10-2.5}$, $PM_{2.5}$, $PM_{2.5-0.25}$, $PM_{0.25}$) in distinct urban and roadway environments. Target sites ranged from highly-polluted metropolitans to desert-like locations in the Greater Beirut area, Milan and the Los Angeles basin. PM chemical composition was determined by conducting a chemical mass closure. Specific emphasis was given to the organic and elemental aerosol fractions. PM oxidative potential was quantified using a macrophage-based *in vitro* reactive oxygen species (ROS) assay. Its association with size-fractionated and chemically-speciated particle components was determined using linear regression analysis. The role of water-soluble metals in PM-induced redox activity was particularly investigated. At near-freeway and urban settings in the Greater Beirut area, Mn, Cu, Co, V, Ni and Zn, many of which are air toxics, were mostly distributed in $PM_{2.5-0.25}$ and $PM_{0.25}$, with high water-solubility in these modes (> 60%). These physico-chemical characteristics may lead to increased adverse biological effects. Of particular concern were water-soluble metals which strongly correlated with ROS formation. In $PM_{10-2.5}$, Mn and Co, which are road dust components, were highly associated with ROS-activity. Cu -a tracer of vehicular abrasion- and Co -a

road dust element- were potential mediators of $PM_{2.5-0.25}$ -based ROS-activity. In $PM_{0.25}$, V and Ni, both originating from fuel oil combustion, were strongly correlated with ROS formation. Water-soluble organic carbon was also implicated in $PM_{2.5}$ -induced ROS generation. Moreover, intrinsic (i.e. PM-mass normalized) ROS-activity displayed a particle size-dependency, with lowest activity associated with $PM_{10-2.5}$. The intrinsic ROS-activity of PM collected from a variety of worldwide urban settings, including Milan, Beirut and Los Angeles, was also quantitatively assessed and compared across areas. Additionally, monthly variation in primary and secondary $PM_{2.5}$ sources was quantified using the Chemical Mass Balance (CMB) model and fixed tracer-to-OC ratios applied to fine PM collected at a centrally-located urban site in Milan for a year-long period. Spatial variability in quasi-ultrafine PM ($PM_{0.25}$) in the Los Angeles basin was examined using coefficients of divergence analysis. While $PM_{0.25}$ mass is relatively spatially homogeneous in the basin, some of its components, mainly elemental carbon, nitrate and several toxic metals, were unevenly distributed, suggesting that population exposure to quasi-ultrafine particles can vary substantially over short spatial scales.

Findings from this work provide additional insight on PM composition, variability, sources and their relation to particle oxidative potential. Advancing our knowledge of PM characteristics that are mostly influential in particle toxicity is essential for establishing more cost-effective and source-specific regulatory strategies for mitigating PM toxicity. Furthermore, an improved understanding of the spatial and temporal complexities of hazardous particle components provides guidance for more carefully-targeted epidemiological studies for personal exposure assessment.

Chapter 1 Introduction

The rise in environmental and health concerns due to air pollution has challenged the scientific community to effectively characterize particulate matter (PM) and assess its contribution to air pollution. Efficient regulation of particle pollution to mitigate climate change and protect human health, in particular, requires a comprehensive understanding of PM properties, variability and sources.

1.1 Background

Particulate matter (PM) is a mixture of solid or liquid particles suspended in a gas. Those can have various sizes, shapes (e.g. spherical, cylindrical) and be composed of hundreds of different chemicals. Chemical components of PM include carbonaceous species, inorganic ions, metals and trace elements as well as organic compounds. The organic fraction of PM is particularly complex since it comprises hundreds of individual organic components. PM can be directly emitted by natural (biogenic) and anthropogenic sources or formed in the atmosphere from the photo-oxidation of gas-phase precursors (e.g. SO₂, NO_x) (Robinson et al., 2007). Natural sources include, but are not limited to, windblown dust, sea spray and biological material (Seinfeld and Pandis, 2006) while major anthropogenic sources comprise industrial processes and fossil fuel combustion (e.g. vehicular emissions and biomass burning). Particles that are directly emitted into the atmosphere are known as primary pollutants whereas particles formed in the atmosphere are referred to as secondary pollutants. Secondary PM is composed of both inorganic and organic compounds. The most abundant inorganic secondary PM components are sulfate, nitrate and ammonium, formed from the oxidation of precursor gases (SO₂, NO_x, NO) (Fine et al., 2008; Seinfeld and Pandis, 2006). Secondary organic aerosol is formed from the reaction of volatile organic compounds with atmospheric oxidants (e.g. OH, ozone) to form low-volatility products (e.g. organic acids, nitro-polycyclic aromatic hydrocarbons) that subsequently condense onto

pre-existing particles (Fine et al., 2008). After emission or formation, PM is subject to removal or transformation by various chemical and physical processes (Hinds, 1999). Particles can change their size and composition by vapor condensation, evaporation, coagulation with other particles or chemical reaction (Seinfeld and Pandis, 2006). PM can also be removed by gravitational settling or diffusion. The presence of PM in the atmosphere has important implications on the environment, such as climate change and visibility impairment, and human welfare. Determining the physical, chemical and toxicological characteristics as well as sources of ambient PM is thus essential, not only for our mechanistic understanding, but also for assessing its environmental and health effects.

1.2 PM Characteristics: Particle-Size

Particle size is an important parameter governing PM behavior. All particle properties (e.g. physical, optical and chemical) are size-dependent, with some varying strongly with PM size (Hinds, 1999). Although atmospheric particles are not always spherical, particle size is commonly expressed as aerodynamic diameter, d_p , with d_p defined as the diameter of a unit density sphere having the same settling velocity as the given particle.

Airborne particles can range from few to several micrometers in size. Particles with d_p less than 10 μm (PM_{10}) are generally of concern because they can enter the intra-thoracic airways (Anderson, 2000). These inhalable particles can be classified into different size ranges, including coarse ($2.5 \mu\text{m} < d_p < 10 \mu\text{m}$, $\text{PM}_{10-2.5}$) and fine PM ($d_p < 2.5 \mu\text{m}$, $\text{PM}_{2.5}$). $\text{PM}_{2.5}$ can be sub-divided into accumulation ($0.1 \mu\text{m} < d_p < 2.5 \mu\text{m}$) and ultrafine ($d_p < 0.1 \mu\text{m}$) particles. These PM modes have distinct sources, chemical composition, respiratory deposition and atmospheric lifetimes. Coarse particles are predominantly generated by mechanical disruption and attrition processes. Major components include resuspended soil, sea-salt, biological material and road dust (Hwang

et al., 2008; Paode et al., 1999). Because of their relatively larger size, coarse particles have higher gravitational settling velocities than smaller-sized particles, and are thus removed from the atmosphere within hours (EPA, 2004; Sioutas et al., 2005). Coarse particles also primarily deposit in the upper respiratory tract. Accumulation-mode particles are mostly anthropogenic in origin, formed mainly by coagulation of particles in the nuclei mode ($d_p < 10$ nm) and condensation of vapors onto pre-existing particles (Seinfeld and Pandis, 2006; Sioutas et al., 2005). This mode has an atmospheric lifetime of the order of days because its removal mechanism is neither dominated by gravitational settling nor diffusion processes (Hinds, 1999). Ultrafine particles are emitted by incomplete combustion processes but can also be formed through gas-to-particle atmospheric conversion processes (Kim et al., 2002; Sardar et al., 2005a; Westerdahl et al., 2005). Despite their very low contribution to overall PM mass, ultrafine particles dominate ambient particle number concentrations (Morawska et al., 1998) and have a large surface area (Hughes et al., 1998) relative to larger particles. Because of their increased number and surface area, ultrafine particles can carry substantial amounts of toxic air pollutants, such as organic carbon (OC) and polycyclic aromatic hydrocarbons (PAHs) (Eiguren-Fernandez et al., 2004; Li et al., 2003; Oberdörster, 2000). Ultrafine particles also have a high pulmonary deposition efficiency compared to larger-sized particles (Chalupa et al., 2004) since they are capable of avoiding phagocytosis by alveolar macrophages and gain entry to pulmonary interstitial sites (Nemmar et al., 2002; Oberdörster et al., 2002).

1.3 PM Exposure and Health Effects

Compelling epidemiological and toxicological evidence indicates consistent associations between exposure to PM and increased risk of adverse health outcomes (Peters, 2001; Pope, 2002). A considerable body of data suggests a significant increase in respiratory,

neurodegenerative and cardiovascular diseases as well as mortality after both short- and long-term exposure to atmospheric PM (Hong et al., 2007; Morgan et al., 2011; Sørensen et al., 2003). Many of the health endpoints may result, at least in part, from oxidative stress initiated by the formation of reactive oxygen species (ROS) at the surface of and within target cells (Ayres et al., 2008; Nel, 2005). Specific health outcomes associated with cellular oxidative stress include the ability of PM to induce pro-inflammatory effects in the nose, lung and cardiovascular system (Ayres et al., 2008). ROS is a collective term comprising chemically reactive oxygen radicals or oxygen-derived species (e.g. hydroxyl radical and hydrogen peroxide) (Halliwell and Cross, 1994). While ROS is continually formed in the human body as a natural byproduct of aerobic metabolism, high levels of ROS can cause a change in the redox status of the cell, leading to severe responses such as pulmonary inflammation and, at higher concentrations, apoptosis (Nel, 2005; Squadrito et al., 2001).

1.4 Rationale of Current Work

1.4.1 Motivation

Ambient PM mass has been consistently associated with significant adverse human health outcomes (Peters, 2001; Pope, 2002). However, while particle mass has been clearly proven useful in demonstrating the association between PM exposure and increased health effects, the contribution of specific particle characteristics to PM toxicity remains largely unknown. Aerosol mass is probably only a surrogate for the real causative particle components (NRC, 2004) and may therefore be a relatively poor metric for regulating PM. Current standards for controlling atmospheric levels of PM are based on measurements of mass concentration of PM₁₀ and PM_{2.5}. Determining the association between PM and particle-induced toxicity is complicated by the fact that airborne PM is composed of a complex mixture of compounds

having different sizes, chemical composition and originating from various sources, both primary and secondary. Many of PM chemical constituents are also highly correlated and could serve as surrogates for other components. Specific particle characteristic(s) (physical or/also chemical) that are mostly influential in PM-induced redox activity remain to be identified, despite attempts at linking health endpoints or toxicity measurements with PM properties. Particle compounds implicated in ROS formation include OC, PAHs and quinones (Cho et al., 2005; Nel et al., 2001; Squadrito et al., 2001). PM oxidative potential may also be largely related to the PM content of soluble species, particularly transition metals (Goldsmith et al., 1998; Prophete et al., 2006). Metals such as iron, copper and vanadium, can initiate ROS formation both directly and indirectly through redox-mediated mechanisms (Fantel, 1996; Valko et al., 2005). Particle-size and number concentration could also be critical in mediating PM toxicity. Because of their increased number concentration, large surface area and high pulmonary deposition efficiency (Morawska et al., 1998), ultrafine particles may be more biologically potent than larger coarse or fine particles (Cho et al., 2005; Ntziachristos et al., 2007a). This association between health endpoints and numerous potentially toxic PM chemical constituents and physical characteristics is daunting and further complicated by the variability (both temporally and spatially) of PM composition. Additional research is therefore needed to identify specific PM characteristic(s) that mostly contribute to its redox activity. Characterization of individual agents (and their potential sources) of PM toxicity is crucial for linking aerosol toxicity with specific air pollution sources that have the most significant effects on public health. More rationally-targeted and cost-effective PM control strategies, focusing on these critical PM components rather than total aerosol mass concentration, can thus be ultimately established.

1.4.2 Objectives

An accurate identification of specific PM components (and their sources) contributing to aerosol toxicity, with subsequent targeted emission controls, necessitates an improved understanding of PM composition, variability, sources and their relation to particle oxidative potential. The overarching objectives of this dissertation were therefore to:

- Evaluate the variation in PM-chemical composition and -redox activity with particle-size, location and season.
- Apportion primary and secondary sources to fine OC and particle mass.
- Determine the association between PM toxico-chemical properties and identify specific chemical components implicated in the induction of PM oxidative potential.
- Quantify and compare the intrinsic ROS-activity of PM from diverse urban settings.

These objectives were accomplished through a series of investigations aiming at determining the chemical and oxidative characteristics of size-resolved (coarse, fine, accumulation and ultrafine) PM in distinct urban and roadway environments. Study sites ranged from highly-polluted metropolitans to desert-like locations in the Greater Beirut area, Milan and the Los Angeles basin. PM chemical composition was determined using chemical fractionation tools and by conducting a chemical mass closure. Particular focus was devoted to the organic fraction as well as elemental composition and associated water-solubility. PM-induced redox activity was quantified by applying a macrophage-based *in vitro* ROS assay to the particle samples. The association between size-fractionated PM chemical properties and ROS-activity was determined using univariate and multivariate linear regression analyses. Furthermore, monthly variation in primary and secondary PM_{2.5} sources was quantified using the Chemical Mass Balance (CMB) model and fixed tracer-to-OC ratios applied to fine PM collected at a centrally-located urban site

in Milan for a year-long period. Spatial variability in quasi-ultrafine PM ($PM_{0.25}$) in the Los Angeles basin was examined by calculating coefficients of divergence (COD) for each pair of sites and mass or associated components.

Findings from this dissertation contribute to the current state of scientific knowledge by providing a quantitative assessment of size-resolved PM-induced redox activity. Results also provide additional and much-needed insight on PM sources, variability, chemical composition and their relation to particle oxidative potential. Identifying PM properties that are mostly influential in inducing particle toxicity contributes, not only to our understanding of biological mechanisms of response, but also to the establishment of source-specific and more cost-effective PM control strategies. In addition, an improved understanding of the spatial and temporal variability of hazardous particle components provides a strong scientific basis to help develop air quality monitoring networks to support epidemiological and personal exposure assessment research.

1.5 Dissertation Layout

This dissertation is structured into different chapters.

Chapter 2 provides the much-needed information on the chemical composition as well as seasonal and spatial variability of quasi-ultrafine particles ($PM_{0.25}$). These particles may have significant health responses; greater than- or independent of the effects induced by larger-sized particles (Cho et al., 2005; Li et al., 2003; Ntziachristos et al., 2007a). A year-long sampling campaign was conducted at 10 distinctly different areas in the Los Angeles Basin, including source, near-freeway, semi-rural receptor and desert-like locations. Previous studies conducted in this complex air shed investigated $PM_{2.5}$ and PM_{10} , with a few exploring the properties of ultrafine PM (Cass et al., 2000; Fine et al., 2004a; Hughes et al., 1998; Sardar et al., 2005a).

Moreover, measurements were mostly restricted to few sampling sites and/or limited sampling intervals (few days or weeks). Findings from this work provide data to support epidemiological and toxicity studies for better assessment of population exposure to ultrafine particles.

Chapter 3 focuses on characterizing ambient PM in Milan, Italy. The monthly variation in coarse and fine PM bulk chemical composition, levels in addition to detailed PM_{2.5}-organic aerosol composition are presented. Molecular marker-based source apportionment modeling is also applied to determine the major sources of PM_{2.5}-OC. However, while results provide insights into wood-smoke and secondary organic aerosol source contributions to fine OC, significant sources of water-insoluble OC could not be explained by traditional source profiles, highlighting the need to establish source profiles characteristic of the area of Milan for use in source apportionment. Results of this study also provide a comprehensive understanding of PM_{2.5} chemical composition in Milan to complement an analysis of its particle-associated redox activity (discussed in Chapter 5).

Chapter 4 outlines a comparative and comprehensive analysis of size-resolved ambient PM (PM_{10-2.5}, PM_{2.5-0.25}, PM_{0.25}) in the Greater Beirut area, Lebanon. While atmospheric PM has generally been well-examined in developed countries, particle pollution in developing nations is relatively less explored. Sampling was concurrently conducted at near-freeway and urban background sites, with size-fractionated samples analyzed for their detailed chemical composition. The dependency of PM chemistry on particle-size and location is explored. Results are also evaluated in the context of metropolitans and roadways worldwide. Findings provide insight on commuter exposure in the Beirut area and complement an analysis of PM-induced redox activity in this region and its relation to particle-size and speciated chemical composition (discussed in Chapter 5).

Chapter 5 addresses the role of PM size and chemistry in inducing redox activity. Results presented in this chapter build upon the chemical characterization of samples collected in Milan-Italy (discussed in Chapter 3) and Beirut-Lebanon (discussed in Chapter 4). The high PM levels and diverse particle sources in these sampling areas provided suitable settings to examine the association of redox activity with size-resolved and chemically-speciated PM components. PM_{2.5}-induced ROS-activity in the urban area of Milan is first quantitatively assessed. Its monthly-variation and correlation with specific chemical species are also examined. The oxidative potential of PM_{10-2.5}, PM_{2.5-0.25} and PM_{0.25} samples, collected at near-freeway and urban background sites in the Greater Beirut area, is next quantified and compared among PM modes. The role of water-soluble metals and trace elements in PM-induced ROS-activity is also particularly investigated. Because of their enhanced bioavailability, soluble species may be more toxicologically-relevant (Costa and Dreher, 1997). Lastly, the intrinsic redox activity of PM in Beirut —representative of polluted developing areas— is compared to that of aerosols from other worldwide urban settings, including Milan and Los Angeles, for which ROS-activity data, using the same assay, are available. Comparisons were difficult in the past since investigators use a variety of assays that are not necessarily directly comparable.

Chapter 6 details the major findings of this research work with an emphasis on its contribution to the current state of scientific knowledge about urban air quality and its implications for public health and regulatory policy. The chapter concludes with recommendations for future atmospheric research directions, air quality regulations as well as epidemiological and toxicological studies.

Chapter 2 Chemical Composition of PM and its Seasonal and Spatial Variability: A Case Study of Ambient Quasi-Ultrafine PM (PM_{0.25}) in the Megacity of Los Angeles

What are the chemical composition, seasonal variability and spatial distribution of quasi-ultrafine PM in urban, semi-rural receptor and desert-like locations in the megacity of Los Angeles?

Current regulatory efforts are focused on the reduction of ambient mass levels of PM₁₀ ($d_p < 10 \mu\text{m}$) and PM_{2.5} ($d_p < 2.5 \mu\text{m}$). However, emerging epidemiological evidence (Delfino et al., 2005; Penttinen et al., 2001; Peters et al., 1997) demonstrated a strong correlation between health endpoints and ultrafine particles (UFP, typically defined as particles with $d_p < 0.1\text{-}0.2 \mu\text{m}$ (Sioutas et al., 2005)). Yet, little is known about the chemical composition of ambient UFP. The chemical composition of ultrafine particles is determined by sources, both primary (e.g. motor vehicles) and secondary (Kim et al., 2002). These source emissions are also affected by temporal variations in meteorological conditions. To improve the characterization of UFP, a year-long sampling campaign was conducted at 10 distinct areas in the Los Angeles air shed, including source, near-freeway, receptor and desert-dominated locations. The objective was to determine the chemical composition as well as seasonal and spatial variability of quasi-UFP ($d_p < 0.25 \mu\text{m}$). Previous studies do not provide insight on the large-scale variation of UFP in the Los Angeles basin (Hughes et al., 1998; Sardar et al., 2005a). Understanding PM spatial and temporal complexities is necessary for personal exposure assessment. Findings of this work provide data to support regulatory agencies as well as epidemiological and toxicity studies.

This chapter is based on the following publication:

Daher N., Hasheminassab S., Shafer M. M., Schauer J. J., Sioutas C., 2013. Seasonal and spatial variability in chemical composition and mass closure of ambient ultrafine particles in the megacity of Los Angeles. *Environmental Science: Processes & Impacts*, 15, 283-295.

2.1 Introduction

In urban areas, ultrafine particles (UFP, typically defined as particles with $d_p < 0.1\text{-}0.2 \mu\text{m}$ (Sioutas et al., 2005)) are primarily emitted from motor vehicles but can also be formed through gas-to-particle atmospheric conversion processes (Kim et al., 2002; Sardar et al., 2005a; Westerdahl et al., 2005). Despite their very low contribution to overall PM mass, ultrafine particles dominate ambient particle number concentrations (Morawska et al., 1998). UFP also have a large surface area relative to fine (PM_{2.5}) or coarse (PM_{10-2.5}, $2.5 < d_p < 10 \mu\text{m}$) PM (Hughes et al., 1998)

and a high pulmonary deposition efficiency (Chalupa et al., 2004). Because of their increased number and surface area, ultrafine particles can carry substantial amounts of toxic air pollutants, such as organic carbon (OC), polycyclic aromatic hydrocarbons (PAHs) and transition metals, many of which have been implicated in inducing inflammatory effects (Kumagai et al., 1997; Saldiva et al., 2002). Some of these PM components, such as PAHs and OC, dominate the ultrafine fraction (Eiguren-Fernandez et al., 2003; Li et al., 2003). Thus, UFP may have significant health responses; greater than- or independent of the effects induced by larger-sized particles, as shown by previous studies which reported that UFP exhibited a greater mass-based redox activity than fine and coarse particles (Cho et al., 2005; Li et al., 2003; Ntziachristos et al., 2007a).

Contrarily to coarse and fine PM, which have distinct sources, a major fraction of accumulation particles ($>$ UFP in diameter and $<$ 2.5 μm) originates from UFP. Consequently, there is no clear cut-point that separates ultrafine from accumulation mode PM. While UFP are conventionally defined as PM accounting for greater than 80% of total particle number concentrations (Morawska et al., 1998), aerosol number median diameters can be as large as 90-150 nm in some polluted urban areas in summer (Fine et al., 2004c; Kim et al., 2002). Therefore, the majority of number-based ambient particles may not always lie below a cut-point of 100 nm. Furthermore, ultrafine soot particles have agglomerate-like structures (Friedlander, 2000), which are characterized by their large surface area and low density compared to equivalent spherical particles. A considerable fraction of these fractal particles would be classified by an inertial separator as ultrafine because of their low density, whereas a particle mobility-based classifier would classify them in the accumulation mode range due to their large surface area (Geller et al., 2006; McMurry et al., 2002; Sioutas et al., 2005). Thus, the cut-point separating accumulation and ultrafine PM can be ambiguous, varying with location and season (Sioutas et al., 2005). The

current study focuses on particles with aerodynamic diameter less than 0.25 μm . We will be referring to these particles as quasi-UFP hereafter.

Lastly, unlike $\text{PM}_{2.5}$ or PM_{10} , for which there is an abundance of continuous and time-integrated mass or chemically speciated data, significantly less is known about the spatial and seasonal variation of ultrafine particles as well as their chemical composition. Determining these PM properties is important in assessing human exposure to ultrafine particles. A recent cohort study conducted in the Los Angeles basin (LAB) reported positive associations of blood biomarkers of inflammation and ambulatory ST-segment depression with quasi-UFP, but no associations with larger accumulation-mode $\text{PM}_{0.25-2.5}$ (Delfino et al., 2009) and $\text{PM}_{10-2.5}$ (Delfino et al., 2011; Delfino et al., 2009). Such differences in systemic responses between particle-size fractions, notably accumulation and ultrafine mode of regulated fine PM, highlight the importance of characterizing particles in the size range $< 0.25 \mu\text{m}$, particularly in impacted communities of the LAB. Previous studies conducted in this area investigated $\text{PM}_{2.5}$ and PM_{10} , with a few exploring UFP properties (Cass et al., 2000; Fine et al., 2004c; Hughes et al., 1998; Sardar et al., 2005a). Moreover, measurements were mostly restricted to few sampling sites and/or limited sampling intervals (few days or weeks). These studies therefore do not provide insight on the larger scale distribution of quasi-UFP in the complex Los Angeles (LA) air shed. To expand the existing knowledge on quasi-ultrafine particles, a year-long sampling campaign was conducted at 10 distinctly different areas in the LAB, including source, near-freeway, semi-rural receptor and desert-like locations. The objective of this study is to provide the much-needed information on the chemical composition as well as seasonal and spatial variability of quasi-UFP. Findings of this work could provide the basis for designing epidemiological and toxicity studies to mitigate population exposure to quasi-ultrafine particles.

2.2 Methodology

2.2.1 Sampling sites

To characterize quasi-UFP, 10 sampling sites, impacted by different PM sources and representing distinct areas of the Los Angeles basin, were selected and set up. These included source, near-freeway, semi-rural receptor and desert-like areas. A three letter code is used to designate the sites throughout this manuscript. Their location, along with nearby major freeways, is shown in Figure 2.1. Detailed description of the sampling locations and selection criteria is provided in a separate publication (Pakbin et al., 2010).

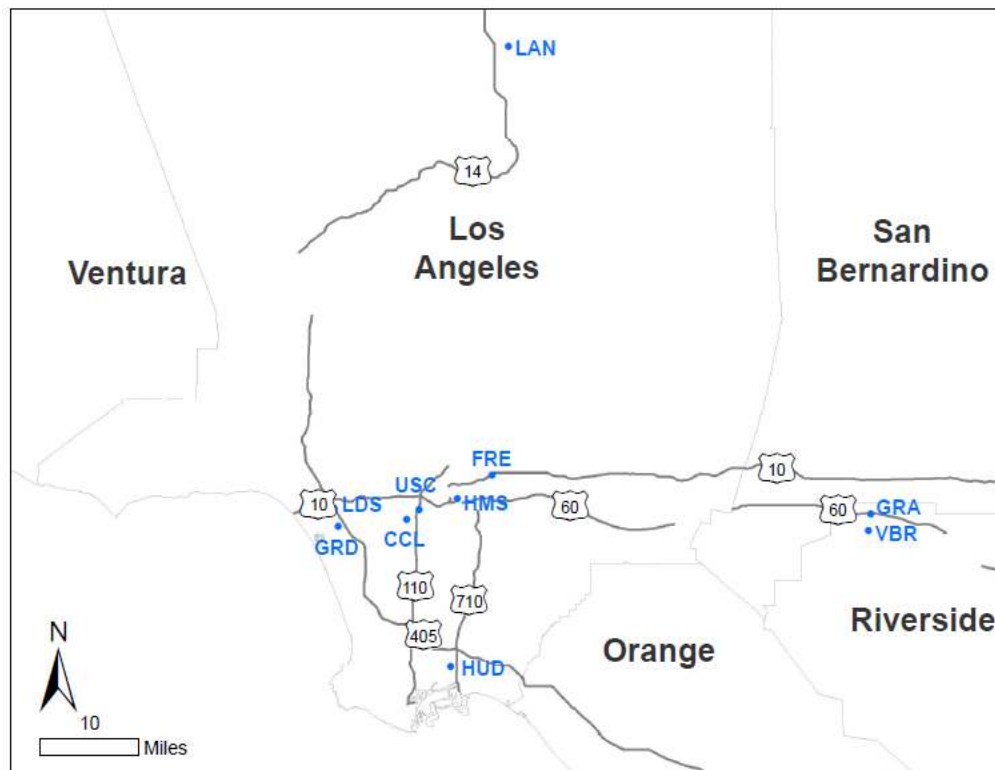


Figure 2.1 Location of the sampling sites.

Briefly, the 10 sites can be classified according to their geographical location into Long Beach (HUD), western LA (GRD, LDS), central LA (CCL, USC), eastern LA (HMS, FRE), Riverside County (VBR, GRA) and Lancaster (LAN); in order of their increasing distance from

the coast. The Long Beach site, HUD, is located about 2 km inland of the ports of LA and Long Beach in a mixed residential and industrial area. It is also immediately to the east of Terminal Island Freeway (ca. 100 m) and 1.2 km west of I-710, both of which have a high fleet and fraction of heavy duty diesel vehicles (HDDV) (up to 25% on I-710 (Moore et al., 2009)) serving to transfer cargo from the ports to inland locations (Moore et al., 2009; Pakbin et al., 2010). Because of its surrounding environment and location, HUD is considered as a source site in the LAB. In contrast, Riverside sites (VBR and GRA), which are located in a mostly rural-agricultural area about 80 km inland from downtown LA, represent pollutant receptor areas in the basin. Given their location on the prevalent air trajectory crossing the LAB from coast to inland, these sites are considerably affected by advected, aged and photochemically-processed PM from upwind regions (Kim et al., 2002; Pakbin et al., 2010). Furthermore, while both sites are relatively close to major streets, GRA is in the vicinity of CA-60 freeway (~300 m north). GRA may therefore be more significantly impacted by freeway emissions than VBR. Further inland across the basin, LAN represents a typical desert-like site, located in a rural region of Lancaster city to the north of the LAB. This monitoring site is over 2 km away from the nearest freeway (CA-14), but near local arterial roadways (Moore et al., 2010; Pakbin et al., 2010). The 6 remaining sites, situated in the LA area, represent urban sites. The western LA sites (GRD and LDS) correspond to coastal areas, with LDS immediately to the southwest of I-405 freeway. The eastern LA (HMS, FRE) and central USC sites are located within 50-800 m of nearby freeways. Moreover, although not located next to a freeway, CCL is adjacent to surface streets with significant motor vehicle traffic.

2.2.2 Sample Collection

Twenty-four-hour time-integrated samples were concurrently collected at the 10 sampling sites for a year-long period extending from April 2008 to March 2009. Samples were collected once per week on a weekday. Two parallel Sioutas Personal Cascade Impactor Samplers (Misra et al., 2002; Singh et al., 2002) (Sioutas™ PCIS, SKC Inc., Eighty Four, PA, USA), operating at 9 lpm, were deployed at each site to collect size-fractionated particles in the following size ranges: <0.25µm (quasi-UFP), 0.25-2.5 µm, and 2.5-10 µm. However, the present study only focuses on the quasi-UFP fraction. The coarse PM chemical composition is discussed in detail in other publications (Cheung et al., 2011a; Cheung et al., 2011b; Cheung et al., 2012a; Pakbin et al., 2010). For the purpose of chemical analyses, one PCIS was loaded with Teflon filters (Pall Life Sciences, Ann Arbor, MI) while the other one with quartz microfiber filters (Whatman International Ltd, Maidstone, England). 37-mm filters were used as collection media for the quasi-ultrafine particles.

2.2.3 Sample Analysis

Mass concentration of the quasi-UFP samples was determined by pre- and post-weighing the 24-hour time-integrated Teflon filters using a Microbalance (Mettler Toledo Inc., Columbus, OH, USA), following equilibrium under controlled temperature and relative humidity conditions (22-24°C and 40-50%, respectively).

To perform chemical analyses of the PM_{0.25} samples, the collected Teflon and quartz filters were sectioned into portions. Elemental and organic carbon (EC and OC, respectively) measurements were performed on individual quartz filter portions while all other analyses were conducted on monthly composites of sectioned filters. Water-soluble inorganic ions and total elements were quantified from monthly composites. EC and OC contents of the filters were

determined using the NIOSH Thermal Optical Transmission method (Birch and Cary, 1996). The ionic content of the filters was quantified by ion chromatography (IC) (Stone et al., 2009) following water extraction and filtration of the samples. The elemental mass of the filter substrates was measured using a high resolution magnetic sector Inductively Coupled Plasma Mass Spectrometry (Thermo-Finnigan Element 2) (Zhang et al., 2008a). A mixed-acid (nitric acid, hydrochloric acid and hydrofluoric acid) microwave-aided digestion was applied for extraction of total elements. Lastly, concentration values that were below the limit of detection ($< 2 \times$ total analytical uncertainty) were assumed as half the detection limit.

2.3 Meteorology

Select meteorological parameters, organized by sites' clusters and season, are listed in Table 2.1. Parameters include mean temperature, relative humidity, precipitation as well as vector-average wind speed and direction. Data was acquired from the online database of the California Air Resources Board. Mean temperature and relative humidity exhibited more seasonality in the inland areas at Riverside and Lancaster, compared to Long Beach and urban LA. Across the air basin, temperatures were coolest in winter while warmest in summer. Mean temperatures were also relatively warm in fall, spanning a range of 18.8-22°C across the sites' clusters. These meteorological conditions are typical of the LAB, where the warm period extends to September and October (Kim et al., 2002). Mean relative humidity was highest in the coastal areas (Long Beach and west LA) and reached peak values in summer (76.8 and 81%). Furthermore, excluding Lancaster, humidity levels increased in summer in the basin. Lancaster, on the other hand, was characterized by an intense seasonal variability in its temperature and relative humidity. Its average temperature varied from a low of 8.7°C in winter to a high of 27.9°C in summer. Its relative humidity also dropped from a maximum of 55.9% in winter to a

minimum of 26.9% in summer and was generally substantially lower than levels at the other sites. These extreme meteorological patterns are consistent with the desert-like and distinct nature of LAN. At all sites, total precipitation was negligible in summer and spring but greatest in fall and winter. Additionally, wind speeds were generally stronger away from the coast, with more calms (< 0.5 m/s) observed in fall and winter. Wind speed during spring and summer was also higher than during fall and winter. Moreover, wind direction was consistent with the prevailing air trajectory crossing the LAB from coast to inland (Hughes et al., 2000). Wind blowing from the coast was predominantly westerly or southwesterly during summer and spring, resulting in strong onshore flows that transport pollutants across the basin. In winter, the wind shifted and had a predominantly northerly component across the sites' clusters, with the exception of Lancaster. In Lancaster, winds mainly originated from the west irrespective of the season.

2.4 Results and Discussion

In the following sections, all reported seasonal concentrations correspond to arithmetic averages with seasons segregated into spring (March–May), summer (June–August), fall (September–November) and winter (December–February). Respective errors represent one standard error, unless otherwise noted. Moreover, all 10 sampling sites presented in figures and tables of this manuscript are arranged from coastal to inland (HUD, GRD, LDS, CCL, USC, HMS, FRE, VBR, GRA and LAN).

Table 2.1 Select meteorological parameters at sites clusters during spring (March-May), summer (June-August), fall (September-November) and winter (December-February). *Data corresponds to December.

		Temperature (°C)	Relative humidity (%)	Precipitation	Wind (vector-average)	
		Average±stdev	Average±stdev	(mm) Total	Speed (m/s) (calm%)	Prevailing direction
Long Beach	Spring	16.3±5	65.2±23.6	12.0	1.6(4.1)	SW
	Summer	21.3±3.8	76.8±17.7	0.7	1.9(3.3)	SW
	Fall	19.9±4.9	67.8±28.7	54.8	1.2(5.6)	W
	Winter	13.8±5	61.6±29.8	168.9	0.7(2.9)	NW
Western LA	Spring	15±4.4	69±18.5	10.9	1.7(9.8)	W
	Summer	19.4±2.7	81±7.9	1.5	0.7(26.2)	W
	Fall	19±4.2	65.3±24.3	98.0	0.2(50.2)	NE
	Winter	13.9±4.8	58.3±26.1	215.8	0.2(26.2)	NW
Central and Eastern LA	Spring	17.2±5.8	59±18.4	9.7	2.1(0.6)	SW
	Summer	22.8±4.8	66.7±13.7	0.0	3.6(1.2)	SW
	Fall	20.9±5.7	55.5±21.4	184.9	1.6(4.6)	SW
	Winter	14.1±5.6	55.6±21.4	182.6*	1.5(0.6)	NE
Riverside	Spring	17.4±6.7	63.4±26.8	1.8	2.6(5)	NW
	Summer	25.6±6.4	65±23	5.6	3.6(2.7)	W
	Fall	22±7.1	56.8±28.1	1.5	1.6(6.5)	NW
	Winter	13.8±6.1	61.8±31.5	78.5	1.3(3.9)	N
Lancaster	Spring	15.2±6.6	40.5±16.7	NA	4.1(13.5)	W
	Summer	27.9±5.4	26.9±9.3	NA	4.3(11.6)	W
	Fall	18.8±7.3	36.5±17.7	NA	1.5(30.5)	W
	Winter	8.7±4.7	55.9±19.7	NA	1.5(33.6)	W

Table 2.2 Seasonal mass concentration (average ± standard error) of quasi-UFP (dp<0.25 µm) at the 10 sampling sites.

	Long Beach	Western LA		Central LA		Eastern LA		Riverside		Lancaster
	HUD	GRD	LDS	CCL	USC	HMS	FRE	VBR	GRA	LAN
Spring	7.9±0.8	6±0.7	5.4±0.7	6.6±0.5	9.2±1.4	7.4±0.7	7.7±0.8	8.8±1.2	10.0±1.7	7.5±1.3
Summer	9.4±0.5	7.1±0.5	7.0±0.4	7.6±0.6	8.7±1.4	9.4±1.1	10.4±0.8	9.7±0.7	12.6±0.9	13.2±1.9
Fall	13±1.6	10.7±1.2	9.9±1.0	11.2±1.1	13.3±1.4	11.4±1.2	12.6±1.4	14.9±2.0	13.1±1.4	8.8±0.9
Winter	16.1±2.8	8.4±1.0	8.5±0.9	10±0.9	11.4±1.4	9.1±0.8	9.7±0.9	9.8±1.4	10.3±1.2	5.9±0.7

2.4.1 Particulate Mass

Seasonal-average mass concentration of quasi-UFP in the Los Angeles basin is presented in Table 2.2 at each of the sampling sites. As can be inferred, the mass levels of quasi-UFP spanned a broad range of 5.9-16.1 $\mu\text{g}/\text{m}^3$ across the seasons and basin. Spatially, the mass concentration in winter, when emissions from local primary sources predominate, was greatest at HUD. This site is located in a pollutant source region of the LAB close to I-710 and Terminal Island freeways, as well as industrial sources and ports of Los Angeles and Long Beach (Pakbin et al., 2010). On the other hand, the wintertime concentration was lowest at the desert-like LAN site due to its remote location from urban sources. In contrast, concentrations were highest at receptor GRA and LAN sites in warm summer or also spring seasons, likely due to increased secondary aerosol formation and particle advection from upwind “source” areas. The strong and predominantly westerly/southwesterly wind in spring and summer (Table 2.1) transports primary PM and gaseous precursors from the western to the eastern edge of the basin (Allen et al., 2000; Pandis et al., 1992), resulting in an elevation in concentration and a photochemically-processed aerosol at the inland locations. Similar observations have been extensively reported for the receptor area of Riverside (Kim et al., 2002; Sardar et al., 2005a). Among urban LA sites, concentrations were lowest at the western/coastal sites (GRD, LDS).

Seasonally, a pronounced variability was observed at HUD and LAN. At source site HUD, peak concentrations occurred in winter and fall (16.1 ± 2.8 and 13 ± 1.6 $\mu\text{g}/\text{m}^3$, respectively) as opposed to spring and summer (7.9 ± 0.8 and 9.4 ± 0.5 $\mu\text{g}/\text{m}^3$, respectively). Higher atmospheric stability conditions, enhanced particle formation by condensable vapors, freshly emitted from vehicles (Kim et al., 2002) and peak cargo activity in the fall (Pakbin et al., 2010) likely contributed to the elevated levels. At LAN, the mass concentration varied from a low of 5.9 ± 0.7

$\mu\text{g}/\text{m}^3$ in winter to a high of $13.2\pm 1.9 \mu\text{g}/\text{m}^3$ in summer. As aforementioned, this trend can be associated with increased eastward PM advection and secondary aerosol formation in summer which offset atmospheric dilution effects. Conversely, peak levels were generally measured in fall at urban LA and Riverside sites. This pattern, which is in agreement with findings of Sardar et al. (2005a), could be attributed to limited particle dispersion due to the low wind speeds (≤ 1.6 m/s, Table 2.1) combined with extended secondary PM formation into early fall and particle formation from directly emitted condensable vapors (Kim et al., 2002). Secondary aerosol production is also supported by the mean peak levels of ozone, an indicator of photochemical activity, which had appreciable concentrations in early fall (Figure 2.2). Moreover, the low temperature coupled with increased relative humidity and stagnant conditions in the evening and early night in fall may enhance the partitioning of low vapor pressure compounds to the particle phase compared to spring/summer, as observed in earlier investigations conducted in this basin (Hudda et al., 2010; Moore et al., 2009). These combined effects lead to more pronounced concentrations in fall relative to the other seasons.

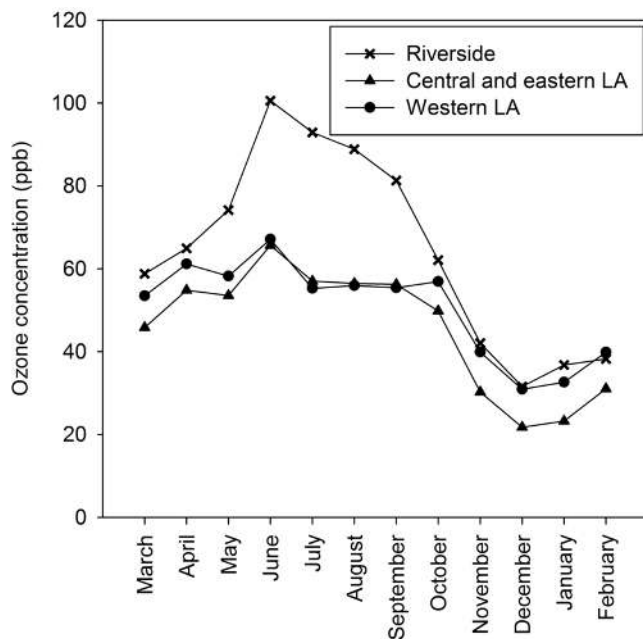


Figure 2.2 Mean peak levels of ozone in Riverside, central and eastern LA as well as western LA. Data acquired from the online database of the California Air Resources Board.

2.4.2 Mass Reconstruction

To determine the bulk composition of quasi-ultrafine particles in the LAB, a chemical mass reconstruction was conducted at each of the sampling sites during spring, summer, fall and winter, as shown in Figure 2.3a-d. PM chemical species were grouped into organic matter (OM), EC, secondary ions (SI), trace ions as well as metals, including crustal material (CM) and trace elements (TE). To account for the contributions of non-carbon atoms (e.g. oxygen, hydrogen) to the total mass of OM, a factor of 1.6 ± 0.2 and 2.1 ± 0.2 is recommended for urban and non-urban aerosols, respectively (Turpin and Lim, 2001). In this study, a factor of 1.8 is used to convert OC to OM for all sites and seasons. SI included ammonium, nitrate and sulfate, while trace ions comprised chloride, sodium and potassium. The proportion of CM in quasi-UFP was determined by summing the oxides of crustal metals, Al, K, Fe, Ca, Mg, Ti and Si, using the following equation (Chow et al., 1994; Hueglin et al., 2005; Marcazzan et al., 2001):

$$CM = 1.89Al + 1.21K + 1.43Fe + 1.4Ca + 1.66Mg + 1.67Ti + 2.14Si \quad (2.1)$$

Si concentration was estimated as $3.41 \times Al$ (Hueglin et al., 2005) since it was not measured in this study. Lastly, TE consisted of the remaining measured elements such as Cu, Zn and Cr.

On a yearly-average basis, the chemical composition of quasi-UFP in the LAB consisted of 49-64% OM, 3-6.4% EC, 9-14.5% SI (5-8.6% sulfate, 0.5-3.8% nitrate and 2.6-5.4% ammonium), 0.9-1.3% trace ions and 5.7-17% CM and TE, as shown in Table 2.3. These proportions are within the ranges previously reported for ultrafine particles in Southern California (Cass et al., 2000; Ning et al., 2007; Sardar et al., 2005a). As can be deduced, OM is the dominant constituent of $PM_{0.25}$, accounting for close to half of its mass. SI and metals were next most abundant, contributing to quasi-UFP in similar amounts.

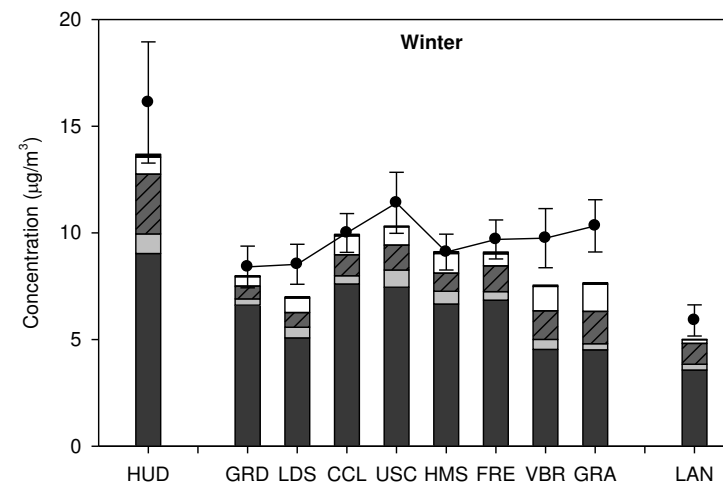
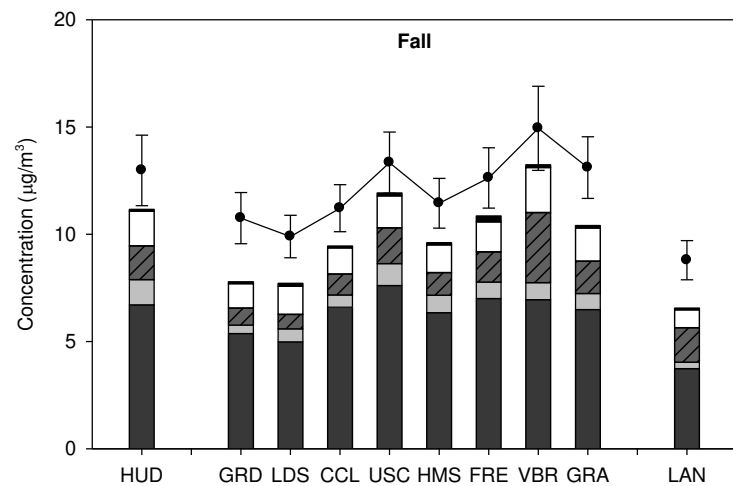
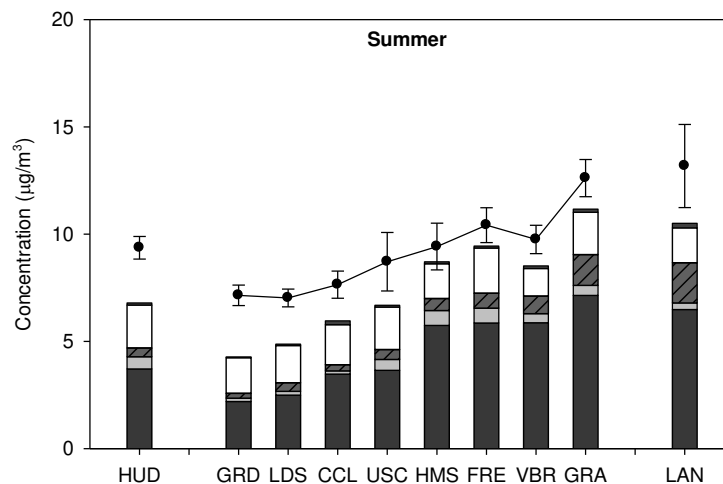
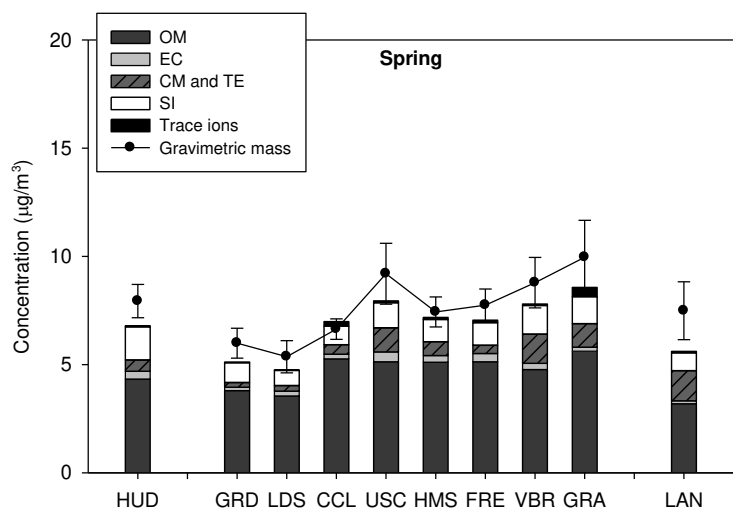


Figure 2.3a-d Chemical composition and gravimetric mass concentration of quasi-UFP ($dp < 0.25 \mu\text{m}$) by site in a) spring; b) summer, c) fall and d) winter. Error bars correspond to one standard error.

Table 2.3 Yearly-average (\pm standard error) percent fraction of quasi-UFP ($dp < 0.25 \mu\text{m}$) components.

	OM	EC	SO ₄ ²⁻	NO ₃ ⁻	NH ₄ ⁺	Trace ions	CM+TE
Long beach	52.6 \pm 5	6.4 \pm 0.8	8.6 \pm 1.3	0.5 \pm 0.1	5.4 \pm 1	0.8 \pm 0.1	10 \pm 1.7
Western LA	54.6 \pm 4	3.8 \pm 0.4	8.1 \pm 0.9	0.8 \pm 0.2	5.2 \pm 0.6	0.7 \pm 0.1	5.7 \pm 0.6
Central LA	58.9 \pm 2.8	5 \pm 0.5	7.8 \pm 1	1.7 \pm 0.3	4.7 \pm 0.6	1.3 \pm 0.3	8.6 \pm 0.9
Eastern LA	63.8 \pm 2.2	5.9 \pm 0.4	7.2 \pm 0.7	0.9 \pm 0.1	4.8 \pm 0.5	1.2 \pm 0.2	8.2 \pm 0.9
Riverside	51.4 \pm 1.5	4 \pm 0.3	5.4 \pm 0.6	3.8 \pm 0.6	4 \pm 0.3	1.3 \pm 0.3	13.4 \pm 1
Lancaster	48.9 \pm 3.1	3.1 \pm 0.4	5 \pm 0.9	1.3 \pm 0.2	2.6 \pm 0.5	0.9 \pm 0.1	16.8 \pm 1.6

The agreement between the gravimetric and reconstructed mass concentrations is overall good as indicated by the ratio of reconstructed to gravimetric mass, which respectively averaged 0.87 ± 0.02 , 0.80 ± 0.03 , 0.83 ± 0.02 and 0.88 ± 0.02 during spring, summer, fall and winter across all sites. These ratios are in the range of 23-40% and 6-45% of unidentified material, reported in other studies for PM_{0.1} and quasi-UFP in the LAB (Arhami et al., 2009; Hughes et al., 1998). This agreement between the two PM mass concentrations is further corroborated by applying a least squares linear regression to the average gravimetric and reconstructed mass concentrations of monthly samples from all sites, as displayed in Figure 2.4a-d. As can be seen, the coefficient of determination (R^2) and slope respectively spanned a range of 0.71-0.82 and 0.77-1.01 across the seasons, indicating a good agreement between the two mass concentrations. This agreement, however, exhibited a seasonal dependence, with a higher fraction of undetermined particulate mass observed during the warm summer season in consistence with other studies (Ho et al., 2006; Hueglin et al., 2005; Sardar et al., 2005a). This fraction, which was highest at the coastal (27-40%) and inland LAN (20%) sites, could be primarily associated with the uncertainty in the OC multiplication factor. As aforementioned, a factor of 1.8 is used for all sites and seasons in this study. Nevertheless, this factor may vary with location, season and time of day (Turpin and Lim, 2001). Applying the same multiplication factor for all sites and seasons may introduce some uncertainty in the estimation of the organic mass. OM may be underestimated in summer, when the aerosol is composed of photochemically-processed and advected particles. Secondary

organic aerosol (SOA) constituents are more oxygenated and polar than primary aerosol components, resulting in an increase in the average organic molecular weight to carbon weight ratio (MWt/C Wt) (Turpin and Lim, 2001). Furthermore, as the aerosol ages during air mass transit, its composition may be altered due to the addition of semi-volatile products of photochemical reactions, leading also to an increase in MWt/C Wt (Turpin and Lim, 2001). In addition, the fraction of unaccounted mass could also be related to uncertainties in the multiplication factors used to convert metals to oxides and un-estimated aerosol-bound water, especially for the coastal sites.

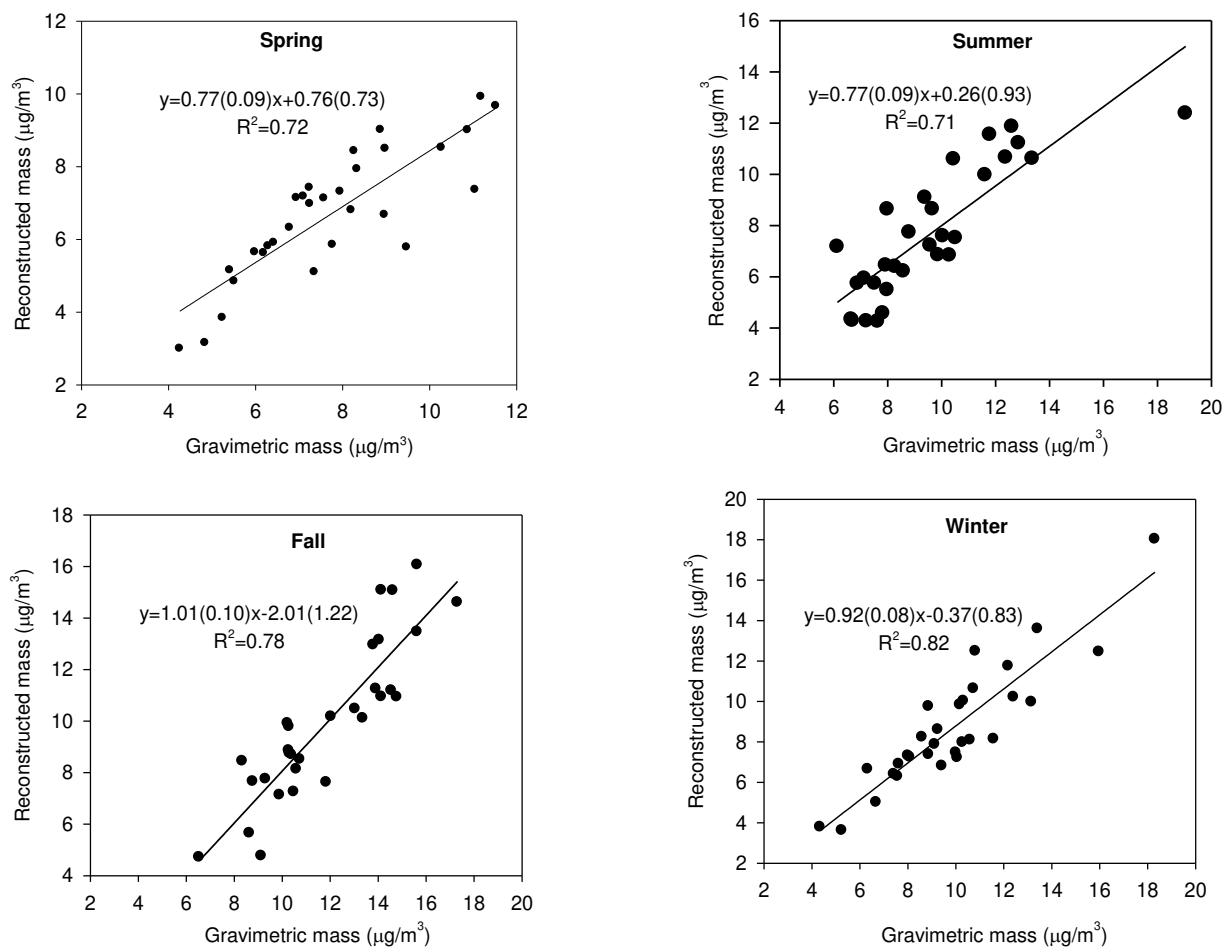


Figure 2.4a-d Linear regression plot of monthly reconstructed and gravimetric mass concentrations in a) spring, b) summer, c) fall and d) winter.

2.4.3 Chemical Composition

2.4.3.1 Carbonaceous Species

Elemental Carbon. EC, a key tracer of diesel exhaust (Schauer, 2003), was a minor constituent of PM_{0.25}, accounting for 3-6.4% of its mass with levels ranging from 0.13 to 1.17 µg/m³ across the seasons and basin, as displayed in Table 2.3 and Figure 2.5a-d. EC levels and contribution to quasi-UFP (~3%) were generally lowest at remote LAN site, which is 2 km away from the nearest freeway. Low levels were also measured at community-based (away from freeway) GRD and CCL sites as well as coastal LDS, particularly in spring/summer when values were mostly close or below the detection limit. In contrast, the largest EC contribution (6.4±0.8%) to PM_{0.25} occurred at source site HUD due to its close proximity to freeways with high volume of HDDV in port service (Moore et al., 2009; Pakbin et al., 2010). Accordingly, HUD exhibited highest EC concentrations across the basin during fall (1.17±0.16 µg/m³) and winter (0.92±0.18 µg/m³), when emissions from local primary sources dominate. Fall- and winter-time EC levels were next most dominant at USC in central LA (1.02±0.16 and 0.82±0.12 µg/m³, respectively) followed by HMS in eastern LA (0.81±0.12 and 0.60±0.13 µg/m³, respectively). These sites are located in close-to-modest proximity (within 150-800 m) to heavily-trafficked freeways. In urban LA and Long Beach, EC concentrations were highest during stagnant fall or also winter seasons compared to warmer summer and spring. Similarly, EC concentration peaked in fall at Riverside. However, notable is that comparable/greater EC levels were measured in summer compared to winter at receptor VBR/GRA sites. Given the greater atmospheric dilution of primary emissions in summer, these higher summertime concentrations of primary species such as EC are mainly attributed to the increased advection of air parcels from upwind sources in the western part of the basin.

Lastly, it is noteworthy that EC concentrations significantly declined compared to earlier studies in this basin. Current $PM_{0.25}$ -EC levels at Riverside are about 15 and 54% lower than those reported by Fine et al. (2004a) in $PM_{0.18}$ during summer and winter, respectively. Additionally, quasi-ultrafine EC levels at USC and Long Beach are 30 and 48% lower than those reported by Minguillón et al. (2008) during March-May, respectively. These reductions in EC concentration reflect improved diesel engine emission controls and the effectiveness of the Clean Trucks Program of Long Beach and Los Angeles ports (San Pedro Bay Ports Clean Air Action Plan).

Organic Matter. OM was the predominant component in quasi-UFP throughout the seasons, accounting for 49-64% of its mass on a yearly-average basis, as presented in Table 2.3. Remote LAN site exhibited the lowest fraction while central (CCL, USC) and eastern LA sites (FRE, HMS) displayed the greatest proportions. The high fractions possibly reflect contributions from vehicular emissions, which constitute a major source of ultrafine particles in urban areas of LA (Sardar et al., 2005a).

OM can be directly emitted from primary sources, such as fossil fuel combustion, or produced in the atmosphere via SOA formation processes (Turpin and Lim, 2001). To evaluate the extent of primary and secondary contributions to OM, the seasonal variation of OC and OC/EC ratio were investigated as illustrated in Figure 2.5a-d and Table 2.4 at each of the sampling sites. EC, which predominantly originates from combustion processes, is used as a tracer of primary combustion-generated OC (Turpin and Lim, 2001). OC concentrations were higher in fall and winter compared to spring and summer at all locations, with the exception of Riverside (VBR, GRA) and LAN where noticeable peaks were apparent in summer. With the exception of GRD and CCL, where EC levels were mostly close to the detection limit, the elevated winter- and fall-time concentrations were overall accompanied by low OC/EC ratios

compared to spring or summer. These ratios, however, exceeded those commonly reported for urban areas (Castro et al., 1999; Turpin et al., 1991), likely due to the very low EC levels relative to OC, particularly in winter. Nonetheless, the seasonality in OC/EC ratio and stronger OC-EC correlation in fall/winter (Table 2.4) indicate that OC is of predominately primary origin during fall and winter. The elevated fall- and winter-time OC concentrations can be attributed to atmospheric stability conditions and favored particle formation or growth by condensable organics freshly emitted from vehicles (Kim et al., 2002) as well as SOA formation driven by the low mixing height (Strader et al., 1999), to a much lesser extent. Wintertime OC concentration varied from ~ 2 to 5 $\mu\text{g}/\text{m}^3$ across the basin, with greater levels measured in the urban areas where local primary sources are more abundant than inland. In particular, wintertime OC concentrations were greatest at source site HUD and central USC, highlighting the importance of primary combustion emissions at these near-freeway sites. Conversely, OC levels were highest at receptor Riverside (VBR, GRA) and LAN sites in summer, averaging 3.3-4 $\mu\text{g}/\text{m}^3$. These levels, which followed a similar pattern to mass and exceeded wintertime concentrations, can be attributed to a combination of increased PM advection and SOA formation in summer, as documented in previous studies (Kim et al., 2002; Pandis et al., 1992). SOA production at these locations, enhanced by the accumulation of organic gases in the advected air parcel during transit from coast to inland (Pandis et al., 1992), is supported by the significant summertime increase in OC/EC ratio, which varied from 5.9-9.4 in fall/winter to 8.4-14.6 in summer at these locations, as well as low OC-EC correlations ($R=0.36-0.41$). Moreover, excluding CCL and GRD where EC levels were close to the detection limit in spring/summer, OC/EC ratios were greatest at the semi-rural/rural areas (VBR, GRA, LAN) compared to the urban sites, reflecting the importance of SOA formation at these inland locations.

Table 2.4 Average ratio (\pm standard error) of organic carbon (OC) to elemental carbon (EC) and Pearson correlation coefficient between OC and EC at the 10 sampling sites. Missing value indicates that EC concentrations were mostly below detection limit.

		Long Beach	Western LA		Central LA		Eastern LA		Riverside		Lancaster
		HUD	GRD	LDS	CCL	USC	HMS	FRE	VBR	GRA	LAN
OC/EC	Spring	9.9 \pm 2.6	14.7 \pm 2.2	10.1 \pm 1	16.3 \pm 2.2	8.8 \pm 2.4	13.7 \pm 2.8	11.7 \pm 3.1	13.5 \pm 2.8	19.9 \pm 3.2	14 \pm 1.5
	Summer	4.1 \pm 0.5	9.1 \pm 0.9	9.3 \pm 1	15.5 \pm 1.3	4.9 \pm 1	6.6 \pm 1.9	5.1 \pm 0.8	8.4 \pm 0.9	10 \pm 1.9	14.6 \pm 1.9
	Fall	3.9 \pm 0.8	7.9 \pm 0.9	5.6 \pm 0.7	7.9 \pm 1.6	4.4 \pm 0.4	5.3 \pm 0.8	4.9 \pm 0.4	5.9 \pm 0.8	5.1 \pm 0.4	9.4 \pm 1.5
	Winter	6.9 \pm 1.3	19.6 \pm 4.6	5.9 \pm 0.7	15.9 \pm 4.3	5.3 \pm 0.4	5.7 \pm 0.8	5.9 \pm 1	5.8 \pm 0.8	8.2 \pm 1.6	9.8 \pm 2.3
R(OC-EC)	Spring/summer	0.44	-	-	-	0.34	0.37	0.43	0.36	0.41	-
	Fall/winter	0.54	0.25	0.71	0.72	0.78	0.77	0.53	0.80	0.56	0.44

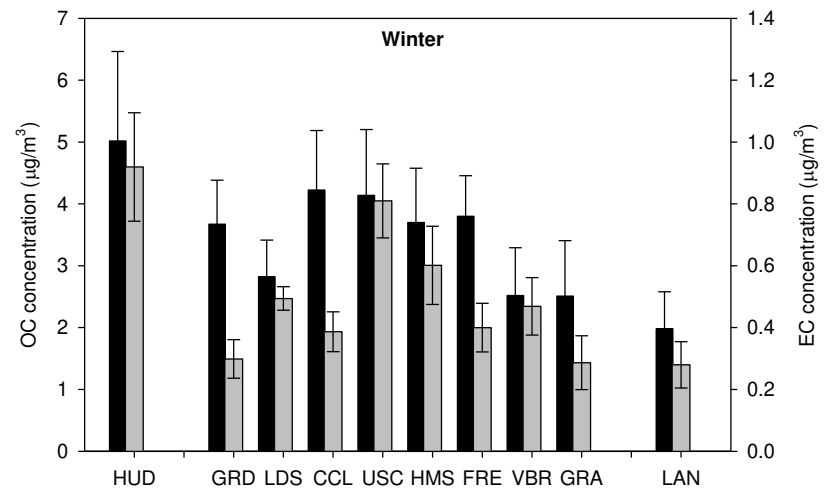
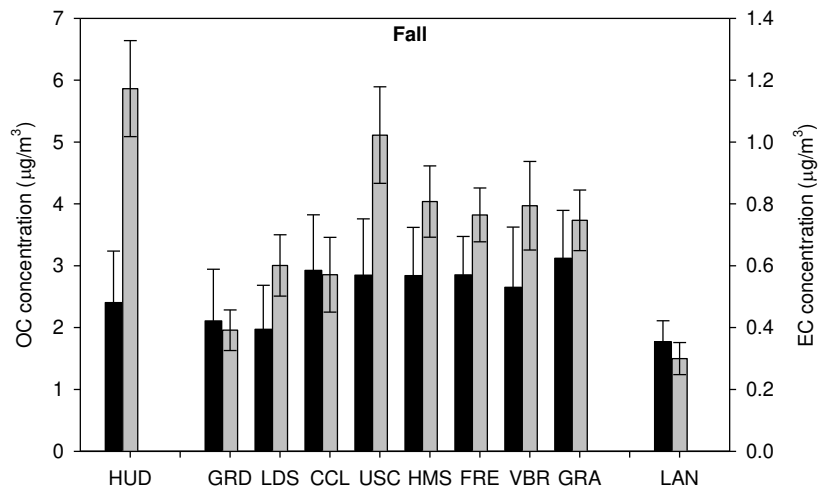
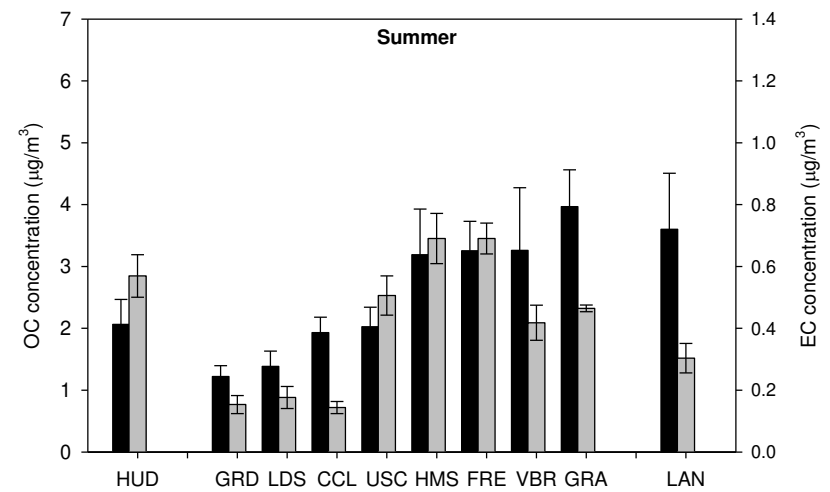
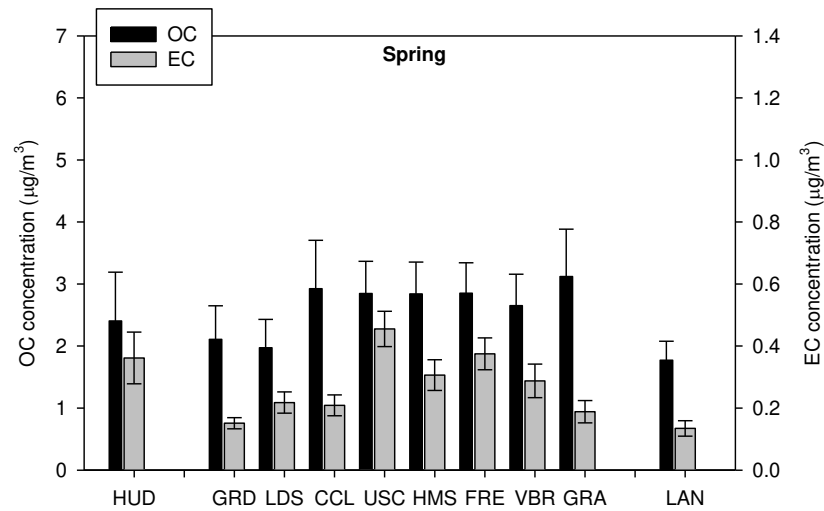


Figure 2.5a-d Average concentration of organic carbon (OC) and elemental carbon (EC) in quasi-UFP ($d_p < 0.25 \mu\text{m}$) by site in a) spring, b) summer, c) fall and d) winter. Error bars correspond to one standard error.

2.4.3.2 Secondary Ions

Figure 2.6a-d shows mean seasonal concentrations of secondary ions (SI), nitrate, sulfate and ammonium, at the sampling sites. These ionic species are mostly secondary aerosol components formed from the reaction of ammonia with nitric acid and sulfuric acid, as indicated by previous studies conducted in the LAB (Hughes et al., 2000; Hughes et al., 2002). Sulfate was mostly prevalent among SI, accounting for 13.3-67.1% of their mass. It exhibited a similar trend at all monitoring sites, displaying wintertime minima while summertime peaks due to increased photochemical activity. Sulfate also lacked an obvious spatial trend during the seasons, with the exception of winter. In winter, when emissions from local primary sources prevail, sulfate concentrations were lowest at Riverside (VBR, GRA) and LAN sites, likely because sources of sulfate or its sulfur dioxide precursor (e.g. fuel combustion, ship emissions) are less abundant inland compared to upwind urban LA and Long Beach areas (Mysliwiec and Kleeman, 2002). Contrary to sulfate, nitrate concentration varied from maxima in winter and fall to minimum or non-detectable amounts in summer and spring. The higher temperature in summer and spring seasons favors the dissociation of particulate ammonium nitrate (Mozurkewich, 1993). Spatially, nitrate showed a strong variability across the basin, reaching generally highest concentrations and contributions to $PM_{0.25}$ (~4% on a yearly-average basis) in Riverside, in agreement with previous studies (Cass et al., 2000; Sardar et al., 2005b). In the remaining areas, nitrate nominally contributed to quasi-UFP, accounting for 0.5-1.7% of its mass. VBR and GRA in Riverside are immediately downwind of local agricultural and Chino dairy farms, which constitute major ammonia sources (Geller et al., 2004; Hughes et al., 1999). These high ammonia emissions favor ammonium nitrate formation by reaction with nitric acid, even in warm summer. As the air parcel originating from the western part of the basin is advected inland, nitric acid

accumulated in the parcel encounters these elevated ammonia levels, resulting in large production of ammonium nitrate (Allen et al., 2000; Geller et al., 2002). Ammonium was the predominant cation in quasi-UFP. Similarly to sulfate, the concentration of ammonium was highest in summer across the basin, possibly because of the greater availability of gaseous sulfuric acid, which forms primarily from photochemically initiated reactions. Its spatial variability was mostly noticeable in winter, when ammonium levels were greater in Riverside, peaking at $0.48 \pm 0.15 \mu\text{g}/\text{m}^3$ at GRA, due to the greater ammonia source strength in this area.

In addition, an ion balance was conducted by determining concentration ratios (in charge equivalents) of the amount of measured ammonium to the amount of ammonium required to fully neutralize measured sulfate and nitrate, as plotted in Figure 2.7a-d for all sampling sites on a seasonal-average basis. A value of 1 suggests that sulfate and nitrate are fully neutralized by ammonium in the form of ammonium nitrate and ammonium sulfate. A value below 1 implies that particles are partially acidic, mostly in the form of ammonium bisulfate (Zhang et al., 2004). As can be inferred, ammonium is generally present in sufficient amounts to fully neutralize sulfate and nitrate, with some values exceeding 1. The latter indicate the presence of excess ammonium, possibly bound to organic acids (Dinar et al., 2008). With the exception of GRA and LAN, lower ionic ratios were observed in fall and winter than spring and summer at the sampling sites. This trend implies a lesser amount of excess ammonium in fall and winter, consistent with an increased formation of ammonium nitrate during cooler periods. Furthermore, ratios in fall and summer were overall lower at the semi-rural/rural inland locations (VBR, GRA, LAN) than urban areas, with ratios dropping below unity at VBR (0.79 ± 0.21) and LAN (0.93 ± 0.16) in fall and summer, respectively. These results indicate a somewhat lower degree of neutralization at these inland receptor sites and a slightly acidic aerosol at VBR and LAN, possibly due to long-

range transport of gaseous acidic precursors. In contrast, ratios were highest at semi-rural GRA in winter, when PM advection is limited, which can be attributed to the greater ammonia emissions in this area, resulting in increased aerosol neutralization. On the other hand, wintertime ratios were lowest and approaching unity at source site HUD in Long Beach and urban central USC in winter, implying a lesser degree of neutralization likely due to their close proximity to heavily-trafficked freeways. It is possible that ammonia cannot fully access sulfuric acid because of organic coatings on the sulfate core or sulfate could be interacting with EC, as argued in previous investigations at USC site (Ning et al., 2007). Thus, ammonia preferentially reacts with larger size accumulation mode particles (Ning et al., 2007).

2.4.3.3 Metals and Elements

The contribution of total metals (CM and TE) to quasi-UFP varied from a low of $5.7\pm 0.6\%$ in Western LA to a high of 13.4 ± 1 and $16.8\pm 1.6\%$ in Riverside and Lancaster, on a yearly-average basis. The greater fractions at the inland areas, which are largely comprised of CM, could be associated with their semi-rural/rural nature. TE were the least abundant species in quasi-ultrafine particles, accounting for $< 1\%$ of $PM_{0.25}$ on a yearly basis. Nonetheless, several of these trace metals (e.g. Cu, Cr) are toxicologically relevant (Becker, 2005). The metals' temporal variation was investigated by examining the concentration of select potentially toxic elements, as shown in Figure 2.8a-d on a seasonal-average basis. Clusters comprised Long Beach (HUD), LA (GRD, LDS, CCL, USC, FRE, HMS), Riverside (VBR, GRA) and Lancaster (LAN). Potential sources of trace elements and metals in quasi-UFP are addressed in detail by Saffari et al. (2013b). Five groups, accounting for about 85% of the total variance of quasi-ultrafine elemental content, were identified using principal component analysis (PCA).

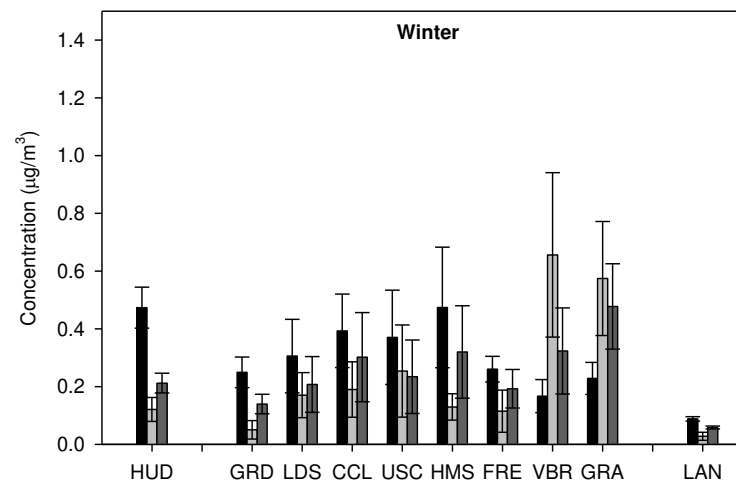
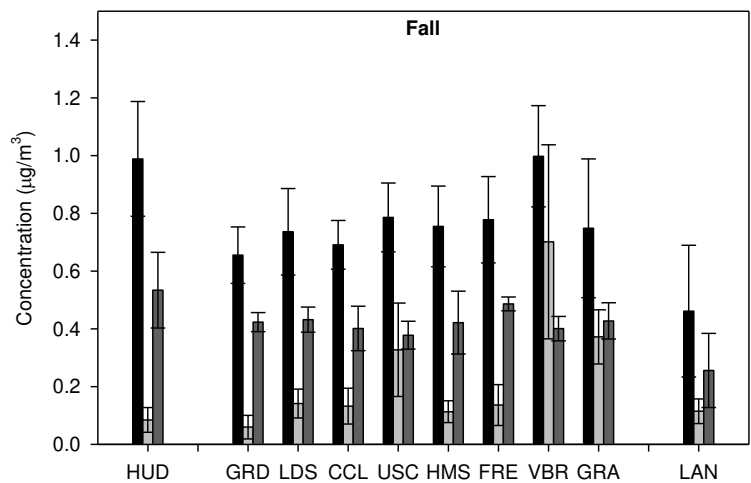
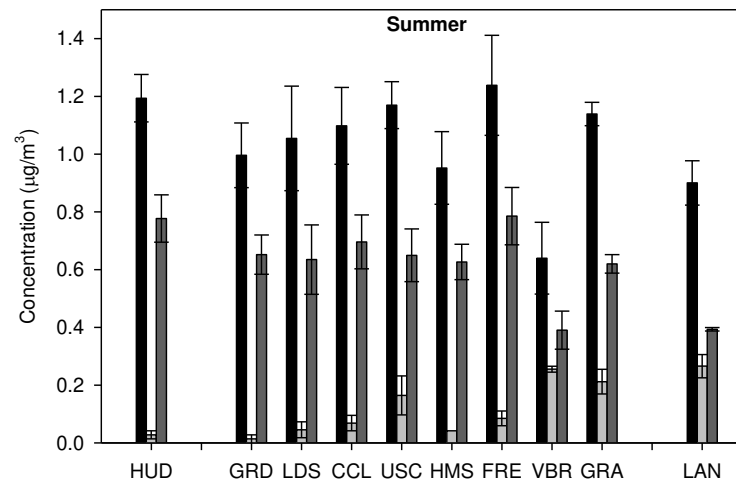
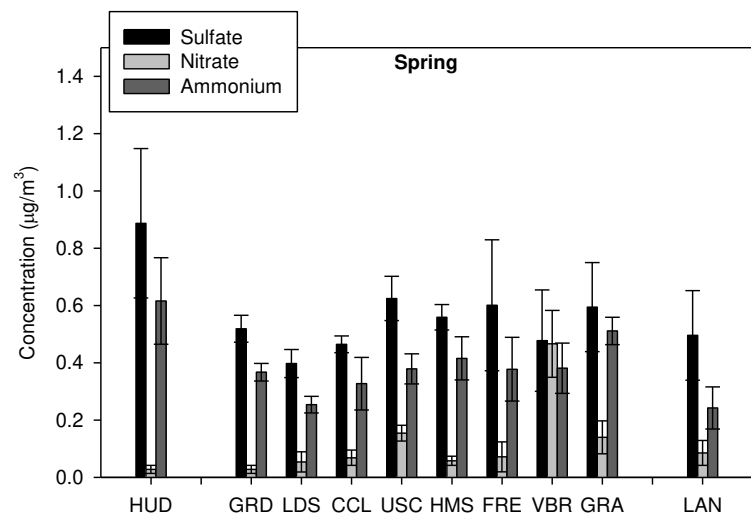


Figure 2.6a-d Average concentration of sulfate, nitrate and ammonium in quasi-UFP ($dp < 0.25 \mu\text{m}$) by site in a) spring, b) summer, c) fall and d) winter. Error bars correspond to one standard error.

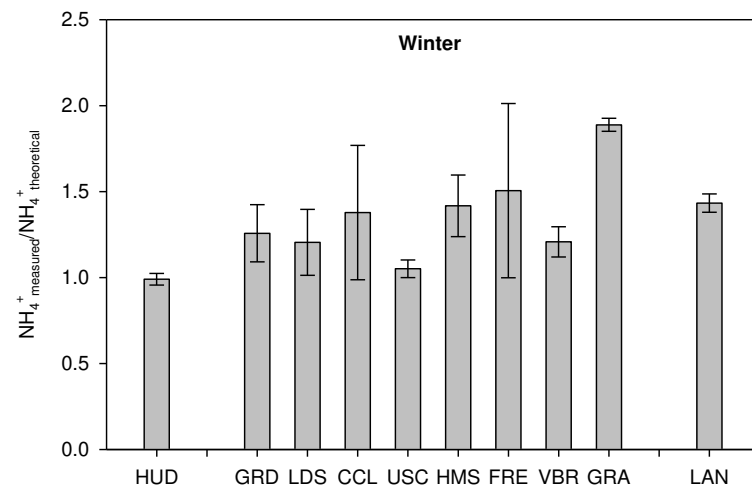
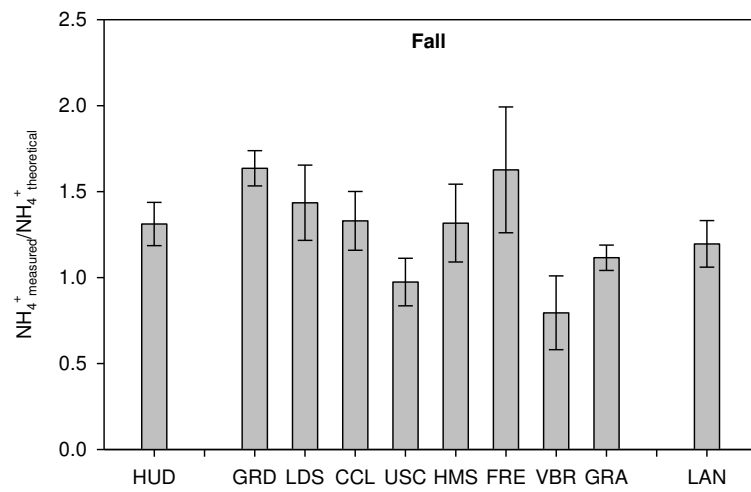
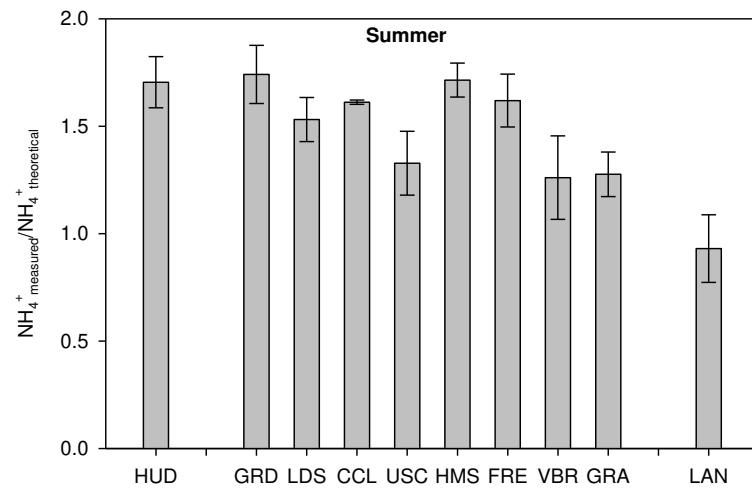
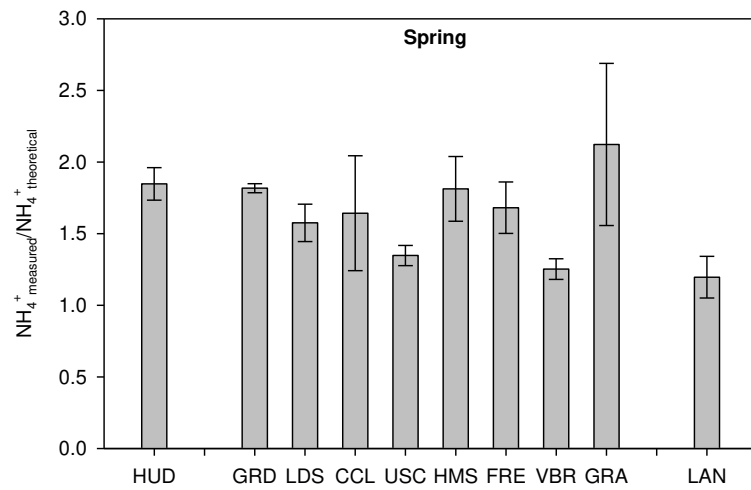


Figure 2.7a-d. Average molar concentration ratio of measured ammonium to theoretical ammonium required for complete neutralization of nitrate and sulfate ions in a) spring, b) summer, c) fall and d) winter. Error bars represent one standard error.

As can be inferred, S and Fe, followed by Zn, V and Cu, were predominant across all sites and seasons. V and S were mostly prevalent at Long Beach during all seasons, with their concentration gradually decaying from coast to inland. These species are associated with residual oil combustion (Saffari et al., 2013b), with bunker-fuel combustion from ship emissions from the ports of LA and Long Beach as a likely source (Isakson et al., 2001; Lu et al., 2006). These results are in agreement with findings of Arhami et al. (2009). Moreover, it should be noted that S reached peak concentrations in summer at all sites, possibly indicating its mixed primary and secondary origin as suggested by its significant correlation with ammonium and sulfate ($R > 0.60$). At Long Beach, Ni was highly correlated with V ($R = 0.72$) while less associated with Cr ($R = 0.62$), suggesting fuel oil combustion from marine vessels as its main source in this area (Arhami et al., 2009). On the other hand, at the remaining sites, Ni was more significantly associated with Cr ($R = 0.84-0.96$) and displayed overall higher concentrations at either Riverside or urban LA, suggesting industrial emissions, particularly metal plating (Pakkanen et al., 2001; Saffari et al., 2013b), as contributing sources. In winter, when emissions from local primary sources are dominant due to atmospheric stagnation conditions, Fe, Zn, Cu, Ba, Mn, Co and As were mostly abundant at the mixed industrial/residential Long Beach site, followed by urban LA then inland Riverside and Lancaster sites. Conversely, these species presented peak concentrations at Riverside or also Lancaster in spring and summer, a likely result of increased eastward PM advection. As the air parcel travels eastwards in the LAB, it passes over highly polluted areas where a multitude of local vehicular sources contribute to their concentrations (Singh et al., 2002). Saffari et al. (2013b) attributed Fe, Mn and Co to road dust, possibly enriched with vehicular-related elements from sources such as lubricating/motor oil (Ntziachristos et al., 2007b) or tire wear (Dahl et al., 2006). Road dust emissions may include

sub-micrometer particles originating from tire-pavement interactions, with a mean particle number diameter around 15-50 nm (Dahl et al., 2006; Gustafsson, 2008). Remaining elements, Zn, Cu, Ba and As, were associated with vehicular abrasion, with brake abrasion (Garg et al., 2000; Sanders et al., 2003) and tire attrition (Singh et al., 2002) as likely sources. Earlier investigations near freeways and major roadways demonstrated that a significant fraction of these elements exist in the sub-200 nm range (Lin et al., 2005; Ntziachristos et al., 2007b; Singh et al., 2002). Moreover, Sanders et al. (2003) showed, using dynamometer experiments, that brake wear particles can be found in the ultrafine size range. Pb and Cd varied from a high at Long Beach to a low at desert-like LAN in winter/fall, with Pb existing in comparable amounts at Riverside and urban LA, indicating strong local sources. Saffari et al. (2013b) associated these elements, mainly Cd, with cadmium emissions. Sources included, but were not limited to, exhaust emissions, plastic production (Hasselriis and Licata, 1996), phosphate fertilizers use and industrial metallurgical activities (Thomaidis et al., 2003), with vehicular emissions dominating at the urban sites while the remaining sources prevailing at the receptor locations (Saffari et al., 2013b). In summer and spring, the concentration of Pb and Cd peaked at Riverside or also Lancaster, likely due to long-range PM transport from upwind urban areas.

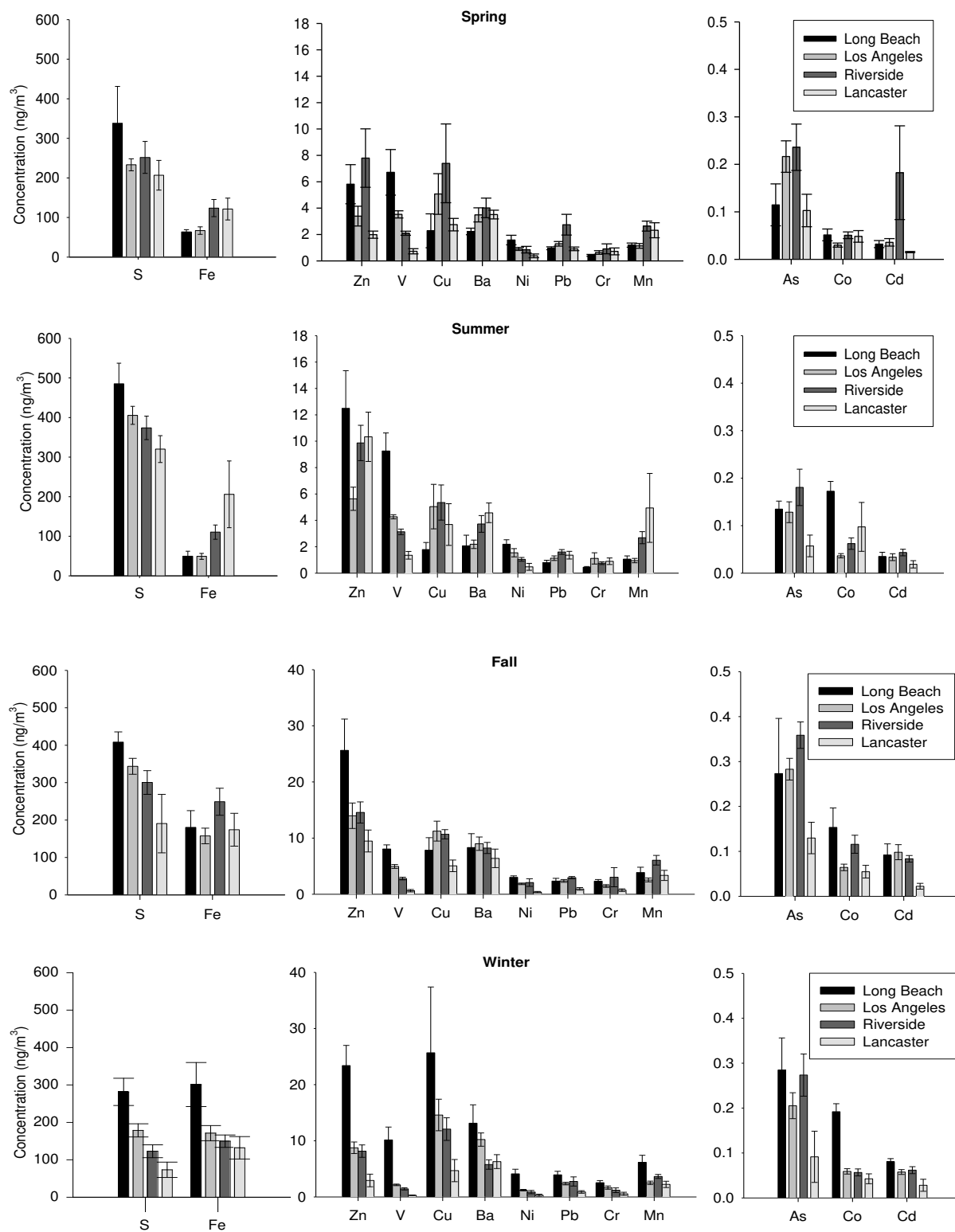


Figure 2.8a-d Average concentration of total metals and elements in quasi-UFP ($dp < 0.25 \mu\text{m}$) by sites' cluster in a) spring, b) summer, c) fall and d) winter. Error bars represent one standard error.

2.4.4 Spatial Variability

To determine the spatial variation of $PM_{0.25}$ in the Los Angeles basin, coefficients of divergence (COD) were calculated between sites' pairs for quasi-UFP mass and its main components. COD provides information on the degree of uniformity between sites, necessary to determine the density of monitoring networks required to accurately assess personal exposure to PM in large metropolitan areas. The COD for a given site pair is defined as follows:

$$COD_{fn} = \sqrt{\frac{1}{n} \sum_{i=1}^n \left(\frac{x_{if} - x_{ih}}{x_{if} + x_{ih}} \right)^2} \quad (2.2)$$

where x_{if} is the i^{th} concentration measured at site f , f and h are two different sites and n is the number of observations.

The COD for paired sites can vary from 0 to 1, with a value of 0 indicating that concentrations are identical at both sites and a COD of 1 implying that concentrations are highly different. In general, small COD values (< 0.2) suggest homogeneity between sites, whereas COD values greater than 0.2 indicate heterogeneity (Wilson et al., 2005). The CODs were estimated between site pairs using monthly concentrations, as illustrated in Figure 2.9.

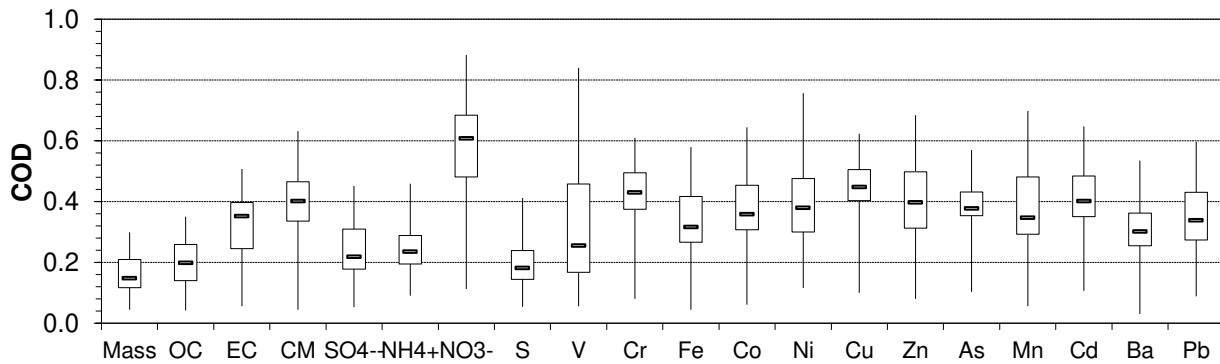


Figure 2.9 Coefficient of divergence (COD) between sites pairs across the year. Box plots show the minimum, first quartile, median, third quartile and maximum observed values.

Overall, findings showed a fairly homogeneous spatial variability for quasi-UFP mass but heterogeneous distribution for some of its components, mainly EC, CM, select toxic metals and

nitrate. These results imply that differences in source contributions may account for the divergence observed for some of $PM_{0.25}$ species. The low median COD value (0.15) and narrow interquartile range (of the order of 0.1 units) for mass indicate its relatively spatial homogeneity throughout the year. The prevalence of similar local sources at most of the sampling locations, namely vehicular emissions, as well as regional PM transport across the basin contribute to this limited variability among sites. The maximum observed COD of 0.30 is associated with sites' pairs including the distinct desert-like LAN site. Accordingly, the median COD for OC, largest contributor to quasi-UFP, equaled 0.20, indicating its moderately homogeneous spatial distribution. OC is attributed to primary combustion sources and SOA formation processes. The latter are regional in nature, resulting in a homogenous dispersion of OC (Turner and Allen, 2008). On the other hand, high heterogeneity is observed for EC, which displayed a median COD of 0.35. This disparity among sites can be related to their varying proximity to freeways and dissimilar HDDV traffic density. Similarly, CM and specific toxic metals were unevenly distributed, in agreement with their unequal abundance at the urban and inland sites, as discussed earlier. A great heterogeneity (median $COD > 0.3$) is observed for elements of industrial emissions (Cr, Cd, Pb) and road dust/vehicular emissions (Fe, Zn, Cu, Ba, Mn, Co, As) because their concentration heavily depends on their proximity to sources and traffic patterns. V, an element of bunker-fuel combustion from marine vessels, also exhibited an uneven distribution in accordance with its decreasing concentration from coast to inland. Similarly, a strong heterogeneity was noted for Ni, which originated from oil combustion at Long Beach whereas industrial sources at the remaining sites, as argued earlier. S, on the other hand, was relatively homogenous across the basin (median $COD = 0.18$), consistent with its partly secondary origin. Moreover, a very strong variability is observed for nitrate throughout the year (median $COD =$

0.61), which can be largely associated with differences in the source strength of its precursor gases at the sites, particularly Riverside. Contrarily, sulfate and ammonium displayed a modest heterogeneity (median COD=0.22, 0.23) but high maxima (>0.45). The latter were driven by the low wintertime levels at remote LAN, due to its distinct meteorology and lack of acidic gaseous precursors.

These results suggest that the variability in some of quasi-UFP chemical constituents on “inter-community” scales in the LAB may lead to considerably variable population exposure to quasi-ultrafine particles in this basin. It is, however, important to acknowledge that these results are based on 24-hour time-integrated data and do not reflect the spatial distribution in quasi-UFP over finer time scales. Previous studies conducted in eastern and source regions of the LAB examined the spatial variability in particle number concentrations on diurnal scales, using hourly CODs (Hudda et al., 2010; Krudysz et al., 2009). Their findings showed greater spatial heterogeneity during morning commute and late evening hours. Such variability, which is relevant to acute exposures, may not be fully captured by this time-integrated approach.

2.5 Summary and Conclusions

To provide insight on the spatial variability in chemical composition of quasi-UFP, a year-long sampling campaign was conducted at 10 distinct areas in the Los Angeles basin. Chemical mass closure showed that the composition of $PM_{0.25}$ is in the range of 49-64% OM, 3-6.4% EC, 9-15% SI, 0.7-1.3% trace ions, and 5.7-17% CM and TE, on a yearly-average basis. Quasi-UFP, which mostly consisted of OC, varied from 5.9 to 16.1 $\mu\text{g}/\text{m}^3$ across the sites and seasons. In winter, mass and OC levels were higher in the urban areas, specifically at source site HUD, where local primary sources are more abundant than inland. These elevated concentrations can be attributed to atmospheric stability conditions and favored particle formation by condensable

organic vapors. Conversely, summertime levels peaked at inland Riverside and LAN sites due to increased SOA formation and $PM_{0.25}$ advection from upwind polluted urban areas. EC levels were highest at HUD due to its proximity to freeways with a large fleet of HDDV while minimal at the community-based and desert-like sites. Among SI, sulfate and ammonium displayed summertime maxima due to increased photochemical activity. In contrast, nitrate levels dropped from a high in winter/fall to a low in summer/spring, reflecting the partitioning of ammonium nitrate to its gaseous precursors with increasing temperature. Furthermore, an ion balance revealed a generally neutral aerosol, with lesser degree of neutralization at near-freeway HUD and USC sites. Furthermore, toxic metals of anthropogenic origin overall peaked at urban LA and Long Beach sites in stagnant winter while receptor Riverside and Lancaster in summer. Lastly, inter-urban variability was investigated by calculating COD between sites' pairs. Results showed that while quasi-UFP mass is relatively spatially homogeneous in the basin, some of its chemical components, mainly EC, nitrate as well as CM and several toxic metals, were unevenly distributed.

In conclusion, findings of this study indicate that the composition and concentration of quasi-UFP are considerably affected by location and season. The spatial and temporal variability of quasi-ultrafine particles should thus be considered in the design of epidemiological studies in order to accurately assess population exposure to PM in complex urban air sheds, such as the megacity of Los Angeles.

2.6 Acknowledgements

This study was funded by the South Coast Air Quality Management District (SCAQMD) (award #11527). We wish to acknowledge the support of USC Provost's Ph.D. fellowship. We also

would like to thank the staff at the Wisconsin State Laboratory of Hygiene for their assistance with the chemical analyses.

Chapter 3 Chemical Composition of PM and its Relation to Sources: A Case Study of Ambient Fine and Coarse PM in Milan

*What are the major primary and secondary sources of $PM_{2.5}$ in the urban area of Milan?
What are their respective contributions to $PM_{2.5}$ mass?*

The composition of particulate matter (PM) at a given location is a function of sources and their relative strengths. A given urban area hosts a multitude of sources encompassing both primary (e.g. biomass burning, heavy- and light-duty vehicles) and secondary (e.g. biogenic- and anthropogenic-derived secondary organic aerosol (SOA)) sources. Reducing ambient PM concentrations, and associated toxicity, thus requires an understanding of PM chemical characteristics, major sources and their temporal fluctuations. In an effort to understand the association between PM composition and sources, necessary for regulatory decision making, fine ($d_p < 2.5 \mu\text{m}$) and coarse ($2.5 \mu\text{m} < d_p < 10 \mu\text{m}$) PM samples were collected for a year-long period at a centrally-located site in Milan. Milan provided a suitable setting to investigate this relationship since it is afflicted with high particle levels, frequently exceeding PM_{10} standards (Lonati et al., 2008). A molecular marker chemical mass balance (MM-CMB) model was applied to apportion primary sources to fine PM while contributions of secondary sources were evaluated using SOA tracers that are unique to their precursor gases. Results provide insights on particle sources in Milan. They also provide a comprehensive understanding of PM chemical composition and variability to complement an analysis of its $PM_{2.5}$ -associated redox activity (discussed in Chapter 5).

This chapter is based on the following publication:

Daher N., Ruprecht A., Invernizzi G., De Marco C., Miller-Schulze J., Heo J. B., Shafer M. M., Shelton B. R., Schauer J. J., Sioutas C., 2012. Characterization, Sources and Redox Activity of Fine and Coarse Particulate Matter in Milan, Italy. *Atmospheric Environment* 49, 130-141.

3.1 Introduction

The association between exposure to particulate matter (PM) and increased risk of adverse health outcomes is firmly established in epidemiological research (Peters, 2001; Pope, 2002). Milan, one of the largest cities in Italy, is afflicted with high particle levels, frequently exceeding PM_{10} standards (Lonati et al., 2008). It has also been classified as one of the most polluted areas in Western Europe (Putaud et al., 2004). The city is characterized by a highly dense population, a large fleet of vehicles and is located in the center of the Po valley, one of the most industrialized regions in Northern Italy with frequently occurring wintertime inversions. These conditions

contribute to elevated particle emission levels. Reducing the concentration and associated-toxicity of ambient PM in Milan therefore requires an accurate characterization of its composition and sources.

The chemical composition of PM in Milan has been quite extensively investigated (Marcazzan et al., 2001; Vecchi et al., 2004). However, its particle sources have been less explored and their characterization have been mostly based on PM elemental and ionic contents (D'Alessandro et al., 2003; Marcazzan et al., 2004; Marcazzan et al., 2001). In this study, we examine the chemical composition of fine ($PM_{2.5}$, $d_p < 2.5 \mu m$) and coarse PM ($PM_{10-2.5}$, $2.5 \mu m < d_p < 10 \mu m$) ($PM_{2.5}$ and $PM_{10-2.5}$, respectively) in addition to major $PM_{2.5}$ sources in Milan. $PM_{2.5}$ and $PM_{10-2.5}$ samples were collected for a year-long period. Samples were then analyzed for their detailed chemical composition. Following the chemical speciation, a molecular marker chemical mass balance (MM-CMB) model was applied to apportion primary and secondary sources to fine PM, using existing source profiles, mostly for the US. Unlike the findings of studies conducted in various cities around the world (Sheesley et al., 2004; Stone et al., 2010; Stone et al., 2008; Zheng et al., 2005), current results demonstrate that significant sources of water-insoluble organic carbon cannot be explained by traditional source profiles. Further work is therefore needed to establish source profiles characteristic of the Milan area for use in source apportionment. Results of this study provide additional insight on the composition, levels and sources of $PM_{2.5}$ and $PM_{10-2.5}$ in Milan to complement an analysis of its particle-associated redox activity (discussed in Chapter 5). Findings can be used to inform policy makers and ultimately implement more effective and source-specific regulatory strategies in this area.

3.2 Methodology

3.2.1 Sample Collection

Fine and coarse PM ($PM_{2.5}$ and $PM_{10-2.5}$, respectively) samples were collected at about 10 m above ground level in the outside area of Santa Maria Delle Grazie Church in the city center of Milan (+45° 27' 59.51", +9° 10' 14.26"). The sampling campaign lasted from December 2009 to November 2010. During this period, twenty-four-hour size-segregated PM samples were collected on a weekly basis by means of two SioutasTM Personal Cascade Impactor Samplers (SioutasTM PCIS, SKC Inc., Eighty Four, PA, USA (Misra et al., 2002). Each PCIS was operated at a flow rate of 9 lpm as well as loaded with 37 and 25 mm filters for $PM_{2.5}$ and $PM_{2.5-10}$ analyses, respectively. For the purpose of chemical speciation, one PCIS was loaded with Teflon filters (Pall Life Sciences, Ann Arbor, MI) while the other one with quartz microfiber filters (Whatman International Ltd, Maidstone, England). To determine PM mass concentration, the weekly Teflon filters were pre-weighed and post-weighed after equilibration, using a Mettler 5 Microbalance (Mettler Toledo Inc, Columbus, OH, USA) under controlled conditions (relative humidity of 40-45% and temperature of 22-24 °C).

3.2.2 Chemical Analyses

To conduct chemical analyses of the size-fractionated PM samples, the Teflon and quartz filters were sectioned into portions. The fractions used for elemental and organic carbon (EC and OC, respectively) determination were grouped into weekly samples and quantified using the NIOSH Thermal Optical Transmission method (Birch and Cary, 1996). All remaining sections were composited monthly and analyzed for water-soluble OC (WSOC), water-soluble inorganic ions (Cl^- , Na^+ , SO_4^{2-} , NH_4^+ , NO_3^- , K^+ , PO_4^{3-}), total metals and organics (for $PM_{2.5}$ only). WSOC and ionic contents of the samples were measured using a Sievers 900 Total Organic Carbon

Analyzer (Stone et al., 2009) and ion chromatography (IC), respectively. However, we should note that no ionic data is available for PM_{2.5-10} March sample because the sample vial broke during IC analysis. The total elemental mass of the filter fractions was measured by means of a high resolution magnetic sector Inductively Coupled Plasma Mass Spectrometry (Thermo-Finnigan Element 2) (Zhang et al., 2008a). A microwave-aided Teflon bomb digestion protocol using a mixture of 1 mL of 16 M nitric acid, 0.25 mL of 12 M hydrochloric acid, and 0.10 mL of hydrofluoric acid was used for this analysis. Moreover, organic speciation was conducted on PM_{2.5} filter composites using gas chromatography mass spectrometry (GC-6980, quadrupole MS-5973, Agilent Technologies). PM_{2.5-10} lacked sufficient mass for this analysis. Briefly, the quartz filter composites were spiked with isotopically-labeled standard solutions prior to extraction. Samples were then extracted by dichloromethane and acetone using Soxhlets, followed by rotary evaporation and reduction in volume under high-purity nitrogen. Extracts were analyzed twice by GC/MS after derivitization of carboxylic acids with diazomethane and after silylation of hydroxyl groups. Additional details can be found in Stone et al. (Stone et al., 2008).

3.2.3 Source Apportionment

Primary and secondary source contributions to monthly ambient fine OC were estimated using a molecular marker chemical mass balance model (MM-CMB). The model was mathematically solved with the US Environmental Protection Agency CMB (EPA-CMB8.2) software by applying the effective variance weighted least squares algorithm to apportion the receptor data to the source profiles (Watson, 1984).

Table 3.1a-b Average source contribution estimates (SCE) to ambient: a) fine organic carbon, b) PM_{2.5} in Milan and associated standard errors (SE). Statistically significant sources (> 2 × SE) are shown in bold. *uncertainty of analytical measurement

a)

Month	Monthly average source contribution estimate (SCE) and standard error (SE) in µg/m ³																			
	R ²	χ ²	Vegetative		Wood-smoke		Natural Gas		Diesel		Gasoline		Urban soil		Coal soot		Biogenic SOA		Toluene SOA	
			SCE	SE	SCE	SE	SCE	SE	SCE	SE	SCE	SE	SCE	SE	SCE	SE	SCE	SE	SCE	SE
Decembe	0.93	5.1	0.18	0.023	0.23	0.07	0.06	0.018	0.00	0.28	1.6	0.19	0.14	7.0e-03	0.27	0.042	0.012	0.006		
January	0.91	5.2	0.26	0.031	0.43	0.14	0.11	0.029	0.00	0.38	1.7	0.21	0.06	4.6e-03	0.36	0.054	0.17	0.041		
February	0.92	5.9	0.18	0.022	0.53	0.17	0.033	0.012	0.06	0.21	1.2	0.14	0.07	4.1e-03	0.21	0.032	0.067	0.020		
March	0.93	5.2	0.14	0.017	0.61	0.20	6.9e-03	4.8e-03	0.15	0.12	0.58	0.073	0.07	3.8e-03	0.080	0.014	0.074	0.026		
April	0.93	5.2	0.13	0.017	0.12	0.03	4.5e-03	3.0e-03	0.28	0.088	0.51	0.062	0.09	4.7e-03	0.032	0.086	0.048	0.020	0.07	0.03
May	0.92	5.4	0.12	0.015	0.09	0.02	0.00	1.7e-03	0.29	0.061	0.33	0.043	0.10	5.3e-03	8.5e-	5.1e-	0.078	0.024	0.17	0.06
June	0.95	3.7	0.094	0.012	0.14	0.04	9.5e-04	1.2e-03	0.26	0.072	0.20	0.026	0.11	5.4e-03			0.20	0.071	0.61	0.22
July	0.94	4.1	0.062	8.2e-03	0.06	0.02	4.5e-04	8.6e-04	0.21	0.045	0.08	0.014	0.11	5.5e-03			0.20	0.071	0.50	0.18
August	0.93	2.8	0.070	9.0e-03	0.06	0.02	0.00	8.0e-04	0.23	0.049	0.16	0.021	0.04	3.1e-03			0.39	0.13	0.39	0.14
Septembe	0.96	2.5	0.14	0.017	0.22	0.07	0.00	2.3e-03	0.32	0.094	0.54	0.058	0.04	2.5e-03			0.087	0.041	0.31	0.12
October	0.98	1.2	0.24	0.030	0.61	0.20	0.037	0.011	0.11	0.22	2.1	0.19	0.11	5.8e-03			0.053	0.026	0.38	0.14
Novembe	0.95	3.5	0.18	0.022	0.62	0.20	0.022	0.011	0.09	0.18	1.6	0.18	0.04	2.5e-03	0.18	0.030	0.054	0.014		

b)

Month	Monthly average source contribution estimate (SCE) and standard error (SE) in µg/m ³																							
	Vegetative		Wood-smoke		Natural gas		Diesel		Gasoline		Urban soil		Coal soot		Biogenic		Toluene		Nitrate		Sulfate		Ammonium	
	SC	SE	SCE	SE	SCE	SE	SC	SE	SC	SE	SC	SE	SCE	SE	SCE	SE	SC	SE	SC	SE*	SC	SE*	SC	SE*
Decembe	0.57	0.07	0.25	0.08	0.070	0.021	0.00	0.7	2.1	0.25	1.7	0.08	0.67	0.10	0.01	9.0e-			9.7	0.73	3.0	0.3	4.6	0.35
January	0.79	0.09	0.45	0.15	0.13	0.034	0.00	0.9	2.2	0.27	0.75	0.05	0.90	0.13	0.30	0.07			15	1.1	4.3	0.4	7.6	0.57
February	0.54	0.06	0.56	0.18	0.038	0.014	0.15	0.5	1.5	0.18	0.92	0.04	0.51	0.07	0.12	0.03			13	1.0	4.0	0.4	6.8	0.51
March	0.43	0.05	0.64	0.21	8.1e-03	5.7e-	0.37	0.3	0.75	0.09	0.90	0.04	0.20	0.03	0.12	0.03			10	0.78	2.9	0.2	4.5	0.34
April	0.42	0.05	0.12	0.04	5.3e-03	3.6e-	0.69	0.2	0.66	0.08	1.1	0.05	0.07	0.02	0.07	0.03	0.14	0.06	3.6	0.27	2.4	0.2	1.5	0.12
May	0.36	0.04	0.09	0.03	0.00	2.0e-	0.71	0.1	0.43	0.05	1.3	0.06	0.02	0.01	0.14	0.03	0.33	0.13	2.1	0.16	2.7	0.2	1.4	0.11
June	0.29	0.03	0.15	0.04	1.1e-03	1.4e-	0.64	0.1	0.26	0.03	1.3	0.06			0.32	0.10	1.2	0.44	0.91	0.06	2.8	0.2	1.3	0.09
July	0.19	0.02	0.06	0.02	5.3e-04	1.0e-	0.52	0.1	0.11	0.01	1.3	0.06			0.34	0.10	0.99	0.36	0.77	0.05	3.7	0.3	1.7	0.12
August	0.22	0.02	0.06	0.02	0.00	9.4e-	0.57	0.1	0.20	0.02	0.51	0.03			0.64	0.19	0.76	0.28	0.65	0.04	2.1	0.2	0.9	0.07
Septembe	0.44	0.05	0.23	0.07	0.00	2.7e-	0.79	0.2	0.69	0.07	0.56	0.03			0.12	0.05	0.62	0.23	3.0	0.22	1.7	0.1	1.6	0.12
October	0.75	0.09	0.64	0.21	0.044	0.013	0.26	0.5	2.7	0.25	1.4	0.06			0.07	0.03	0.75	0.27	11	0.80	2.8	0.2	4.9	0.37
Novembe	0.57	0.06	0.65	0.21	0.026	0.013	0.24	0.4	2.0	0.23	0.56	0.03	0.44	0.07	0.11	0.02			8.7	0.65	2.2	0.2	4.3	0.32

MM-CMB was conducted using molecular source tracers that were quantified in the fine PM samples. Molecular marker compounds that are chemically stable during transport from source to receptor were selected as fitting species (Schauer et al., 1996). These included levoglucosan, $\alpha\beta\beta$ -20R&S-C₂₇-cholestane, $\alpha\beta\beta$ -20R&S-C₂₉-sitostane, 17 α (H)-22,29,30-trisnorhopane, 17 α (H)-21 β (H)-hopane, 17 β (H)-21 α (H)-30-norhopane, benzo(b)fluoranthene, benzo(k)fluoranthene, indeno[c,d]pyrene, benzo(ghi)perylene, picene, EC, aluminum (Al), titanium (Ti), calcium (Ca) and n-alkanes C₂₉, C₃₁, and C₃₃. The model input source profiles were based on the observed primary markers and assumed representative of sources in Milan. These profiles included wood-smoke (Fine et al., 2004b; Sheesley, 2007), vegetative detritus (Rogge et al., 1993c), coal soot (Zhang et al., 2008b), natural gas (Rogge, 1993), urban soil (Rutter et al., 2011), diesel emissions and gasoline vehicles (Lough et al., 2007). The selected urban soil profile is not characteristic of the area of Milan. However, electing this profile is not crucial for the overall apportionment of fine OC, as it minorly contributes to total OC mass (Rutter et al., 2011). Its selection was nevertheless based on a comparison of the elemental ratios of the measured data to those of available soil profiles. The urban soil profile of St. Louis, Missouri (Rutter et al., 2011), provided the most adequate fit.

Contributions of secondary sources, biogenic- and toluene (anthropogenic)-derived secondary organic aerosol (SOA), were evaluated using SOA tracers that are unique to their precursor gases. Tracers for biogenic-derived SOA comprised α -pinene (3-hydroxyglutaric acid, pinic acid, 3-acetylhexanedioic acid, 2-hydroxy-4-isopropyladipic acid, pinonic acid), β -caryophyllene (β -caryophyllinic acid) and isoprene (2-methylthreitol, 2-methylerythritol) derivatives (Kleindienst et al., 2007). On the other hand, tracers for toluene-derived SOA only included toluene derivative (2,3-dihydroxy-4-oxopentanoic acid) (Kleindienst et al., 2007).

These secondary sources were, however, not included in the MM-CMB model. Their contributions were separately estimated using fixed tracer-to-OC ratios (Kleindienst et al., 2007).

MM-CMB model results were considered to have acceptable statistical fit if $R^2 \geq 0.91$ and $\chi^2 < 6$ (Table 3.1a). R^2 corresponds to the variance in ambient species concentrations explained by their calculated concentration. χ^2 represents the weighted sum of squares of the differences between calculated and measured fitting species concentrations.

3.3 Results and Discussion

3.3.1 Particulate Mass and Composition

To determine the bulk composition of ambient $PM_{2.5}$ and $PM_{10-2.5}$ in Milan, a chemical mass reconstruction was conducted on the monthly PM samples as shown in Figure 3.1a-b. PM chemical species were classified into organic matter (OM), elemental carbon (EC), crustal material (CM), sulfate, nitrate, ammonium, other ions (Cl^- , Na^+ , PO_4^{3-}) and trace elements (TE). As can be observed from the plots, ambient PM levels in Milan were dominated by $PM_{2.5}$ concentration, which ranged from $12.4 \mu g/m^3$ in August to $74.7 \mu g/m^3$ in January and averaged (\pm one standard deviation) $34.5 \pm 19.4 \mu g/m^3$ throughout the year. This yearly $PM_{2.5}$ average, which is in accordance with the $32.8 \mu g/m^3$ value reported by Lonati et al. (2005), exceeds the EU annual $PM_{2.5}$ mean limit of $25 \mu g/m^3$, set for 2015 (Council Directive 2008/50/EC). Higher $PM_{2.5}$ concentrations were recorded in cold months (October-March), while lower in warm months (April-September), consistent with a series of published data on PM pollution in this city (Lonati et al., 2005; Lonati et al., 2008; Marcazzan et al., 2001). The increase in cold months occurred when the concentration of OM and secondary ions (NH_4^+ , NO_3^- , SO_4^{2-}) was greatest, and can be mainly attributed to the typical meteorological conditions of the Po valley. The cold period is characterized by frequent and persistent thermal inversions which limit the dispersion of

pollutants in the atmosphere, while the warmer season is characterized by a deeper mixing layer which enhances the dispersion of pollutants (Giuliaci, 1988; Marcazzan et al., 2001). Conversely, $PM_{10-2.5}$ concentrations displayed less variability, reaching an annual average of $6.79 \pm 1.67 \mu\text{g}/\text{m}^3$ with peak concentrations in July and October, likely due to enhanced re-suspension favored by increased soil dryness as well as higher wind speeds.

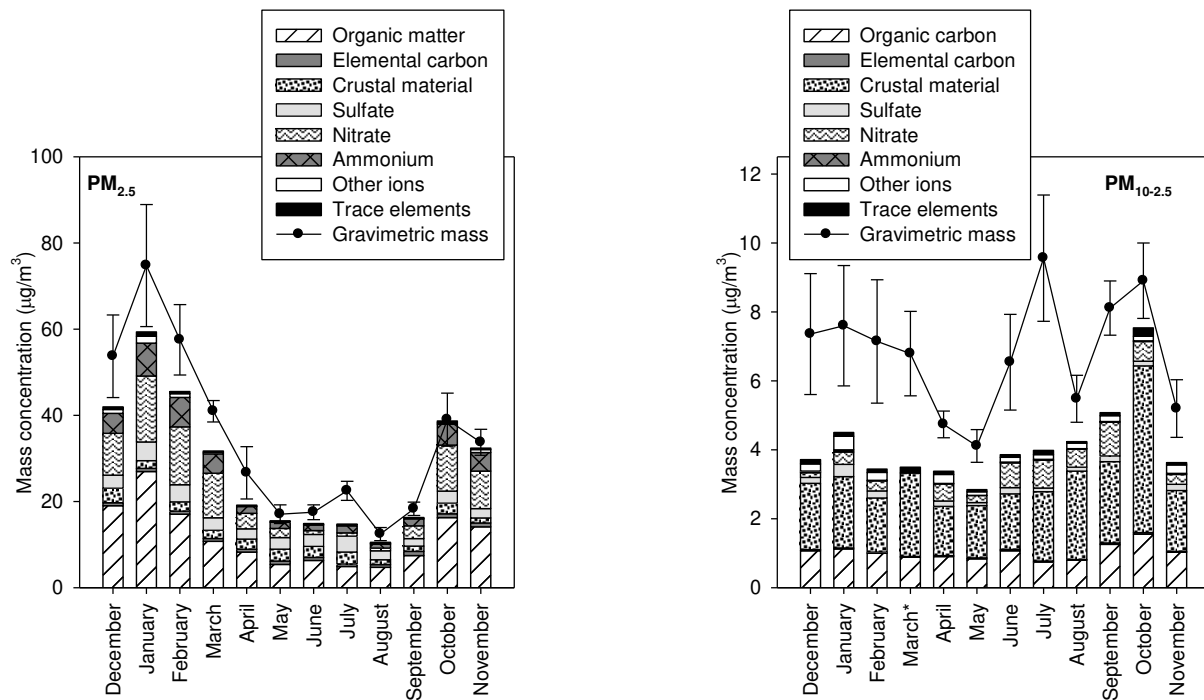


Figure 3.1a-b Monthly bulk composition and average gravimetric mass (standard error) of ambient a) $PM_{2.5}$ and b) $PM_{10-2.5}$ in Milan. * indicates coarse ions sample for March was lost during chemical analysis.

3.3.1.1 Crustal Material and Trace Elements

Yearly-average crustal enrichment factors (CEFs) were determined to assess the relative contributions of anthropogenic and natural sources to select elements, as displayed in Figure 3.2. For a given element, CEF was estimated as the ratio of its abundance in a PM sample to its average abundance in the upper continental crust (UCC) after normalization to Al, which is selected as a reference element. The UCC composition was retrieved from Taylor and McLennan (1985). Typically, elements with a CEF greater than 10 are considered to be mostly of

anthropogenic source, whereas elements with a CEF approaching 1 are of crustal origin (Birmili et al., 2006). A notably strong enrichment is observed for Cu, Zn, Pb, Mo, Sn, Sb and S in both size fractions (CEF > 100), indicating their anthropogenic origin. Potential sources of Cu, Zn, Pb, Mo, Sn and Sb include vehicular emissions and motor oil combustion (Lough et al., 2005; Singh et al., 2002) while S is predominantly of secondary origin, likely in the form of ammonium sulfate as indicated in previous studies conducted in Milan (Marcazzan et al., 2003; Marcazzan et al., 2001). These elements were also more enriched in the fine fraction. Similarly, elements including Ni, Cr, and Ba in both PM modes as well as PM_{2.5}-bound Mn were enriched but to a lesser extent, suggesting their mainly anthropogenic source such as oil combustion, vehicular emissions and industrial activities (Lough et al., 2005; Marcazzan et al., 2001; Singh et al., 2002). CEF for fine K also indicated a moderate enrichment, but was associated with a large standard deviation as it ranged from 2.4 in May to 27 in January, indicating the mixed crustal and anthropogenic origin of K. A potential source is wood combustion (Kim et al., 2003) for domestic heating, as suggested by its seasonal trend. On the other hand, CEFs slightly higher than unity were observed for coarse-PM K and Mn in addition to Ca, Fe, Na and Sr in both PM fractions, indicating a strong natural component for these elements. Moreover, CEFs of about unity were observed for Ti and Mg, which were equally enriched in both PM modes, implying their crustal origin.

The amount of CM in PM_{2.5} and PM_{2.5-10} was determined by summing the oxides of crustal metals, Al, K, Fe, Ca, Mg, Ti and Si, using the following equation (Chow et al., 1994; Hueglin et al., 2005; Marcazzan et al., 2001):

$$CM = 1.89Al + 1.21K + 1.43Fe + 1.4Ca + 1.66Mg + 1.7Ti + 2.14Si \quad (3.1)$$

Si concentration, which was not measured in this study, was estimated as $3.41 \times \text{Al}$ (Hueglin et al., 2005). Moreover, only the crustal component of fine K, approximated as the ratio of its measured concentration to its CEF, is included in CM estimation.

In the coarse mode, crustal elements were the dominant constituent of $\text{PM}_{10-2.5}$ accounting for about $32 \pm 10\%$ of its mass and exhibited generally higher concentrations during August and October as shown in Figure 3.1b and Table 3.2. This increase is likely due to re-suspension favored by the greater wind speeds as well as soil dryness during these months. In the fine mode, CM contribution to PM was lower, averaging $7.9 \pm 4.5\%$ of $\text{PM}_{2.5}$.

TE mainly comprised elements such as Cu, Zn, Cr, Ba, Pb, Ni in addition to non-crustal fine K, and marginally contributed to PM mass ($\sim 1.5\%$) in both size modes. These elements also displayed a similar trend, reaching generally higher concentrations (Table 3.2) during October-March while lower during the remaining months, due to better atmospheric dispersion.

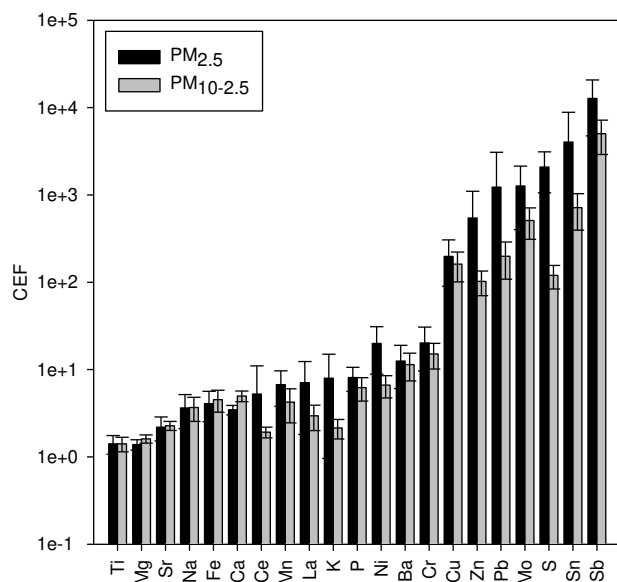


Figure 3.2 Yearly average (standard deviation) crustal enrichment factor (CEF) of select total elements in ambient $\text{PM}_{2.5}$ and $\text{PM}_{10-2.5}$ in Milan.

Table 3.2 Monthly concentration of total metals and elements in ambient PM_{2.5} and PM_{10-2.5} in Milan.

		Monthly concentration (ng/m ³)													
		Mg	Al	S	K	Ca	Ti	Cr	Mn	Fe	Ni	Cu	Zn	Ba	Pb
PM _{2.5}	December	71.2	209	1154	411	366	20.4	4.11	10.6	504	2.95	27.0	76.6	11.5	35.3
	January	42.0	91.4	1831	624	180	8.81	3.75	10.6	418	3.71	28.1	168	13.1	108
	February	45.4	125	1384	343	217	10.2	3.62	10.5	399	2.96	22.2	53.9	9.30	25.6
	March	51.1	109	1037	221	215	10.0	2.59	7.64	332	1.94	16.6	39.1	6.20	13.2
	April	60.0	145	780	125	266	12.9	2.46	7.60	350	1.49	14.6	32.5	7.22	10.9
	May	52.8	192	885	116	244	16.1	2.02	15.9	324	1.80	11.7	25.9	6.16	10.5
	June	63.7	168	1079	126	295	15.1	2.04	8.11	300	1.83	11.6	27.2	6.56	9.95
	July	70.3	197	1251	145	291	15.6	2.69	7.76	282	2.19	11.8	28.3	5.76	8.21
	August	31.9	75.7	699	64.4	122	5.55	1.13	3.59	144	1.40	6.27	10.3	3.44	4.21
	September	30.6	73.3	575	87.6	124	6.69	2.33	6.54	215	1.66	11.5	38.6	4.43	9.89
	October	53.7	134	932	280	273	18.8	4.52	13.0	476	2.88	23.2	61.3	10.7	22.1
November	24.4	59.6	804	216	110	8.95	3.14	9.23	273	2.59	15.6	46.3	6.57	14.7	
PM _{10-2.5}	December	45.2	98.9	73.3	43.1	241	9.27	2.28	4.51	375	0.726	16.6	11.0	7.09	3.28
	January	52.0	111	84.9	47.4	285	10.2	2.00	4.42	348	0.737	12.6	10.1	6.29	4.62
	February	39.7	84.2	53.8	35.3	216	7.27	1.59	3.37	261	0.650	9.5	6.35	4.62	3.38
	March	72.1	143	59.3	55.0	324	10.4	1.81	4.23	316	0.645	10.2	7.28	5.50	3.41
	April	34.9	80.2	29.7	38.6	192	7.08	1.26	3.07	216	0.438	7.5	6.45	3.83	1.77
	May	29.6	87.1	40.2	48.4	172	8.85	1.37	9.14	248	0.481	8.9	7.69	4.56	2.81
	June	36.8	81.6	44.5	72.4	246	11.4	1.55	4.76	246	0.623	9.1	7.62	4.47	2.77
	July	61.3	117	48.1	65.8	272	8.99	1.27	3.71	251	0.521	8.1	5.37	4.63	1.40
	August	64.8	161	44.9	87.3	329	13.8	1.70	5.12	273	0.713	9.3	8.08	5.34	2.25
	September	58.3	117	49.6	77.6	346	12.4	2.65	5.93	410	0.946	16.0	13.7	7.74	4.44
	October	108	226	98.5	137.5	678	23.9	6.23	13.4	996	2.00	39.2	27.3	19.7	15.6
November	37.4	84.0	52.4	47.5	221	9.54	2.47	4.77	385	0.881	16.6	9.94	8.74	3.85	

3.3.1.2 Carbonaceous Compounds

To account for the contributions of elements associated with OC (e.g. oxygen, hydrogen) to the total mass of OM, a factor of 1.6 ± 0.2 and 2.1 ± 0.2 is recommended for urban aerosols and non-urban aerosols, respectively (Turpin and Lim, 2001). We used a factor of 1.8 to convert OC to OM in this study. OM was a major component of $PM_{2.5}$ while a minor species of $PM_{10-2.5}$ accounting for $34 \pm 6.3\%$ and $16 \pm 3.4\%$ of their masses on a yearly-based average (\pm one standard deviation), respectively. Coarse mode OM lacked a discernible seasonal pattern, averaging $1.0 \pm 0.22 \mu\text{g}/\text{m}^3$. On the other hand, fine OM concentration presented a marked seasonality, ranging from a high of $26.9 \mu\text{g}/\text{m}^3$ in January to a low of $\sim 4.81 \mu\text{g}/\text{m}^3$ in July and August. EC had a minimal contribution to $PM_{2.5-10}$, accounting for less than 0.50% and $0.047 \mu\text{g}/\text{m}^3$ of its mass. Its contribution to $PM_{2.5}$ was more significant but still quite low, accounting for $2.8 \pm 1.5\%$ of its mass. Moreover, $PM_{2.5}$ -EC reached higher concentrations in winter with peak occurrence in January ($0.73 \mu\text{g}/\text{m}^3$), while lower concentrations in summer with a minimum in July ($0.55 \mu\text{g}/\text{m}^3$). The variation in fine OM and EC concentration can be partly attributed to the change in mixing height, as aforementioned.

To further investigate the variability of OC in $PM_{2.5}$, the monthly mass ratio of fine OC to EC was estimated as illustrated in Figure 3.3. This ratio, which is commonly used to determine the extent of secondary OC formation (Cabada et al., 2004; Turpin and Huntzicker, 1995) attained highest values during December-February (13.2-20.4) while lowest during May-September (3.7-5.1). Interestingly, these ratios exceed those reported for other urban areas (Castro et al., 1999; Turpin and Huntzicker, 1995), particularly in winter when minimum ratios were frequently recorded and used as a threshold to indicate SOA formation. The high wintertime ratios in this study are consistent with the low levels of EC. The latter is largely from

biomass smoke in winter. Biomass burning was considerable in winter as indicated by the monthly trend of levoglucosan in Figure 3.5a. Levoglucosan, a tracer for biomass burning (Simoneit et al., 1999), exhibited higher concentrations in winter, relative to other periods. On the other hand, emissions from diesel vehicles were insignificant in winter, as shown later. Furthermore, WSOC, an indicator of biomass burning and SOA formation processes (Weber et al., 2007), exhibited higher concentrations in winter. Thus the peak wintertime OC/EC ratio is likely strongly impacted by primary fossil fuel combustion and biomass burning.

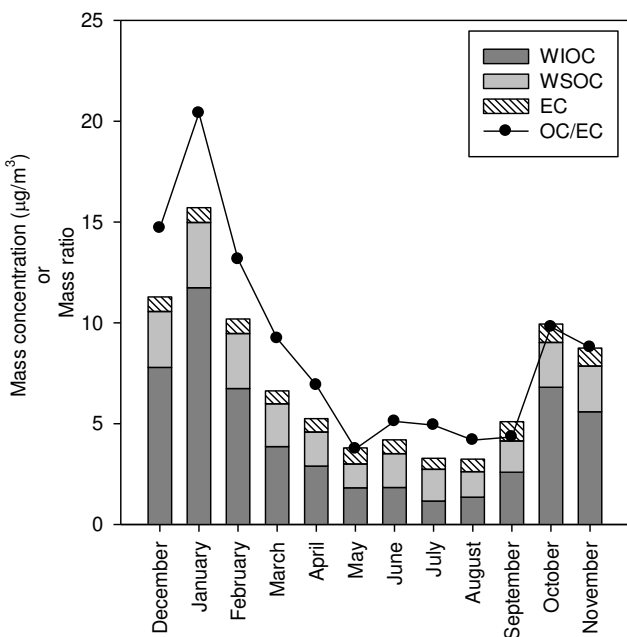


Figure 3.3 Monthly variation in the concentration ($\mu\text{g}/\text{m}^3$) of $\text{PM}_{2.5}$ water-insoluble organic carbon (WIOC), water-soluble organic carbon (WSOC) and elemental carbon (EC) as well as in the concentration ratio of fine organic carbon-to-EC (OC/EC).

3.3.1.3 Inorganic Ions

In the coarse mode, ions lacked any obvious seasonal pattern and reached a collective yearly average (\pm one standard deviation) of $0.88 \pm 0.27 \mu\text{g}/\text{m}^3$ with a relative contribution to $\text{PM}_{10-2.5}$ of $12 \pm 5.2\%$. On the other hand, in the fine mode, ions were a dominant component of $\text{PM}_{10-2.5}$, accounting for $37 \pm 7.3\%$ of its mass on a yearly-average basis. Total $\text{PM}_{2.5}$ ionic mass

ranged between 3.76 and 28.9 $\mu\text{g}/\text{m}^3$ with lowest contributions occurring in summer (June-August) while highest in winter (January-February). The most significant inorganic ions in $\text{PM}_{2.5}$ were nitrate ($16\pm 8.5\%$), sulfate ($10\pm 4.5\%$) and ammonium ($9.4\pm 2.3\%$). In the Po valley, there are large anthropogenic sources of NO_x and agricultural-related sources of NH_3 (Putaud et al., 2004), it is therefore expected that these ions are formed from gaseous precursors such as NH_3 , NO_x and SO_2 . The wintertime increase in $\text{PM}_{2.5}$ -ions can be partly attributed to the low mixing height. Additionally, the low temperature and high relative humidity conditions in winter favor the partitioning of ammonium nitrate to the particulate-phase (Chang et al., 2000; Park and Kim, 2004). Accordingly, their lowest summertime concentrations can be attributed to the evaporation of NH_4NO_3 at high temperatures. In contrast, sulfate maintained a rather stable concentration of $2.9\pm 0.78 \mu\text{g}/\text{m}^3$ in spite of the expected increase in summer, as a result of enhanced photochemical activity. This expected increase is likely offset by the greater summertime atmospheric dispersion.

Lastly, an ion balance was conducted by determining monthly concentration ratios of measured ammonium to the amount of ammonium required to fully neutralize the measured sulfate and nitrate as plotted in Figure 3.4. As can be detected, NH_4 is generally present in sufficient amounts to fully neutralize SO_4 and NO_3 in the form of $(\text{NH}_4)_2\text{SO}_4$ and NH_4NO_3 . Ratios slightly lower than 1 were observed in April and May (0.76 and 0.87, respectively). Nonetheless, these results overall indicate that the cations and anions in $\text{PM}_{2.5}$ were largely in balance, consistent with the findings of Perrone et al. (2010).

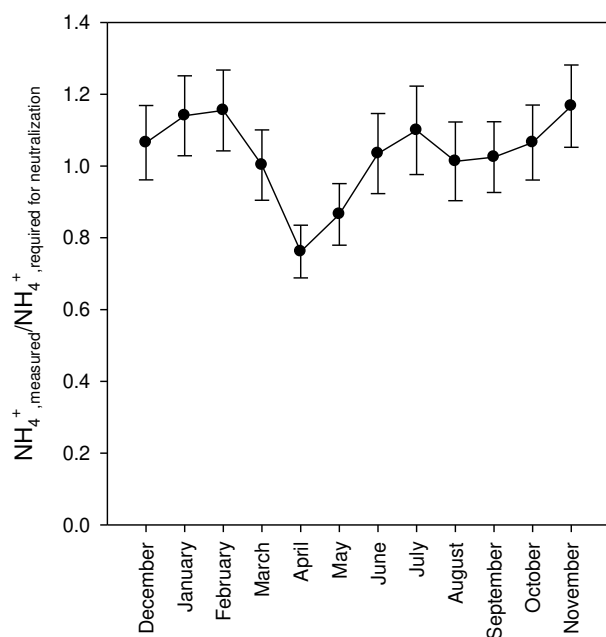


Figure 3.4 Monthly concentration ratio of measured ammonium to required ammonium for complete neutralization of nitrate and sulfate ions in ambient $\text{PM}_{2.5}$ in Milan. Error bars represent the uncertainty of analytical measurement.

3.3.2 Mass Closure

Chemical mass balance results overall show a good agreement between the reconstructed and gravimetric fine PM mass, averaging $83 \pm 9.7\%$. This agreement is comparable to that reported by Putaud et al. (2004) and Hueglin et al. (2005) at various European sites. However, a lesser agreement is observed for the coarse PM fraction, averaging $62 \pm 13\%$. The percent mass discrepancy could be related to un-estimated aerosol-bound water and crustal components as well as uncertainties in the gravimetric mass and chemical measurements. Uncertainties in the multiplication factors used to convert OC to PM and metals to oxides could also contribute to the inconsistency between reconstructed and gravimetric mass. The higher discrepancy observed for coarse PM could be primarily related to an under-estimation of OM. The conversion factor used to convert OC to OM may under-represent the contribution of OM from soils, which is likely to

contain sugars and amino acids that have higher molecular weight per carbon weight ratio (Turpin and Lim, 2001).

3.3.3 Organic Species and Source Identification

The importance and abundance of OM in PM_{2.5} merits a thorough exploration of this component. For this purpose, the monthly variation of select organic molecular markers is examined as illustrated in Figure 3.5a-f.

Levoglucosan, a tracer for biomass burning (Simoneit et al., 1999), contributed to PM_{2.5} throughout the year with lowest levels occurring during warm months while highest during cold months, as displayed in Figure 3.5a. Specifically, levoglucosan concentration ranged from a low of 8.0 ng/m³ in July to a high of ~86 ng/m³ in November/March. This marked seasonal pattern can be associated with increased biomass use for domestic heating.

On the other hand, picene, a molecular marker for coal soot (Oros and Simoneit, 2000), only contributed to PM_{2.5} during November-May, as shown in Figure 3.5b. Its monthly-average concentration was negligible throughout June-October then peaked at 0.54 ng/m³ in January, indicating that coal soot only intermittently contributes to ambient PM_{2.5}.

Select polycyclic aromatic hydrocarbons (PAHs), common products of incomplete combustion (Manchester-Neesvig et al., 2003), followed a temporal trend quite similar to that of PM_{2.5} and OC, as displayed in Figure 3.5c. Their cumulative concentration ranged from 0.15 to 10 ng/m³ with highest levels measured in winter (December-February) while lowest in summer (June-August). The sharp concentration drop in summer can be related to the combined effects of particle-bound PAH volatilization and partitioning to the gas phase (Zheng and Fang, 2000), reaction with oxidizing gases (Arey et al., 1988; Schauer et al., 2003), greater atmospheric dispersion and lack of wintertime heating combustion sources. In comparison to other cities, the

annual average concentrations of these tracers were 0.05-0.45 and 0.65-2.1 times those reported in Thessaloniki, Greece (Manoli et al., 2002) and Augsburg, Germany (Schnelle-Kreis et al., 2007), respectively. Moreover, although only quantified in the fine fraction, benzo(a)pyrene, commonly used as an index for PAH carcinogenicity (Menichini et al., 1999), exhibited a yearly mean concentration ($0.40 \pm 0.49 \text{ ng/m}^3$), much lower than the annual EU limit of 1 ng/m^3 in ambient PM.

Hopanes, which are associated with engine lubricating oil of mobile sources, coal combustion and fuel oil (Oros and Simoneit, 2000; Rogge et al., 1997; Schauer et al., 2002), exhibited some seasonality as shown in Figure 3.5d for select tracers. These, including $17\beta(\text{H})$ - $21\alpha(\text{H})$ -30-norhopane, $17\alpha(\text{H})$ - $21\beta(\text{H})$ -hopane, 22S -homohopane and 22R -homohopane, displayed a collective concentration ranging from a low of 0.12 ng/m^3 in July to a high of 1.7 ng/m^3 in October. Their seasonal variability was however less pronounced than that of PAHs, likely due to their lower volatility and higher atmospheric stability. The concentration drop during warm months is probably related to the increase in atmospheric mixing height.

To investigate the origin of n-alkanes (C_{24} - C_{33}), the carbon preference index (CPI), defined as the concentration ratio of their odd-to-even numbered homologues, was estimated. A CPI about 1 indicates a dominance of anthropogenic sources, whereas a CPI greater than 2 indicates a prevalence of biogenic sources (Simoneit, 1986). These compounds presented a seasonally-dependent CPI as shown in Figure 3.5e. They demonstrated a strong odd-to-even carbon number preference during March-October (CPI=1.7-2.8) with a maximum at C_{31} (hentriacontane), indicative of their modern biogenic source. In contrast, these n-alkanes presented much lower CPI (1.26-1.32) with maximum at C_{24} (tetracosane) during the remaining months, suggesting the predominance of anthropogenic sources, such as fossil fuel utilization and wood-smoke (Rogge

et al., 1993d). These n-alkanes also exhibited a temporal trend similar to PAHs and hopanes. Their collective concentration ranged from a low of 6.84 ng/m³ in July to a high of 48.3 ng/m³ in January. This drastic drop in n-alkanes levels during warm months can again be attributed to the increase in atmospheric mixing height coupled with volatilization of these species from the particulate into the gas phase (Kuhn et al., 2005).

SOA derivatives exhibited a strong seasonal variation, as illustrated in Figure 3.5f. The concentrations of their individual tracers are listed in Table 3.3. Overall, highest levels occurred during summer (June-August) when the intensity of photochemical activity is highest (Ion et al., 2005). These levels, ranging from 35.7-55.6 ng/m³, dropped to as low as 2.88 ng/m³ in December. Isoprene-derived SOA tracers only contributed to ambient PM_{2.5} during May-September with a concentration range of 0.49-6.2 ng/m³, which can also be associated with greater isoprene emission rates at high temperatures and light intensities (Rinne, 2002). On the other hand, while α -pinene derivatives presented highest concentrations during summer, they persistently contributed to ambient PM_{2.5}. This temporal behavior suggests a continual presence of a local biogenic α -pinene source. The concentration of α -pinene derivatives ranged from 2.56 ng/m³ in November to 46.4 ng/m³ in August with a small peak occurrence in January. The latter is likely associated with an accumulation of SOA precursor gases due to the low mixing height (Strader et al., 1999). Similarly, β -carophyllene derivative was almost continually present, reaching a high of 2.3/2.2 ng/m³ in January/August and a low of 0.26 ng/m³ in April. Toluene derivative, linked to motor vehicles emissions, was only detected during April-October with levels varying from 0.58 ng/m³ in April to 4.9 ng/m³ in June.

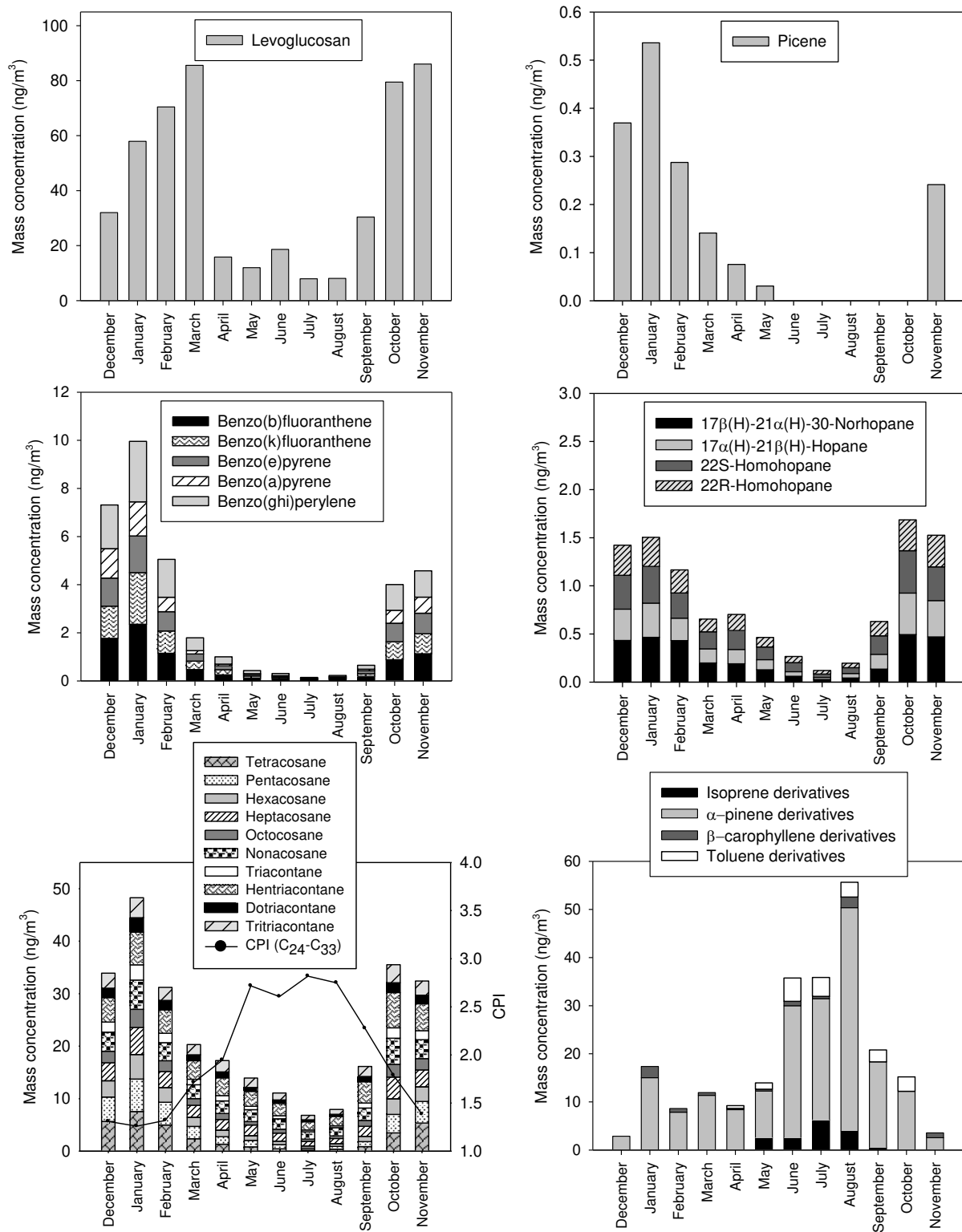


Table 3.3 Monthly concentration of secondary organic aerosol tracers in ambient PM_{2.5} in Milan. n.d. indicates that compound was not detected.

	Monthly concentration (ng/m ³)								
	Isoprene-derivatives			α-pinene derivatives			β-carophyllene derivatives	Toluene-derivative	
	2-methylthreitol	2-methylerythritol	3-hydroxyglutaric acid	Pinic acid	3-acetyl hexanedioic acid	2-hydroxy-4-isopropyladipic acid	Pinonic acid	β-carophyllinic acid	2,3-dihydroxy-4-oxopentanoic acid
December	n.d.	n.d.	n.d.	n.d.	n.d.	2.88	n.d.	n.d.	n.d.
January	n.d.	n.d.	5.98	n.d.	2.11	6.94	n.d.	2.33	n.d.
February	n.d.	n.d.	0.686	n.d.	2.34	4.84	n.d.	0.756	n.d.
March	n.d.	n.d.	2.98	n.d.	3.20	5.18	n.d.	0.578	n.d.
April	n.d.	n.d.	2.98	n.d.	2.13	3.27	n.d.	0.261	0.579
May	0.649	1.91	1.75	0.210	3.35	3.19	1.21	0.371	1.33
June	0.816	1.71	8.19	1.04	15.1	2.37	0.751	0.910	4.85
July	1.80	4.45	8.71	0.846	12.6	2.08	0.952	0.488	3.95
August	1.76	2.18	12.1	2.68	27.3	3.59	0.795	2.21	3.06
September	0.302	0.192	5.82	0.215	10.4	1.09	0.268	n.d.	2.48
October	n.d.	n.d.	5.29	n.d.	3.02	3.89	n.d.	n.d.	3.00
November	n.d.	n.d.	0.529	n.d.	n.d.	2.04	n.d.	0.989	n.d.

3.3.4 MM-CMB results

3.3.4.1 Source Apportionment of Fine OC

The monthly contributions of primary and secondary sources to ambient fine OC, as estimated by the MM-CMB model, are presented in Figure 3.6a and summarized in Table 3.1a. Their associated uncertainties are also reported in Table 3.1a. The uncertainty in source contribution corresponds to the standard error reported by the CMB software. It was analytically estimated using the effective variance weighted least squares algorithm and is based on uncertainty of both the source profiles and ambient concentrations. Nine sources, including vegetative detritus, wood-smoke, natural gas, diesel emissions, gasoline vehicles, urban soil, coal soot, biogenic-derived SOA and toluene-derived SOA, were identified. These sources collectively contributed to a yearly average (\pm standard deviation) of $35\pm 10\%$ of OC. In particular, primary sources contributed to 20-34% of measured fine OC, with lowest percent contribution occurring in July/January and greatest in October. Contributions of secondary sources to OC mass ranged from about 1% in winter to 30% in August. The largest contributors to fine OC varied with season. Gasoline vehicles had the higher contribution from September to May (with the exception of March), accounting for 11-23% of OC mass. In March, contributions from both wood-smoke and gasoline vehicles were predominant (10 and 9.7% of OC, respectively). In warmer months, the contributions of SOA sources became more pronounced. Toluene-derived SOA was the major contributor in June and July with a relative contribution of nearly 18%. Additionally, toluene- and biogenic-derived SOA were both prevailing source contributors in August with similar relative contributions of about 15%. Gasoline vehicles displayed a year-long contribution to OC with higher source contribution estimates (SCEs) in the range of 1.2-2.1 $\mu\text{g}/\text{m}^3$ occurring during October-February. Lowest contribution of 0.085 $\mu\text{g}/\text{m}^3$ was attained in July. Diesel emissions contributed to OC statistically significantly ($> 2\times$ standard error) during

April-September with a SCE range of 0.28-0.32 $\mu\text{g}/\text{m}^3$. Wood-smoke contributed on average (\pm standard deviation) $4.6\pm 2.6\%$ to total OC on a year-long basis. Its SCE varied from a low of $0.061 \mu\text{g}/\text{m}^3$ in July/August to a high of $\sim 0.61 \mu\text{g}/\text{m}^3$ in October/November/March. This seasonal pattern suggests the use of wood-smoke for residential heating during cold months. Vegetative detritus also continually contributed to OC, averaging $2.6\pm 0.67\%$ and ranging from a low of $0.062 \mu\text{g}/\text{m}^3$ in July to a high of $0.26 \mu\text{g}/\text{m}^3$ in January. On the other hand, coal soot contributed to OC significantly only during November-April with an average contribution of $1.9\pm 0.91\%$ and a peak SCE of $0.36 \mu\text{g}/\text{m}^3$ in January. Urban soil accounted for $1.8\pm 1.2\%$ and $0.085\pm 0.032 \mu\text{g}/\text{m}^3$ of fine OC on a yearly-based average (\pm standard deviation). Natural gas contributed the least to OC, with utmost values of 0.74% and 0.11 ± 0.029 (\pm standard error) $\mu\text{g}/\text{m}^3$ in January. As expected, SCEs from toluene-derived SOA exhibited a seasonal dependency. They were measurable only during April-October, with highest contributions occurring in June-August (15-18%) and peaking at $0.61\pm 0.22 \mu\text{g}/\text{m}^3$ in June. Contributions from biogenic-derived SOA were almost continual and reached a peak of $0.39 \mu\text{g}/\text{m}^3$ (15% of OC) in August.

Lastly, unidentified source contributions, denoted as “other WSOC” and “other WIOC”, correspond to water-soluble and water-insoluble OC that could not be apportioned to the considered primary and secondary sources. “Other WSOC” was estimated as the difference between measured WSOC and the sum of SCE of biogenic- and toluene-derived SOA as well as WSOC that is associated with wood-smoke emissions. The contribution of wood-smoke to OC is estimated as 71% water-soluble (Sannigrahi et al., 2006). Likewise, un-apportioned WIOC was determined as the difference between the total concentration of WIOC (OC-WSOC) and the sum of all primary SCEs (excluding wood-smoke) plus the concentration of WIOC from wood-smoke. Total residual OC mass averaged $65\pm 10\%$ and was highest in January. Moreover, as can

be inferred from Figure 3.6a, unattributed OC is mostly water-insoluble ($63\pm 9.2\%$), indicating that uncharacterized OC sources are mainly primary.

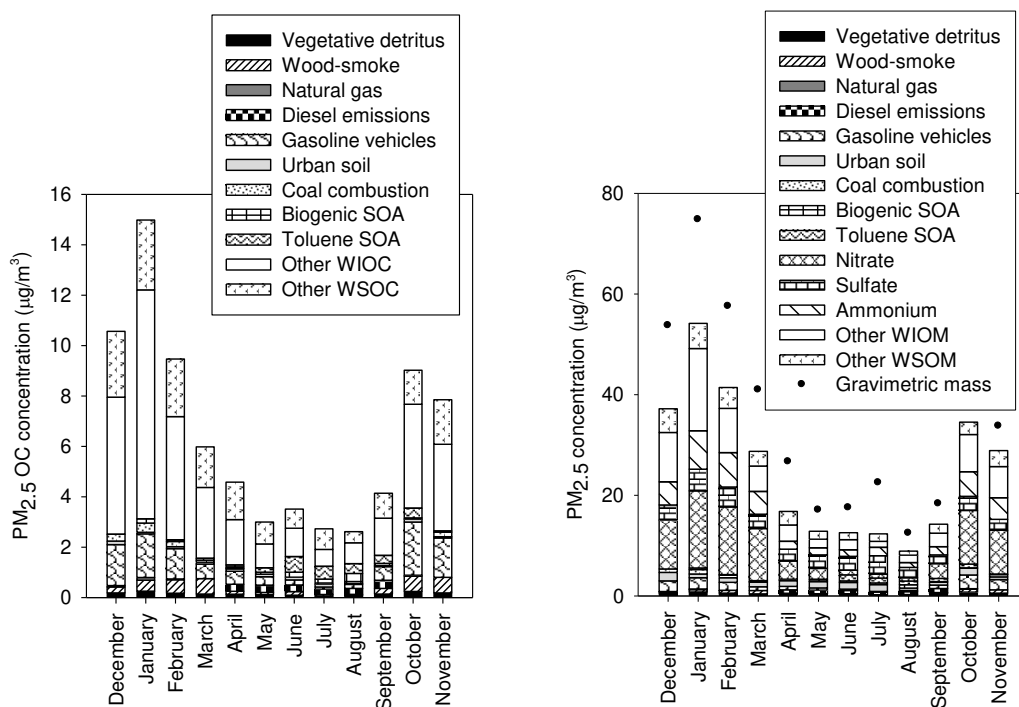


Figure 3.6a-b contribution to ambient a) $PM_{2.5}$ organic carbon (OC) and b) $PM_{2.5}$ mass estimated using a molecular marker chemical mass balance (MM-CMB) model.

To further elucidate the nature of unidentified OC, GC/MS-chromatograms for the monthly composited samples were examined, as displayed in Figure 3.7a-d, for select samples. As can be observed, the chromatograms indicate a dominance of an unresolved complex mixture (UCM) exhibiting two humps. The first hump peaks prior to 25 min during summer months while the second peaks afterwards during winter months. Moreover, the mass spectrum and elution time of the latter UCM hump are very similar to those of motor oil when analyzed by GC/MS. In urban atmospheres, UCM has been associated with contributions from fossil fuel residues (Rogge et al., 1993a; Simoneit, 1984). This hump also appears to exhibit a similar temporal trend to unidentified OC and “other WIOC”, suggesting that un-apportioned OC is likely primarily derived from petroleum-based material.

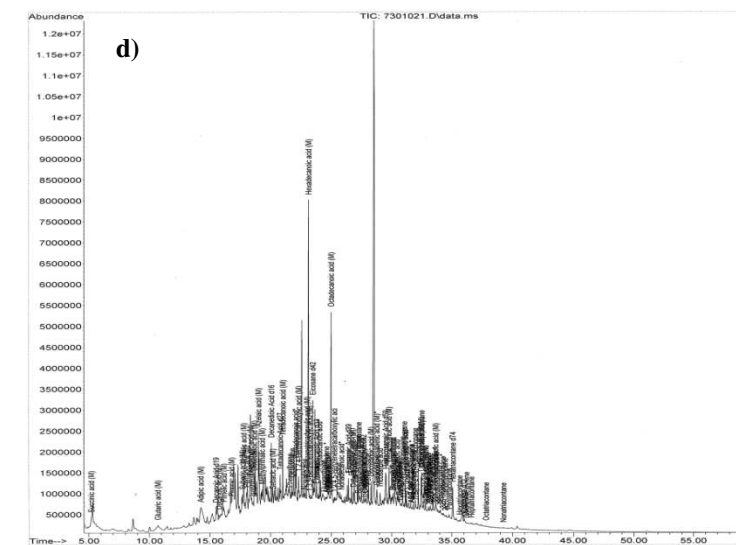
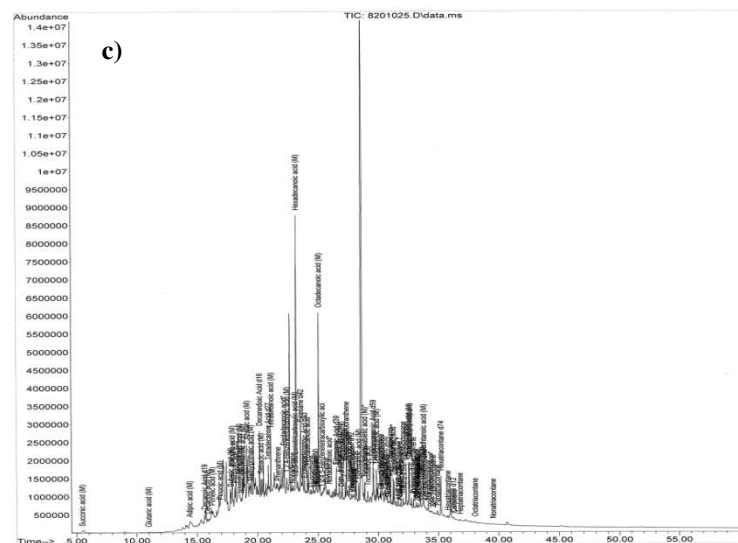
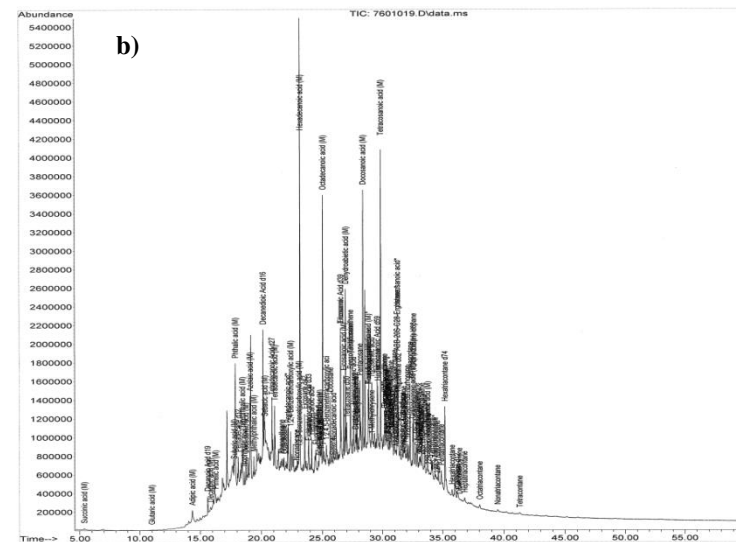
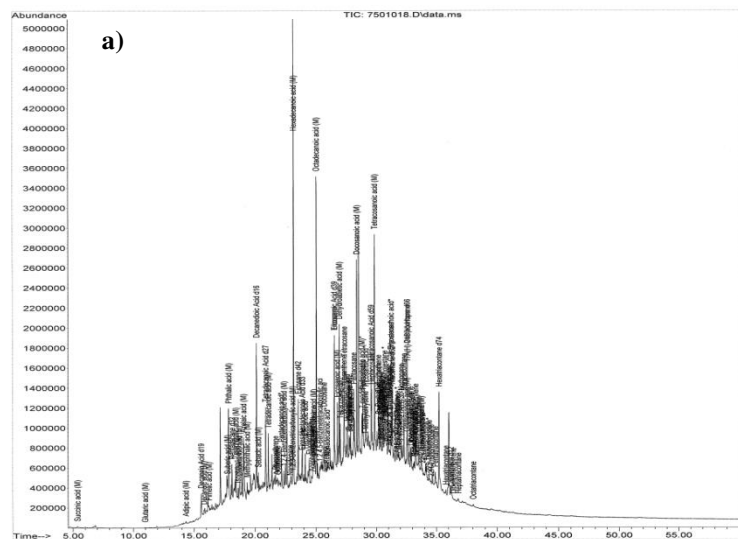


Figure 3.7a-d GC/MS chromatograms of ambient PM_{2.5} in Milan in: a) December, b) January, c) July and d) August monthly samples.

Given that residential heating in Lombardy is mostly based on the use of natural gas, as indicated in a survey conducted in this region (Caserini, 2007), motor vehicles are the most likely source of this petroleum-derived material. These observations indicate that the results of our source apportionment for motor vehicles, should be interpreted with caution, given that they are based on emission profiles that are characteristic of US vehicle fleet and do not adequately represent vehicular emissions in Milan. This inadequacy may be due to the much wider use of diesel PM filters in Western Europe than the US and the higher prevalence of smoking vehicles (vehicles emitting atypically large amounts of lubricating oil) in the US than Western Europe. Additional work is therefore needed to accurately identify and quantify these major petroleum-based PM sources in Milan.

3.3.4.2 Source Apportionment of Total PM_{2.5}

Source contributions to total PM_{2.5} were evaluated by converting MM-CMB apportionment results for fine OC to those of PM_{2.5} using fine OC-to-PM mass ratios for each source (Kleindienst et al., 2007; Lough et al., 2007; Rogge, 1993; Rogge et al., 1993c; Rutter et al., 2011; Sheesley, 2007; Zhang et al., 2008b). In addition to the sources identified in OC apportionment, “other WIOM”, “other WSOM” as well as nitrate, ammonium and sulfate ion concentrations were considered in PM_{2.5} apportionment as displayed in Figure 3.6b and Table 3.1b. “Other WIOM” and “other WSOM” were assessed by multiplying “other WIOC” and “other WSOC” by a factor of 1.8 (Turpin and Lim, 2001). These sources collectively accounted for 73±9.0% of the measured PM_{2.5} mass. Some of the discrepancy in apportionment could be related to uncertainties associated with the conversion factor from OC to OM and source profiles compositions. The contributions of these sources to PM_{2.5} also exhibited some seasonality. During fall/winter (September-February), the greatest average (±standard deviation)

contributions were from NO_3^- ($10 \pm 4.3 \mu\text{g}/\text{m}^3$, $22 \pm 4.4\%$) followed by “other WIOM” ($8.5 \pm 4.6 \mu\text{g}/\text{m}^3$, $18 \pm 2.7\%$), NH_4^+ ($5.0 \pm 2.1 \mu\text{g}/\text{m}^3$, $11 \pm 1.8\%$), “other WSOM” ($3.5 \pm 1.3 \mu\text{g}/\text{m}^3$, $8.0 \pm 1.5\%$) and SO_4^{2-} ($3.0 \pm 1.0 \mu\text{g}/\text{m}^3$, $6.9 \pm 1.4\%$). Individual contributions of remaining sources were $< 4.4\%$ ($1.9 \mu\text{g}/\text{m}^3$). During spring/summer (March-August), the major contributions were from SO_4^{2-} ($2.7 \pm 0.5 \mu\text{g}/\text{m}^3$, $13 \pm 4.2\%$), NO_3^- ($3.1 \pm 3.7 \mu\text{g}/\text{m}^3$, $11 \pm 8.2\%$), “other WIOM” ($2.5 \pm 1.5 \mu\text{g}/\text{m}^3$, $11 \pm 2.7\%$) followed by, NH_4^+ ($1.9 \pm 1.3 \mu\text{g}/\text{m}^3$, $7.9 \pm 1.7\%$) and “other WSOM” ($1.8 \pm 0.81 \mu\text{g}/\text{m}^3$, $7.9 \pm 1.5\%$). The remaining sources had contributions of about 5.2% ($1.1 \mu\text{g}/\text{m}^3$). These results clearly show that “other WIOM”, which, as argued earlier, is potentially derived from petroleum-based sources, contributes considerably to $\text{PM}_{2.5}$ in Milan, especially in winter and fall.

3.4 Summary and Conclusions

Ambient particle levels in Milan are dominated by $\text{PM}_{2.5}$, which exhibited a yearly average of $34.5 \pm 19.4 \mu\text{g}/\text{m}^3$, in excess of the EU annual mean limit of $25 \mu\text{g}/\text{m}^3$. Secondary inorganic ions and OM were the most prevalent fine PM components, accounting for $36 \pm 7.1\%$ and $34 \pm 6.3\%$ of its mass, respectively. Highest concentrations occurred in winter, when atmospheric dispersion is poorest and combustion-related emissions are high. On the other hand, coarse PM displayed an annual average of $6.79 \pm 1.67 \mu\text{g}/\text{m}^3$ and was dominated by crustal material. Source apportionment results showed that wood-smoke and secondary organic aerosol sources contributed to $4.6 \pm 2.6\%$ and $9.8 \pm 11\%$ of fine OC on a yearly-based average, respectively. The residual OC was mostly attributed to petroleum-based material that is not adequately represented by existing source profiles used in this study.

In conclusion, ambient PM_{10} in Milan, particularly $\text{PM}_{2.5}$, is present in high levels, with petroleum-based fuel emissions as significant sources. Additional studies, aimed at deriving source profiles characteristic of the area of Milan should be undertaken. Findings of these

investigations can ultimately be used to inform policy makers and guide emission reduction strategies for better protection of human health.

3.5 Acknowledgements

This research was supported by Southern California Particle Center (SCPC), funded by US EPA (Grant 2145 G GB139) and the University of Southern California (USC) Viterbi School of Engineering. We would like to thank the superintendent of fine arts and culture in Lombardy for his willingness to accept this study. We also wish to acknowledge the support of USC Provost's Ph.D. fellowship. We thank Jeff DeMinter and the staff at the Wisconsin State Laboratory of Hygiene for their assistance with the chemical measurements. We also wish to thank SIMG-Italian College GPs and ISDE-International Doctors for the Environment for managerial support, Eng. Franco Gasparini, designer of the HVACS for technical help, and the whole management and employees of the Sovrintendenza, particularly Arch. A. Artioli, Arch. G. Stolfi, Arch. Napoleone, Mr. G. Bonnet and Dr. L. Dall'Aglio.

Chapter 4 Chemical Composition of PM and its Relation to Particle-Size: A Case Study of Size-Resolved PM at Near-Freeway and Urban Background Sites in the Greater Beirut Area

How does PM chemical composition vary across and within particle-size modes?

Particle-size and chemical properties of particulate matter (PM) are both potential factors determining PM toxicity (Anderson, 2000). A better characterization of size-resolved PM chemical composition is therefore vital for assessing exposure to PM and determining specific particle components that are mostly critical in inducing adverse health effects. To this end, coarse (PM_{10-2.5}), accumulation (PM_{2.5-0.25}) and quasi-ultrafine (PM_{0.25}) PM samples were concurrently collected at two contrasting locations in the Greater Beirut area during summer of 2012. Sampling sites included near-freeway and urban background locations. The diversity in sources at the monitoring locations provided a suitable setting to investigate the association between PM chemistry and particle-size. The current chapter summarizes the findings of this study. Results provide a comparative and comprehensive analysis of size-fractionated ambient particles in Lebanon, which also complements an investigation of particle-size-resolved redox activity in this area (discussed in Chapter 5).

This chapter is based on the following publication:

Daher, N., Saliba N. A., Shihadeh A.L., Malek J., Baalbaki R., Sioutas C., 2013. Chemical Composition of Size-Resolved Particulate Matter at Near-freeway and Urban Background Sites in the Greater Beirut Area. *Atmospheric Environment*, 80, 96-106.

4.1 Introduction

In urban areas, motor vehicles are the primary source of PM (Sternbeck et al., 2002; Westerdahl et al., 2005), with populations in close proximity to trafficked-roadways being most susceptible to particle-induced health effects (Tonne et al., 2007). PM vehicular emissions, derived from both exhaust and abrasion (Sternbeck et al., 2002), are composed of potentially toxic air pollutants, such as organic carbon (OC), polycyclic aromatic hydrocarbons (PAHs) and transition metals (Cho et al., 2005; See et al., 2007). Some of these components (OC, PAHs) also dominate the ultrafine particle-mode (aerodynamic diameter, $d_p < 0.1-0.2 \mu\text{m}$) because of its increased number and surface area relative to larger coarse (PM_{10-2.5}, $10 \mu\text{m} < d_p < 2.5 \mu\text{m}$) and fine (PM_{2.5}, $d_p < 2.5 \mu\text{m}$) PM (Hughes et al., 1998; Morawska et al., 1998).

Lebanon, a country in the eastern Mediterranean basin, represents one case study of developing regions, where particle levels routinely exceed the World Health Organization (WHO) guidelines (Saliba et al., 2010). Lacking an effective mass transportation system (MoE/URC/GEF, 2012), road traffic emissions are a major cause for its elevated PM levels, particularly in urban areas. Accurate characterization of traffic-associated particle emissions in Lebanon is thus essential.

Investigation of PM in Lebanon has been generally restricted to urban areas and has focused on determining the ionic and elemental content of coarse or fine PM (Kouyoumdjian and Saliba, 2006; Massoud et al., 2011; Saliba et al., 2010). To determine chemically-specified and size-resolved properties of traffic-related particle emissions in Lebanon, coarse, accumulation ($PM_{2.5-0.25}$, $2.5 \mu m < d_p < 0.25 \mu m$) and quasi-ultrafine ($PM_{0.25}$, $d_p < 0.25 \mu m$) PM samples were collected at two contrasting locations in the summer of 2012. Sampling sites included near-freeway and background locations in the Greater Beirut area. To the best of the authors' knowledge, this is the first study to provide a comparative and comprehensive analysis of size-fractionated ambient PM in Lebanon. Results are also evaluated in the context of metropolitans and roadways worldwide. Findings of this work provide insight on commuter exposure to traffic-related PM in the area of Beirut and could ultimately aid in establishing air pollution control strategies, currently very limited, in this region.

4.2 Methodology

4.2.1 Sampling Sites

The sampling campaign was conducted in the Greater Beirut area at two contrasting sites, including urban background and near-freeway locations, as shown in Figure 4.1.

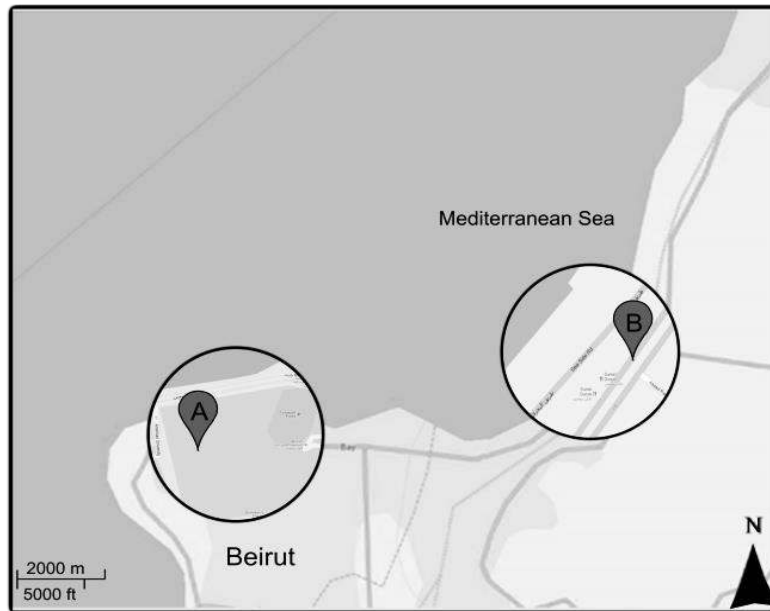


Figure 4.1. Map of the urban background (A) and near-freeway sites (B).

The background site was situated at the American University of Beirut (AUB), in a location overlooking AUB campus from the south/east and the Mediterranean coast from the north/west. It is surrounded by a dense vegetation cover and mostly pedestrian roads, with the nearest street located about 150 m west of the site. This coastal roadway separates the site from the Mediterranean Sea and experiences fairly high traffic activity throughout the day, particularly during rush hours (7-9 a.m. and 4-7 p.m.). The sampling site is also within 1.5 and 2.5 km of a leisure yacht club and the commercial port of Beirut, respectively. Particle levels at this coastal site are commonly influenced by sea and land breeze circulations (Baalbaki et al., 2013). A sea breeze with a predominantly westerly component typically develops in warm seasons during daytime (Baalbaki et al., 2013; Saliba et al., 2010).

The second sampling site consisted of Jal El Dib freeway, along its southbound stretch. This 5-lane freeway serves as a main conduit for vehicles between *Mount/North Lebanon* and the capital Beirut. It experiences heavy traffic throughout the day, with increased congestion during peak hours (7-11 a.m. and 4-7 p.m.), resulting in a daily traffic volume of about 221,409

vehicles/day (LCDR/TEAM, 2000). The sampling point was directly adjacent to the highway at about 1 m from its edge and 1.5 m above ground level. The site was thus directly influenced by road-traffic emissions. The site is also about 0.4 and 3.3 km away from the Mediterranean coast and a yacht port/club, respectively. Lastly, we should note that traffic composition data could not be found for this freeway. The overall Lebanese vehicular fleet, however, consists of 83% gasoline-operated passenger cars and 11.8% heavy-duty vehicles. The remaining 5% includes 2/3-wheelers and agricultural vehicles (MoE/URC/GEF, 2012). Furthermore, sulfur content is 1000 and 5000 ppm by weight in gasoline and diesel fuel, respectively (UNEP/Jordan, 2008; Waked and Afif, 2012).

4.2.2 Sample Collection

Sampling was conducted from 7:00 a.m. to 5 p.m. on weekdays during July-August 2012, with samples concurrently collected at the two sites on a weekly basis. Three parallel Sioutas Personal Cascade Impactor Samplers (Sioutas PCIS, SKC Inc., Eighty Four, PA, USA (Misra et al., 2002)), preceded by PM₁₀ inlets (Chemcomb 3500 speciation sampling cartridge, Rupprecht & Patashnick CO, Inc, Albany, USA) and operating at 9 lpm, were deployed at each site to collect size-fractionated particles in the size ranges: 10-2.5 μm (coarse PM), 2.5-0.25 μm (accumulation PM) and <0.25 μm (quasi-ultrafine PM). For the purpose of chemical speciation, one PCIS was loaded with quartz microfiber filters (Whatman International Ltd, Maidstone, England) while the other two PCISs were loaded with Teflon filters (Pall Life Sciences, Ann Arbor, MI). The quartz substrates were pre-baked at 550 °C for 12 h and stored in baked aluminum foil at - 4°C until field use. 25 mm filters were used as impaction substrates for PM_{10-2.5} and PM_{2.5-0.25} while 37 mm filters were used as collection media for PM_{0.25}. The collected particle mass was determined by pre- and post-weighing the Teflon filters using a UMX2

microbalance (Mettler Toledo GmbH, CH-8606 Greifensee, Switzerland), following equilibration under controlled temperature and relative humidity conditions (22–24°C and 40–50%, respectively).

4.2.3 Sample Analysis

To conduct chemical analyses of the samples, the collected Teflon and quartz filters were sectioned into portions. Quantification of carbonaceous species and organic compounds was conducted on the quartz substrates, while all other measurements were performed on the Teflon filters. Depending on the analytical mass requirements, measurements were performed on either individual weekly samples (carbonaceous species, ions, metals and elements) or composites of the weekly samples (organics and water-soluble organic carbon). Elemental and organic carbon (EC and OC, respectively) were quantified using the NIOSH Thermal Optical Transmission method (Birch and Cary, 1996). The ionic and water-soluble organic carbon (WSOC) contents of the filters were respectively determined by ion chromatography (Model 2020i, Dionex Corp.) and a Sievers 900 Total Organic Carbon Analyzer, following water-extraction and filtration of the samples (Sullivan et al., 2004). The total elemental mass of the filter substrates was measured using a high resolution magnetic sector Inductively Coupled Plasma Mass Spectrometry (Thermo-Finnigan Element 2). A microwave-aided Teflon bomb digestion protocol using a mixture of 1 mL of 16 M nitric acid, 0.25 mL of 12 M hydrochloric acid, and 0.10 mL of hydrofluoric acid was used for extraction of total metals and elements (Herner et al., 2006). Organic speciation was conducted using gas chromatography mass spectrometry (GC-6980, quadrupole MS-5973, Agilent Technologies). The filter substrates were spiked with isotopically-labeled standard solutions prior to extraction. Samples were then extracted in a 50/50 dichloromethane/acetone solution using Soxhlets, followed by rotary evaporation and volume

reduction under high-purity nitrogen. Extracts were analyzed twice by GC/MS after derivitization of carboxylic acids with diazomethane and after silylation of hydroxyl groups. Additional details about the GC method can be found in Sheesley et al. (2004).

4.3 Results and Discussion

4.3.1 Size-Resolved Particle Mass Concentration

Size-resolved PM mass concentrations (average \pm standard error) are presented in Table 4.1 for each location.

Table 4.1. Average (\pm standard error) size-resolved particle mass levels at the near-freeway and urban background sites.

Size range (μm)	Concentration ($\mu\text{g}/\text{m}^3$)	
	Near-freeway	Background
10-2.5	34.0 \pm 1.5	15.8 \pm 0.9
2.5-0.25	13.8 \pm 0.9	8.6 \pm 1.0
<0.25	36.1 \pm 0.9	14.0 \pm 0.4

Overall PM (PM_{10}) mass composition was relatively consistent across the two sites, with $\text{PM}_{0.25}$ and $\text{PM}_{10-2.5}$ prevailing (each constituting 36-43% of PM_{10}). However, despite this comparability, PM concentrations were significantly higher (1.6-2.6 times) at the near-freeway than background site for all particle-size ranges. At the roadside location, PM mass levels varied from a low of 13.8 $\mu\text{g}/\text{m}^3$ in $\text{PM}_{2.5-0.25}$ to a high of 34.0 and 36.1 $\mu\text{g}/\text{m}^3$ in $\text{PM}_{10-2.5}$ and $\text{PM}_{0.25}$, respectively. Particle concentrations at the background site ranged from 8.6 $\mu\text{g}/\text{m}^3$ in the accumulation mode to 15.8 and 14.03 $\mu\text{g}/\text{m}^3$ in the coarse and quasi-ultrafine fractions, respectively. The persistently higher levels at the roadside suggest substantial contributions from vehicular emissions as well as traffic-induced re-suspension to PM levels at the freeway. Compared to other Mediterranean areas, while coarse particle levels at the background site are lower (0.55-0.60 times) than those reported at urban background locations in Athens-Greece (June-July) and Barcelona-Spain (March-May), $\text{PM}_{2.5}$ concentrations are comparable (0.90-1.13

times) (Sillanpää et al., 2005). Conversely, coarse and fine PM levels are 2.4-2.9 times greater than those measured at I-710; a major freeway with the highest ratio (about 11%) of heavy-duty diesel vehicles (HDDVs) in Los Angeles (LA)-California highway network (Kam et al., 2012) .

4.3.2 Size-Resolved Particle Mass Composition

To determine the bulk composition of the PM samples, a chemical mass reconstruction was conducted for each particle mode and sampling site, as displayed in Figure 4.2a-b.

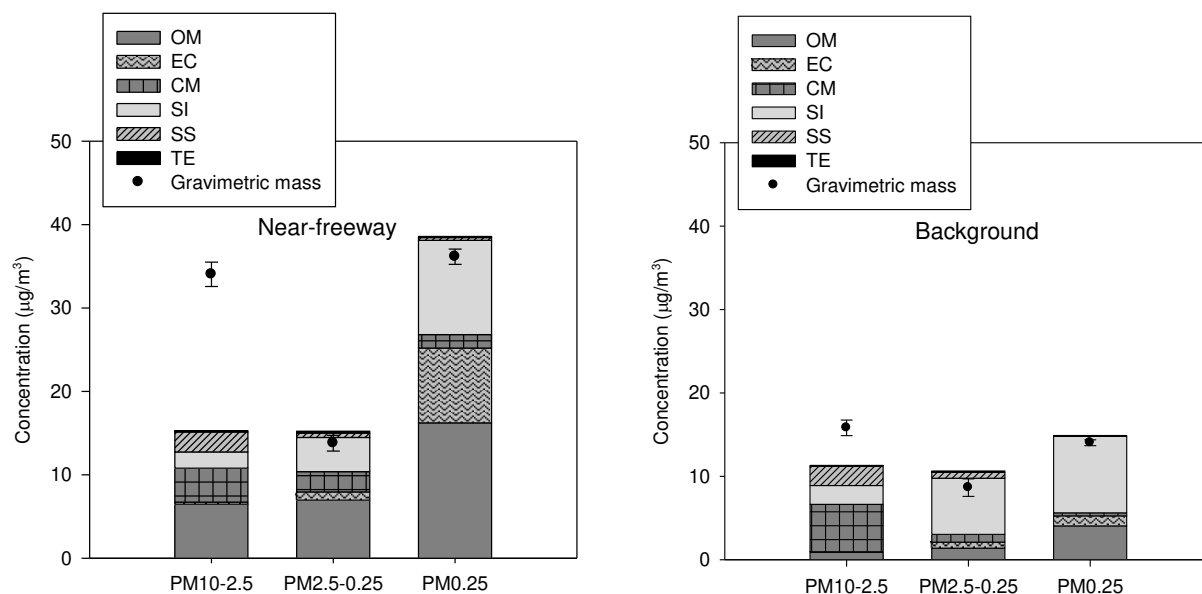


Figure 4.2 a-b. Chemical composition and gravimetric mass concentration of PM_{10-2.5}, PM_{2.5-0.25} and PM_{0.25} at the a) near-freeway and b) urban background sites. Error bars correspond to one standard error.

PM chemical species were classified into organic matter (OM), EC, sea-salt (SS), secondary ions (SI), crustal material (CM) and trace elements (TE). To account for the contributions of non-carbon atoms (e.g. oxygen, hydrogen) to the total mass of OM, a factor of 1.6 ± 0.2 and 2.1 ± 0.2 is recommended for urban and non-urban aerosols, respectively (Turpin et al., 1991). A factor of 1.6 is used to convert OC to OM in this study. SS contribution was estimated as the sum of Na⁺ concentration and sea-salt fractions of Cl⁻, Mg²⁺, K⁺, Ca²⁺, and SO₄²⁻ concentrations, assuming standard sea-water composition (Seinfeld and Pandis, 2006) and using soluble Na⁺ as a tracer for sea-salt. SI includes ammonium, nitrate and non-sea-salt sulfate (nss-sulfate), where

nss-sulfate is obtained by subtracting the sea-salt fraction of sulfate from total measured sulfate. The proportion of CM in the PM samples was determined by summing the oxides of crustal metals, Al, K, Fe, Ca, Mg, Ti and Si, using the following equation (Chow et al., 1994; Hueglin et al., 2005; Marcazzan et al., 2001):

$$CM = 1.89Al + 1.21K + 1.43Fe + 1.4Ca + 1.66Mg + 1.7Ti + 2.14Si \quad (4.1)$$

Ca and Mg correspond to their non-sea-salt portions and Si concentration, which was not measured in this study, was estimated as 3.41x Al (Hueglin et al., 2005).

We should note that multiplying Ca and Mg by their respective factors could lead to an overestimation of their oxides, if Ca and Mg were associated with nitrate or sulfate ions, which are directly measured and included in the mass closure. However, a sensitivity analysis showed that using this approach would only result in a $2 \pm 0.38\%$ (arithmetic mean \pm standard error) overestimation in the reconstructed mass across sites and particle-size fractions. Its impact on the overall mass balance is thus minimal. Lastly, TE consists of the remaining measured elements such as Cu, Zn and Cr.

In the coarse fraction, CM was the predominant component at the background site ($22.9 \pm 8.1\%$), while the second most abundant compound ($12.2 \pm 3\%$), closely following OM ($19.4 \pm 3.4\%$), at the freeway site. These rather low CM fractions will be discussed in a subsequent section. On the other hand, accumulation and quasi-ultrafine PM modes were dominated by OM (46-56%) at the near-freeway site while SI (54-68%) dominated at the background location. This variability in particle composition between sites, mainly for $PM_{0.25}$ and $PM_{2.5-0.25}$, confirms that these modes are strongly dependent on sources in their microenvironment.

4.3.2.1 Carbonaceous Species

In $PM_{2.5-0.25}$ and $PM_{0.25}$, OM was the most prevalent component at the near-freeway location (45.7-55.8%) while the next most prominent species at the background site (15.2-29.3%). Its contribution to the coarse fraction was moderate at both locations, averaging less than 19.4% and $6.5 \mu\text{g}/\text{m}^3$.

To evaluate the extent of primary and secondary contributions to the organic mass, the variation in size-resolved OC, WSOC and EC concentrations is shown in Figure 4.3a-b for each site.

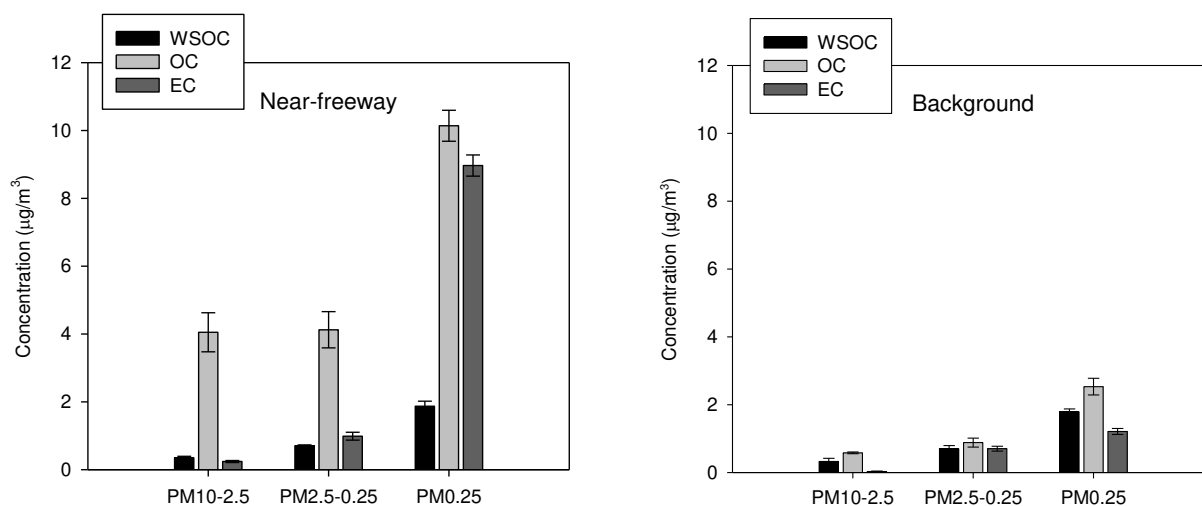


Figure 4.3a-b. Average concentration of water-soluble organic carbon (WSOC), organic carbon (OC) and elemental carbon (EC) in $PM_{10-2.5}$, $PM_{2.5-0.25}$ and $PM_{0.25}$ at the a) near-freeway and b) urban background sites. Error bars correspond to one standard error.

As can be inferred, the majority of these carbonaceous species (55-88%) is confined in the quasi-ultrafine mode. OC in the fine fraction can be directly emitted from primary sources, such as fossil fuel combustion, or produced via secondary organic aerosol (SOA) formation processes; whereas OC in the coarse fraction may also include biological debris (Bauer et al., 2008; Putaud et al., 2004). OC was mostly water-insoluble at the freeway site, corroborating its predominantly primary origin. Its concentration ranged from a low of $4 \mu\text{g}/\text{m}^3$ in $PM_{10-2.5}$ to a high of $10.1 \mu\text{g}/\text{m}^3$ in $PM_{0.25}$ and was 4-7—fold greater than levels at the background site. This trend is

consistent with substantial contributions from vehicular sources at the highly trafficked-freeway site. Although OC concentration significantly varied between locations, mass levels of $PM_{2.5-0.25}$ - and $PM_{0.25}$ -WSOC, indicators of SOA formation processes (Weber et al., 2007), were comparable ($p>0.05$) across the two sites, likely suggesting their regional secondary nature. Moreover, OC was largely water-soluble at the background site, particularly in the quasi-ultrafine ($71.7\pm 0.1\%$) and accumulation ($79.2\pm 0.1\%$) size ranges, indicating its mainly secondary origin. Its water-soluble fraction varied from $0.69 \mu\text{g}/\text{m}^3$ in $PM_{2.5-0.25}$ to $1.79 \mu\text{g}/\text{m}^3$ in $PM_{0.25}$. Lastly, it is noteworthy that size-resolved OC levels are 2-4 times levels at I-710 in Los Angeles, CA (Kam et al., 2012), as can be inferred from Figure 4.4a. I-710 is characterized by a HDDV composition of 11-25% and a total vehicular traffic flow of 4247 vehicles/hour (Kam et al., 2012; Ntziachristos et al., 2007c), roughly half of that estimated for the freeway in this study. In contrast, levels at the background site are comparable to those measured at an urban background location in LA (Kam et al., 2012) (Figure 4.4a).

EC, which could originate from various sources in urban locations such as diesel exhaust and smoking vehicles (Schauer, 2003), minimally contributed to coarse PM at both sites, accounting for less than 0.7% and $0.24 \mu\text{g}/\text{m}^3$ of its mass. Its contribution to fine PM was more significant, with EC dominating the quasi-ultrafine mode and comprising 25.3 ± 0.9 and $8.9\pm 0.9\%$ of $PM_{0.25}$ at the near-freeway and background sites, respectively. Its $PM_{0.25}$ -levels varied from $9.0 \mu\text{g}/\text{m}^3$ at the roadside location to $1.2 \mu\text{g}/\text{m}^3$ at the background site, spanning a 7.4-fold increase, which indicates a considerable impact from HDDVs or also smoking vehicles on particle levels at the freeway. At the coastal background site, EC could partly originate from non-road sources such as diesel generators, largely used due to regular power outages, or also fuel oil combustion given the site's proximity to nearby ports (1.5-2.5 km). Finally, it is worth

noting that $PM_{0.25}$ -EC levels at the freeway site greatly exceed (5-fold) those measured at the I-710 in LA, which is characterized by a high truck flow of 470/hour (Kam et al., 2012) (Figure 4.4b). This is likely due to lack of diesel particulate filters and higher prevalence of smoking vehicles (vehicles emitting atypically large amounts of lubricating oil) in Lebanon than LA. Mobile sources in Lebanon are characterized by a large, old (average age exceeds 13 years) and poorly maintained vehicular fleet (MoE/UNDP/GEF, 2011; MoE/URC/GEF, 2012).

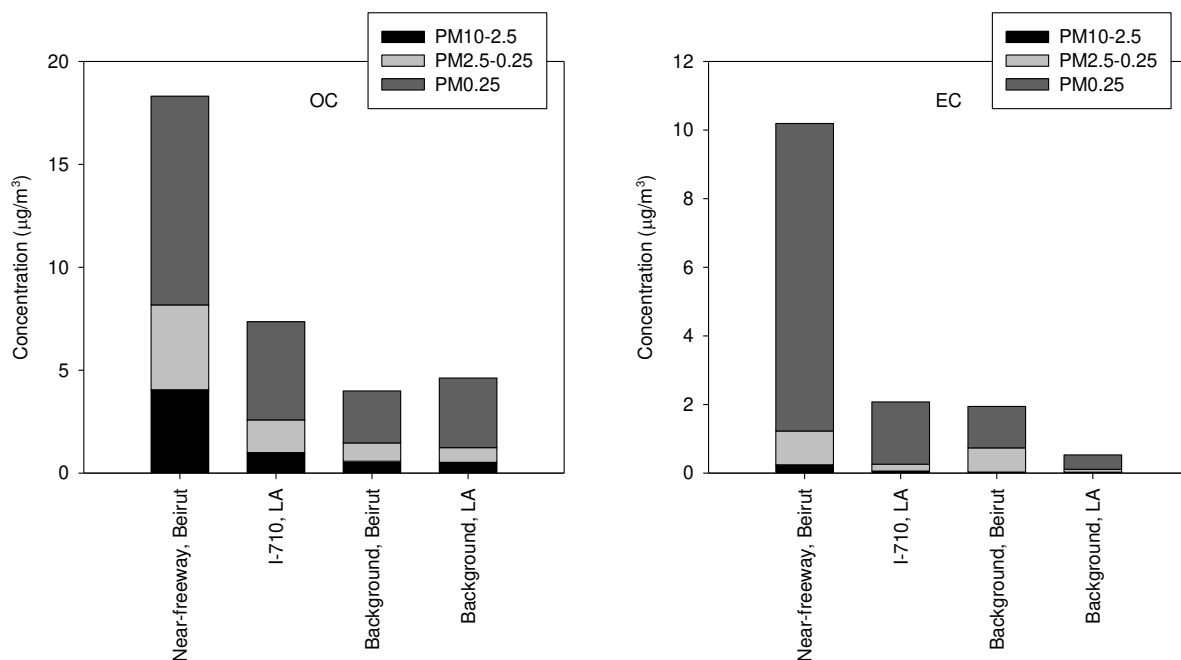


Figure 4.4a-b. Comparison of size-resolved a) organic carbon (OC) and b) elemental carbon (EC) concentrations (current study) with data from I-710 freeway and an urban background site in the Los Angeles (LA) area (Kam et al., 2012).

4.3.2.2 Secondary Ions

Coarse mode-SI contributed only marginally to $PM_{10-2.5}$ (< 14% and $2.3 \mu\text{g}/\text{m}^3$), with nitrate dominating its mass (77-93%, $1.5\text{-}2.1 \mu\text{g}/\text{m}^3$), followed by nss-sulfate (7-23%, $0.2\text{-}0.4 \mu\text{g}/\text{m}^3$), as shown in Figure 4.5a-b. Ammonium was undetected in this mode, consistent with several studies which documented that ammonium particles mostly exist in the fine mode (Karageorgos and Rapsomanikis, 2007; Sillanpää et al., 2006). Coarse nitrate and nss-sulfate,

which exhibited overall comparable concentrations across sites, are likely formed from the respective reactions of nitric and sulfuric acids with soil dust (Noble and Prather, 1996; Zhuang et al., 1999), promoted by the calcium-carbonate-rich soil in Lebanon, as demonstrated by a previous study conducted in the Beirut area (Kouyoumdjian and Saliba, 2006). A significant fraction of these anions could also originate from the reaction of nitric and sulfuric acids with sea salt (Noble and Prather, 1996), given the proximity of the sites to the Mediterranean Sea (150-400 m).

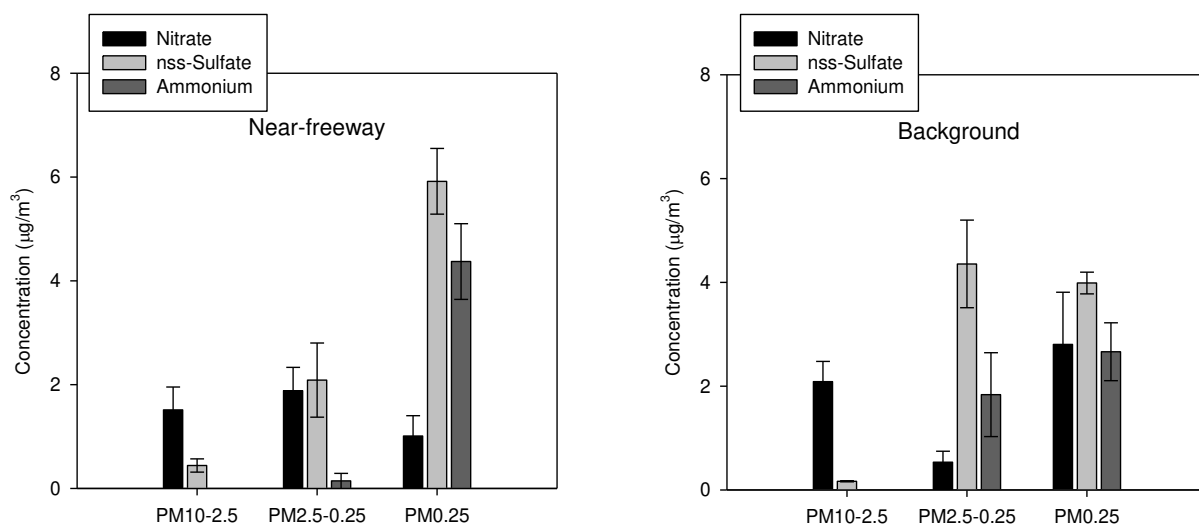


Figure 4.5a-b. Average concentration of nitrate, non-sea-salt sulfate and ammonium in PM_{10-2.5}, PM_{2.5-0.25} and PM_{0.25} at the a) near-freeway and b) urban background sites. Error bars correspond to one standard error.

These observations are further supported by a charge balance, estimated as the ratio of ($\text{Na}^+ + \text{NH}_4^+ + \text{ssCa}^{2+} + \text{ssMg}^{2+}$) to ($\text{Cl}^- + \text{NO}_3^- + \text{SO}_4^{2-}$) in equivalent units. This balance revealed a non-neutralized aerosol in the coarse fraction, indicating that the excess nitrate and sulfate are possibly in the form of soil-associated calcium nitrate and sulfate (Figure 4.6).

In quasi-ultrafine and accumulation PM, SI was the major component at the background location (54-68%) while the next most abundant species at the freeway site (29-31%). Nss-sulfate was mostly prevalent among secondary ions in PM_{0.25} and PM_{2.5-0.25}, accounting for 2.1-

5.9 $\mu\text{g}/\text{m}^3$ and 42–65% of their collective mass across sites and modes. Ammonium and nitrate were less abundant, with ammonium contributing to 0.14/4.4 and 1.8/2.7 $\mu\text{g}/\text{m}^3$ in $\text{PM}_{2.5-0.25}/\text{PM}_{0.25}$ at the near-freeway and background sites, respectively. Nitrate, averaging 1.01 and 2.8 $\mu\text{g}/\text{m}^3$ in $\text{PM}_{2.5-0.25}$ and $\text{PM}_{0.25}$, respectively, at the background location, is potentially in the form of ammonium nitrate formed from the photochemical reaction of nitric acid with ammonia (Robarge et al., 2002). On other hand, nitrate was primarily in the accumulation mode at the near-freeway site, averaging 1.9 and 0.5 $\mu\text{g}/\text{m}^3$ in $\text{PM}_{2.5-0.25}$ and $\text{PM}_{0.25}$, respectively. The dominance of nitrate in $\text{PM}_{2.5-0.25}$ at the roadway could be related to its predominant association with calcium or sodium in this mode. Ammonia is possibly consumed by gaseous precursors of sulfate (i.e. SO_2) at the freeway site, which may be present at higher levels at that site due to additional contributions from traffic emissions. Given the potentially low availability of ammonia, nitric acid is more likely to react with sea-salt or soil. Nss-sulfate, on the other hand, is likely present as ammonium sulfate, formed from photochemical reactions of ammonia with sulfuric acid (Robarge et al., 2002), as suggested by its strong correlation with ammonium at both sites ($R=0.74-0.95$ and $p<0.05$). This observation is in agreement with a previous study conducted in this region (Kouyoumdjian and Saliba, 2006). Additionally, it is noteworthy that sulfate and ammonium display fairly uniform concentrations in $\text{PM}_{2.5}$ across the two sites ($p>0.05$), suggesting their predominantly regional secondary nature due to the long-range transport of their precursor gases. SO_2 levels in the eastern Mediterranean basin and Lebanon, in particular, are highly influenced by air masses originating from eastern and central Europe (Saliba et al., 2007b; Sciare et al., 2003). This was further confirmed by a backward air mass trajectory analysis, using HYSPLIT model (Draxler and Rolph, 2003), which showed predominantly N-NW winds during the sampling campaign (Figure 4.7). Local primary sources

such as diesel-operating buses and ship emissions may also contribute to SO₂ emissions and sulfate formation, to some extent. PM_{0.25}-sulfate could originate from bunker fuel combustion from marine vessels (Arhami et al., 2009), particularly at the background site given its close proximity (ca. 2.5 km) to the commercial port of Beirut.

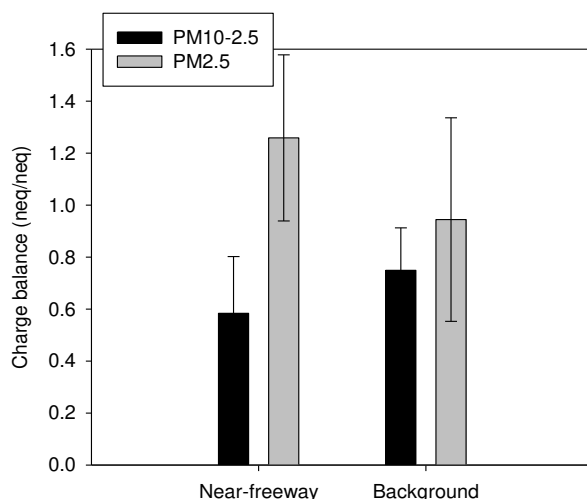


Figure 4.6. Average charge balance ratio of cations (Na^+ , NH_4^+ , ssCa^{2+} , Mg^{2+}) to anions (Cl^- , NO_3^- , SO_4^{2-}). Error bars represent one standard error.

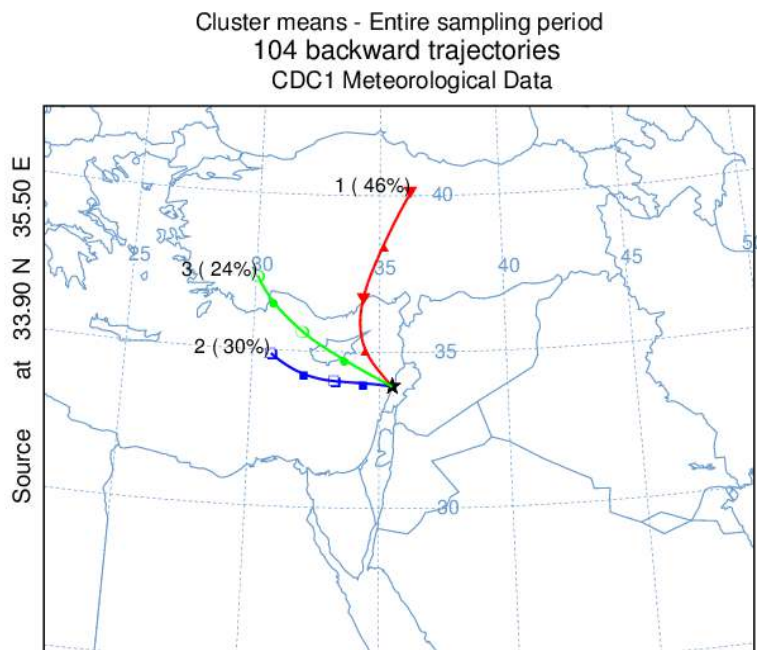


Figure 4.7. Backward air mass trajectories for the entire sampling campaign (July-August 2012), simulated using HYSPLIT model from NOAA. For each sampling day, four 48-hour trajectories were modeled every six hours at 500 m-agl using vertical wind velocity field from the meteorological data.

4.3.2.3 Sea-Salt

Sea-salt mass concentration was considerably higher in $PM_{10-2.5}$ relative to the other two size fractions, with about 75% of sea-spray accounted for in the coarse mode at both sampling locations, consistent with expectations. Furthermore, although $PM_{10-2.5}$ -SS existed in similar amounts at both sites (2.37 ± 0.91 and 2.31 ± 0.46 $\mu\text{g}/\text{m}^3$, on average), sea-salt was a more significant component of coarse PM at the coastal background site than the traffic-impacted freeway location, accounting for 14.7 ± 3.1 and $7.3\pm 2.8\%$ of its mass, respectively.

4.3.2.4 Crustal Material and Trace Elements

At both sites, CM was more prevalent in the coarse mode than accumulation and quasi-ultrafine particle-size fractions. It accounted for 12.2 ± 3.0 and $22.9\pm 8.1\%$ of $PM_{10-2.5}$ at the near-freeway and background locations, respectively. These proportions are, however, low compared to other Mediterranean areas, where 36% (Barcelona) to 65% (Athens) CM mass fractions were reported during spring and summer (Sillanpää et al., 2006). CM may be under-represented using the sum of oxides method since this technique does not include all components known to contribute to dust. Moreover, soil in Lebanon is rich in calcite and limestone rocks (Abdel-Rahman and Nader, 2002; Kouyoumdjian and Saliba, 2006). Its mineral content may therefore be underestimated using a factor of 1.4 to account for Ca oxides. Andrews et al. (2000) reported that, depending on the soil composition, the crustal mass may be underestimated by as much as 50% using the sum of oxides approach. Furthermore, although vehicular-induced resuspension is expected to promote CM concentration at the freeway site, $PM_{10-2.5}$ -CM levels were comparable at the background and near-freeway locations, averaging 3.8 ± 1.6 and 4.1 ± 0.95 $\mu\text{g}/\text{m}^3$, respectively. Soil dust re-suspension at the background site may be enhanced by local sea breeze or also construction activities and vehicular traffic nearby the site. The site is about 150 m away

from a coastal road, where the driving mode involves intermittent acceleration and deceleration of vehicles at intersections and street shops, which could increase dust re-suspension.

Trace metals' contribution was consistently low at 0.5-1.8% for all size fractions and sites.

4.3.2.5 Chemical Mass Closure

Chemical mass balance results show an overall good agreement between the reconstructed and gravimetric PM mass. Percent mass apportioned varied between 45-123% across size fractions and sites, with lesser agreement observed for the coarse mode, particularly at the freeway site. The fraction of unknown mass for PM_{10-2.5} is nonetheless consistent with other studies, which reported a 28-50% range of unaccounted coarse PM mass (Hueglin et al., 2005; Putaud et al., 2004). The unidentified mass could be related to uncertainties in the gravimetric and chemical measurements. Unmeasured crustal components and uncertainties in the correction factors used to account for oxides of metals could also lead to some inconsistency, particularly for the coarse fraction. Uncertainty in the multiplication factor used to convert OC to OM could further explain the discrepancy in the masses. The greater unknown PM_{10-2.5} mass at the roadside than background location, in particular, could be mainly attributed to an underestimation of this factor. The latter depends on sources of organic components, which may display a considerable spatial variation and are generally not well-characterized for coarse particles. Previous studies documented that dicarboxylic acids, including malonic and succinic acids, are present in significant amounts in coarse PM at traffic-impacted sites (Oliveira et al., 2007; Yao et al., 2004). These organics also display a high organic molecular weight per carbon weight ratio. Based on measurements of Rogge et al. (1993d) in downtown LA, Turpin and Lim (2001) estimated the average organic molecular weight per carbon weight ratio of diacids, including an oxalic acid estimate, as 3.29. The application of a fixed conversion factor of 1.6 and

the higher abundance of coarse OM at the near-freeway ($19.4\pm 3.4\%$) than background site ($5.8\pm 0.3\%$) could lead to an underestimation of OM and thus to a significantly greater unknown mass fraction in $PM_{10-2.5}$ at the freeway location.

4.3.3 Organic Compounds Characterization

To further investigate PM-organic composition, size-resolved mass concentrations (arithmetic mean \pm standard error) of PAHs, hopanes, steranes, n-alkanes and carboxylic acids were determined at each sampling site as summarized in Table 4.2 and Figures 4.8a-c and 4.9a-b. Undetected compounds or compounds with a concentration below the limit of detection (LOD) are reported as bdl. These values were also treated as zero in the reported sums. LOD for a given species is estimated as two times its uncertainty measurement in the limit as the concentration of the compound approaches zero. The LODs for speciated organics are listed in Tables 4.2 and 4.3.

4.3.3.1 Polycyclic Aromatic Hydrocarbons (PAHs)

Polycyclic aromatic hydrocarbons (PAHs), many of which have been identified as potent human carcinogens (IARC, 1987) are common products of incomplete combustion (Manchester-Neesvig et al., 2003). Because of their semi-volatile nature, these species can partition between the gaseous and particulate phase, depending on ambient temperature and atmospheric dilution conditions (Mader and Pankow, 2002; Zielinska et al., 2010). Levels at the background site were below detection limit for all size-fractionated PAHs, as shown in Table 4.2. This site is surrounded by mostly pedestrian roads and dense vegetation covers, with the nearest street located about 150 m away. PAH emissions from this adjacent road are likely shifted to the gaseous phase during their advection from the roadway to the sampling site. The high summertime temperatures coupled with frequent daytime on-shore winds and increased atmospheric dilution at this non-enclosed coastal site likely favor the volatilization,

photodegradation and dispersion of PAHs. In contrast, levels of PAHs reached a cumulative concentration of $11.5 \pm 0.6 \text{ ng/m}^3$ at the near-freeway site, with the majority distributed in the quasi-ultrafine size range. Most of the measured compounds displayed concentrations that are about an order of magnitude higher in $\text{PM}_{0.25}$ than $\text{PM}_{2.5-0.25}$. Moreover, while high and medium molecular weight (MW) ($\text{MW} \geq 276 \text{ amu}$ and $\text{MW} = 252 \text{ amu}$, respectively) benzo(ghi)perylene, coronene, benzo(e)pyrene and benzo(b)fluoranthene were the predominant PAHs in $\text{PM}_{0.25}$ and $\text{PM}_{2.5-0.25}$, low MW PAHs ($\leq 228 \text{ amu}$) were also detected in the quasi-ultrafine mode. These results indicate significant contributions from light-duty vehicles (LDVs) as well as HDDVs to PAH levels at the roadway. Previous works showed that both gasoline- and diesel-powered motor vehicles contribute to high MW PAHs, whereas HDDVs are the major source of low MW PAHs (Ning et al., 2008; Schauer et al., 2002). Benzo(a)pyrene, commonly used as an index for PAH carcinogenicity (Menichini et al., 1999), exhibited a cumulative concentration of 0.69 ng/m^3 , exceeding that reported at I-710-freeway in LA by about 7 times (Liacos et al., 2012). Size-segregated overall PAH concentrations were also 1.3-3.9 fold greater relative to those measured at I-710 (Liacos et al., 2012), indicating substantial vehicular combustion emissions at the near-freeway site.

Table 4.2. Average (\pm standard error) concentration and limit of detection (LOD) of PAHs, hopanes and steranes in PM_{10-2.5}, PM_{2.5-0.25} and PM_{0.25} at the near-freeway and urban background sites.

	PM10-2.5		PM2.5-0.25		PM0.25		LOD	
	Near-freeway	Background	Near-freeway*	Background	Near-freeway	Background		
PAHs (ng/m³)	Pyrene	bdl	bdl	bdl	bdl	0.4 \pm 0.01	bdl	0.05
	Benzo(ghi)fluoranthene	bdl	bdl	bdl	bdl	0.8 \pm 0.39	bdl	0.04
	Benzo(a)anthracene	bdl	bdl	bdl	bdl	0.4 \pm 0.02	bdl	0.15
	Chrysene	bdl	bdl	bdl	bdl	0.7 \pm 0.03	bdl	0.07
	Benzo(b)fluoranthene	bdl	bdl	0.11 \pm 0.04	bdl	1.3 \pm 0.04	bdl	0.08
	Benzo(k)fluoranthene	bdl	bdl	0.05 \pm 0.01	bdl	0.64 \pm 0.04	bdl	0.04
	Benzo(e)pyrene	bdl	bdl	0.1 \pm 0.03	bdl	1.4 \pm 0.02	bdl	0.06
	Benzo(a)pyrene	bdl	bdl	0.06 \pm 0.02	bdl	0.63 \pm 0.03	bdl	0.04
	Indeno(1,2,3-cd)pyrene	bdl	bdl	0.1 \pm 0.03	bdl	1.1 \pm 0.06	bdl	0.07
	Benzo(ghi)perylene	bdl	bdl	0.17 \pm 0.02	bdl	2.6 \pm 0.12	bdl	0.07
	Coronene	bdl	bdl	0.1 \pm 0.03	bdl	1.6 \pm 0.03	bdl	0.06
	Total	-	-	0.7 \pm 0.07	-	11.5 \pm 0.59	-	-
Hopanes and steranes (ng/m³)	17 α (H)-22,29,30-Trisnorhopane	bdl	bdl	0.22 \pm 0.02	bdl	0.32 \pm 0.05	bdl	0.08
	17 α (H)-21 β (H)-30-Norhopane	0.2 \pm 0.02	bdl	0.78 \pm 0.08	bdl	2.4 \pm 0.13	0.05 \pm 0.05	0.03
	17 α (H)-21 β (H)-Hopane	0.15 \pm 0.03	bdl	0.62 \pm 0.12	bdl	3.3 \pm 0.12	0.1 \pm 0.09	0.03
	22S-Homohopane	0.15 \pm 0.02	bdl	0.54 \pm 0.04	bdl	4.1 \pm 0.25	0.1 \pm 0.09	0.03
	22R-Homohopane	0.09 \pm 0.02	bdl	0.4 \pm 0.03	bdl	3.3 \pm 0.14	0.1 \pm 0.07	0.03
	22S-Bishomohopane	0.13 \pm 0.02	bdl	0.32 \pm 0.02	bdl	2.9 \pm 0.22	bdl	0.03
	22R-Bishomohopane	0.1 \pm 0.0001	bdl	0.2 \pm 0.02	bdl	2.2 \pm 0.15	bdl	0.03
	22S-Trishomohopane	bdl	bdl	0.2 \pm 0.02	bdl	2.3 \pm 0.08	bdl	0.04
	22R-Trishomohopane	bdl	bdl	0.14 \pm 0.01	bdl	1.3 \pm 0.06	bdl	0.04
	$\alpha\alpha$ -20S-C27-Cholestane	bdl	bdl	0.13 \pm 0.02	bdl	0.38 \pm 0.06	bdl	0.04
	$\alpha\beta$ -20R-C27-Cholestane	bdl	bdl	0.13 \pm 0.01	bdl	0.24 \pm 0.01	bdl	0.04
	$\alpha\alpha$ -20R-C27-Cholestane	bdl	bdl	0.14 \pm 0.02	bdl	0.37 \pm 0.04	bdl	0.04
	Total	0.82 \pm 0.09	-	3.8 \pm 0.16	-	23.1 \pm 0.89	0.29 \pm 0.28	-

bdl indicates an undetected compound or a concentration below detection limit. *Error corresponds to analytical uncertainty

4.3.3.2 Hopanes and Steranes

Hopanes and steranes, which are derived from fuel oil and automotive lubricating oil (Rogge et al., 1993a; Schauer et al., 2002), were several folds greater at the near-freeway site than background location, confirming a strong impact from vehicular exhaust on PM levels at the roadway (table 2.2). Similarly to PAHs, hopanes and steranes were mostly confined in the quasi-ultrafine mode, with 17 α (H)-21 β (H)-hopane, 22S-homohopane and 22R-homohopane prevailing at both sites. In proximity of the freeway, hopanes and steranes displayed a collective concentration ranging from a low of 0.82 ng m⁻³ in PM_{10-2.5} to a high of 23.1 ng m⁻³ in PM_{0.25}. These levels were 2.1-17.4 times those measured at diesel-impacted I-710 freeway in California (Liacos et al., 2012). Additionally, these organic compounds exhibited high hopanes plus steranes-to-total carbon (TC=OC+EC) ratios (0.16-1.1 ng/ μ g) compared to those recorded at I-710 (0.20-0.35 ng/ μ g) (Liacos et al., 2012), which is likely related to different engine operating conditions and configurations (e.g. after-treatment control technologies) or also lubricating oil formulation. The Lebanese vehicular fleet is characterized by a high percentage of non-catalyst equipped vehicles (Waked and Afif, 2012). At the coastal background site, unlike PAHs which were below detection limit, PM_{0.25}-hopanes exhibited a cumulative mean concentration of 0.29 \pm 0.28 ng/m³. Because of their lower vapor pressure, hopanes are more atmospherically stable than PAHs (Zielinska et al., 2004) and may thus be less sensitive to meteorological conditions at this site. The large error associated with the measured levels suggests a change in source strength or an impact from multiple sources, such as vehicular emissions and nearby harbor activities. Marine vessels may contribute to urban concentrations of hopanes (Peters et al., 1992).

4.3.3.3 N-Alkanes

To assess the influence of anthropogenic and biogenic emissions at the sampling sites, size-resolved particle-phase n-alkanes (C_{19} - C_{34}) were quantified, as illustrated in Figure 4.8a-c. The origin of the selected n-alkanes was investigated by estimating their carbon preference index (CPI), defined as the concentration ratio of their odd-to-even numbered homologues (Simoneit, 1989). A CPI about 1 indicates a dominance of anthropogenic sources, whereas a CPI greater than 2 suggests a prevalence of biogenic sources (Arhami et al., 2010; Simoneit, 1989). In both coarse and accumulation modes, overall levels of n-alkanes were several folds greater (4.5-16.6 times) at the near-freeway compared to the background site. While $PM_{2.5-0.25}$ -bound n-alkanes at the roadside displayed notable peaks at C_{29} and C_{31} , a signature of biogenic sources (Rogge et al., 1993c), these compounds were characterized by a predominance of homologues $<C_{25}$ and a CPI approaching 1 (1.31). Coarse mode n-alkanes showed a similar distribution, with a CPI close to 1 (0.70 ± 0.03) and maxima at C_{22} and C_{23} . These profiles confirm a strong impact from vehicular combustion emissions at the freeway site. Rogge et al. (1993a) found that fine particulate n-alkanes emitted from diesel and gasoline exhaust emissions show no carbon number preference but rather high levels of n-alkanes in C_{19} - C_{25} . In $PM_{0.25}$, C_{19} - C_{34} at the near-freeway site, which accounted for most of total n-alkanes mass (86%), averaged 74.6 ± 3.4 ng/m³, with n-alkanes enriched across the entire range of carbon numbers and a CPI of 1.03 ± 0.08 . This distribution indicates both road dust and vehicular exhaust emissions as major sources of n-alkanes in proximity of the freeway. N-alkanes derived from fine particulate road dust exhibit no carbon number preference, but greater concentrations for high MW homologues (Rogge et al., 1993b). At the background site, $PM_{0.25}$ -n-alkanes were consistently lower than those at the freeway location, reaching a total concentration of 18.7 ± 4.3 ng/m³ with a CPI of 1.2 ± 0.06 . These

compounds were also dominated by high MW congeners, spanning homologues up to C₃₃, which suggests road dust as a dominant source of n-alkanes at this site.

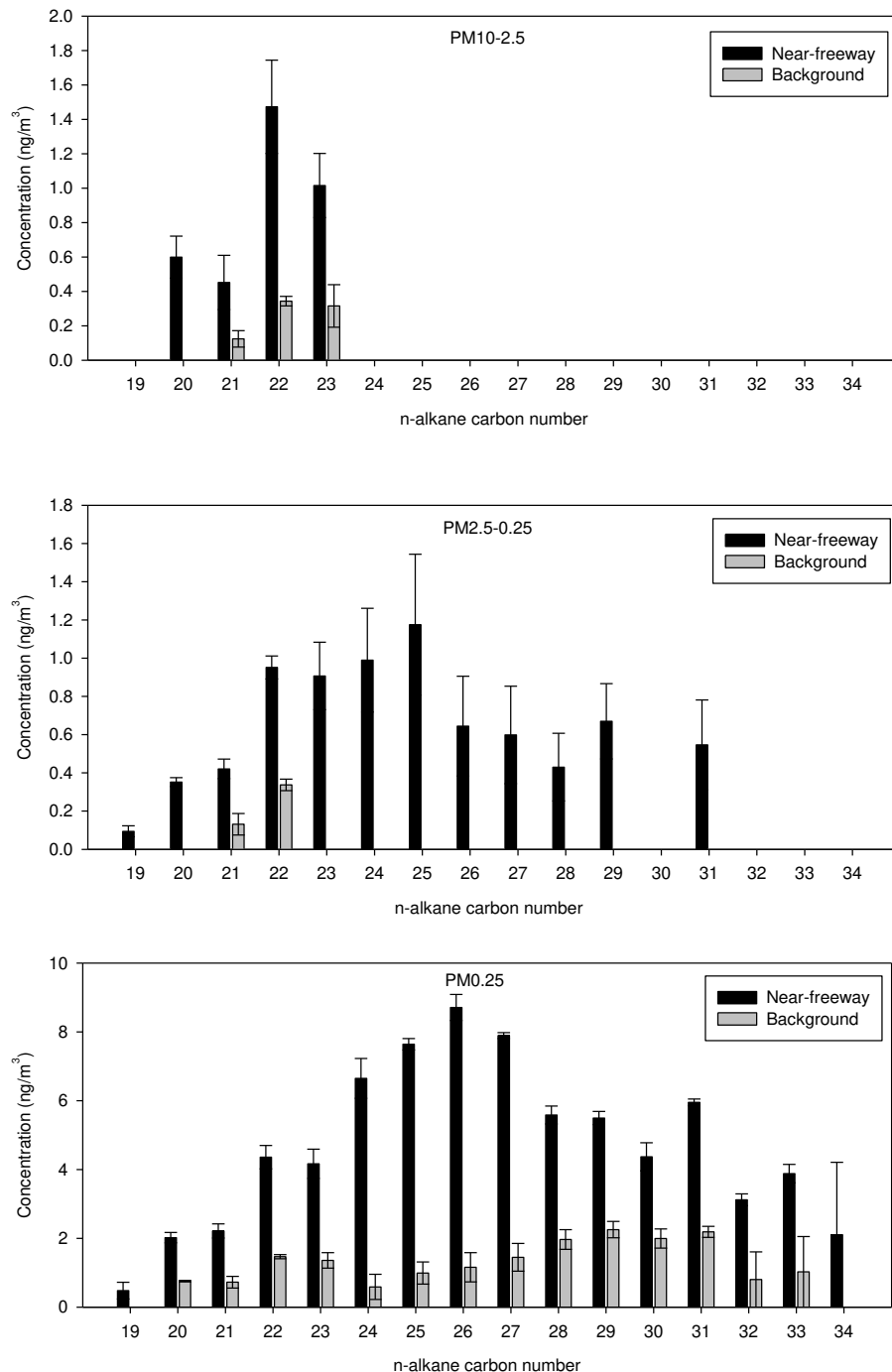


Figure 4.8a-c. Average n-alkanes concentration (C₁₉-C₃₄) in a) PM_{10-2.5}, b) PM_{2.5-0.25} and c) PM_{0.25} at the near-freeway and urban background sites. Only values above the limit of detection (LOD) are shown. Error bars correspond to one analytical or standard error.

Table 4.3 Limit of detection (LOD) of n-alkanes and dicarboxylic acids.

Limit of detection (LOD), ng/m ³					
n-alkanes	Nonadecane	0.13	Dicarboxylic acids	Phthalic acid	0.64
	Eicosane	0.02		Methylphthalic acid	0.68
	Heneicosane	0.15		Azelaic acid	0.58
	Docosane	0.02		Succinic acid	0.56
	Tricosane	0.26			
	Tetracosane	0.37			
	Pentacosane	0.35			
	Hexacosane	0.37			
	Heptacosane	0.62			
	Octacosane	0.45			
	Nonacosane	0.55			
	triacontane	0.56			
	Hentriacontane	0.85			
	Dotriacontane	0.97			
	Tritriacontane	1.08			
	Tetratriacontane	1.00			

4.3.3.4 Dicarboxylic Acids

Dicarboxylic acids have several different sources, including primary traffic emissions and photochemical oxidation of anthropogenic or biogenic volatile organic compounds (Rogge et al., 1993d). Figure 4.9a-b presents the average concentration of select dicarboxylic acids. These acids were mostly partitioned in the quasi-ultrafine mode at both sites. PM_{0.25}-succinic and -azelaic acids displayed generally comparable concentrations (4.8-5.8 and 8.4-9.1 ng/m³) across sampling locations, suggesting photo-oxidation of biogenic unsaturated fatty acids as their potential source (Stephanou and Stratigakis, 1993). A fraction of succinic and azelaic acids (12.3 and 9.4%, respectively) was also observed in the coarse mode at the freeway site, which may be associated with their evaporation from smaller-size modes and subsequent condensation onto coarse particles due to their semi-volatile nature (Limbeck et al., 2001), especially at high

ambient temperatures such as those in Beirut during our sampling period. On the other hand, phthalic and methylphthalic acids in $PM_{0.25}$ varied from a high (13.4 and 4.3 ng/m^3 , respectively) at the near-freeway site to a low (6 and 1.9 ng/m^3 , respectively) at the background location, indicating their potentially engine exhaust source or formation by atmospheric chemical reactions involving directly emitted PAHs (Rogge et al., 1993d).

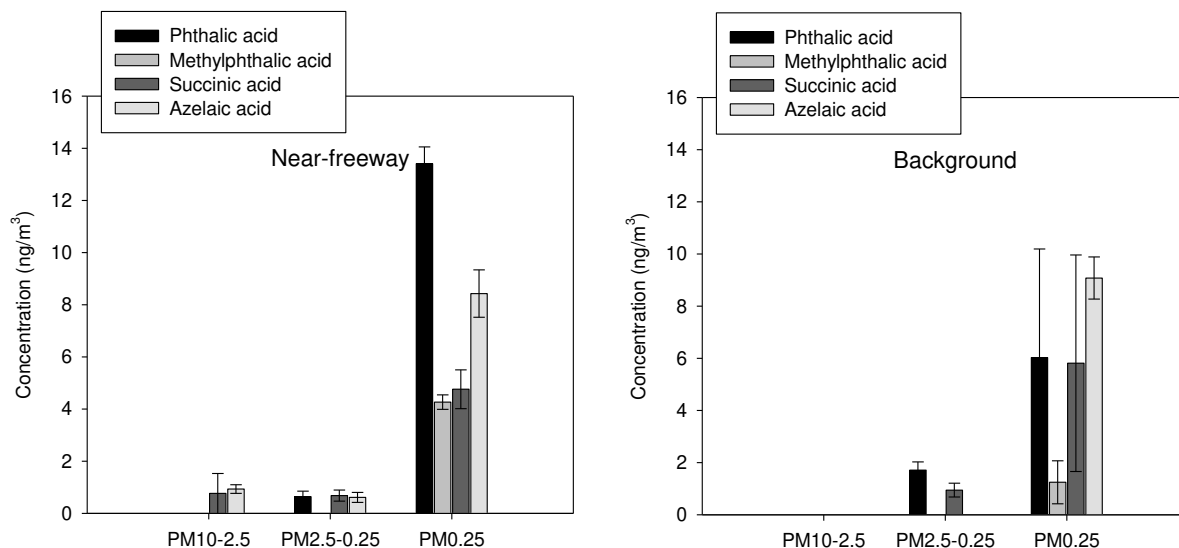


Figure 4.9a-b Average concentration of dicarboxylic acids in $PM_{10-2.5}$, $PM_{2.5-0.25}$ and $PM_{0.25}$ at the a) near-freeway and b) background sites. Only values above the limit of detection (LOD) are shown. Error bars correspond to one standard or analytical error.

4.4 Summary and Conclusions

To investigate road-traffic emissions in the Greater Beirut area, $PM_{10-2.5}$, $PM_{2.5-0.25}$ and $PM_{0.25}$ samples were concurrently collected at near-freeway and background sites. Particle mass levels at the background location were significantly lower than those at the roadway for all size modes. PM at the background site was mainly influenced by secondary sources as evidenced by SI contribution to the overall particle mass (~50%). The prevalence of secondary emissions was further confirmed by OM, which accounted for 17% of PM_{10} and was mostly water-soluble

(70.4%) at this location. Contrarily, particle levels at the near-freeway location were dominated by vehicular emissions from both road dust and tailpipe. OM, which accounted for 46-56% of $PM_{2.5-0.25}$ and $PM_{0.25}$, was mainly water-insoluble at this location, indicating its predominantly primary origin. Moreover, $PM_{0.25} \cdot EC$ varied from $1.2 \mu\text{g}/\text{m}^3$ at the background site to $9.0 \mu\text{g}/\text{m}^3$ in proximity of the freeway, highlighting a strong impact from HDDVs or also smoking vehicles on roadway emissions. The influence of HDDVs in addition to LDVs was further supported by PAHs molecular composition. Both high and low MW PAHs were detected in significant levels near the freeway. Moreover, relative to other roadways, speciated organics exhibited high hopanes plus steranes-to-total carbon ratios (0.16-1.1 ng/ μg), indicating dissimilar engine configurations or also lubricating oil formulation. Lastly, CM, indicative of soil dust resuspension, was a significant component of coarse particles at both sites. Road-dust contribution to PM at both locations was also corroborated by $PM_{0.25}$ -bound n-alkanes which were enriched in high MW congeners and showed no carbon number preference. Dicarboxylic acids were mostly partitioned in $PM_{0.25}$, with phthalic and methylphthalic acids existing in greater amounts at the roadway. Dicarboxylic acids were mostly partitioned in $PM_{0.25}$, with phthalic and methylphthalic acids existing in greater amounts at the roadway.

Results of this work provide insight on commuter exposure to traffic-related PM in the area of Beirut. Compared to I-710—a heavy-duty diesel-impacted freeway in southern California—levels of toxic vehicular tracers were substantially greater at the roadway in this study. This can be attributed to different fuel composition as well as higher prevalence of old and non-catalytic vehicles in the Greater Beirut area. These findings call for pressing and stricter regulations on motor vehicles. Size-resolved PM redox activity at these sites and its association to particle composition is discussed in Chapter 5.

4.5 Acknowledgements

This research was supported by the University of Southern California (USC) School of Engineering Fred Champion Endowment and the American University of Beirut (AUB) Faculty of Engineering & Architecture. We wish to acknowledge the support of USC Provost's Ph.D. fellowship and the NOAA Air Resources Laboratory (ARL) for providing the HYSPLIT model. We would like to thank the staff at Wisconsin State Laboratory of Hygiene for their assistance with the chemical measurements and wish to acknowledge Professor James Schauer and Dr. Martin Shafer. We also would like to thank the staff at AUB chemistry department

Chapter 5 A Comparative Assessment of the Oxidative Potential of PM: The Role of Particle-Size and Chemical Composition

What is the role of PM physico-chemical characteristics in inducing toxicity?

Are PM components from all sources equally toxic or are some components of greater concern?

How does PM intrinsic ROS-activity vary across urban settings?

An increasing body of epidemiological and toxicological evidence indicates robust associations between adverse health effects and mass of particulate matter (PM) (Peters, 2001; Pope, 2002). An emerging hypothesis is that many of the biological effects derive from the ability of PM to generate reactive oxygen species (ROS) at the surface of and within affected cells (Li et al., 2003; Nel, 2005). ROS is a collective term comprising chemically reactive oxygen radicals or oxygen-derived species (e.g. hydroxyl radical and hydrogen peroxide) (Halliwell and Cross, 1994). However, while particle mass has been proven useful in demonstrating the associations between PM exposure and health responses, aerosol mass is probably only a surrogate for causal particle components (NRC, 2004). Specific PM species contributing to aerosol toxicity remain to be identified. Particle compounds implicated in ROS formation include organic carbon, polycyclic aromatic hydrocarbons and quinones (Cho et al., 2005; Nel et al., 2001; Squadrito et al., 2001). Transition metals, particularly water-soluble species, may also act directly to catalyze the formation of ROS via redox reactions (Ciapetti et al., 1998; Prahalad et al., 1999). Particle-size could also be critical in mediating PM toxicity. Because of their large surface area, increased number and high pulmonary deposition efficiency (Chalupa et al., 2004; Hughes et al., 1998; Morawska et al., 1998) ultrafine particles ($d_p < 0.1 \mu\text{m}$) may be more potent than larger coarse ($\text{PM}_{10-2.5}$) or fine ($\text{PM}_{2.5}$) particles (Cho et al., 2005; Ntziachristos et al., 2007a). In an effort to investigate the association of ROS-activity with particle-size-resolved and/or chemically-specified PM, two case studies were considered, where a sensitive rat alveolar macrophage-based *in vitro* ROS assay was coupled with chemical fractionation tools. In the first study, $\text{PM}_{2.5}$ samples were collected for a year-long period at a centrally-located urban site in Milan, Italy. In the second study, coarse, accumulation ($\text{PM}_{2.5-0.25}$) and quasi-ultrafine ($\text{PM}_{0.25}$) particle samples were collected at near-freeway and urban background sites in the Greater Beirut area, Lebanon. Results from both studies are subsequently discussed, with an emphasis on ROS-activity and its relation to PM chemical species and particle-size. These results build upon the chemical characterization of samples from both studies, presented in Chapters 3 and 4. The intrinsic redox activity of PM in Beirut—representative of developing areas lacking air quality regulations—is also compared to that of aerosols from other worldwide urban settings, including Milan and Los Angeles, for which similar ROS data, using the same assay, are available. Comparisons across studies to assess PM intrinsic toxicity have generally been difficult since investigators use different assays to measure particle oxidative potential (e.g. dithiothreitol (DTT), dihydroxybenzoate (DHBA) and macrophage-based ROS assays (Ayres et al., 2008)). Findings from these studies support efforts towards establishing more rationally-targeted and source-specific PM control strategies.

This chapter is based on the following publications:

Daher N., Ruprecht A., Invernizzi G., De Marco C., Miller-Schulze J., Heo J. B., Shafer M. M., Shelton B. R., Schauer J. J., Sioutas C., 2012. Characterization, Sources and Redox Activity of Fine and Coarse Particulate Matter in Milan, Italy. *Atmospheric Environment* 49, 130-141.

Daher, N., Saliba N. A., Shihadeh A.L., Malek J., Baalbaki R., Shafer M. M., Schauer J. J., Sioutas C., 2013. Oxidative Potential and Chemical Speciation of Size-Resolved Particulate Matter (PM) at Near-freeway and Urban Background Sites in the Greater Beirut Area. *Under review*.

1. Oxidative Potential of Fine PM (PM_{2.5}) at an Urban Site in Milan, Italy

5.1.1. Introduction

Milan, one of the largest and most polluted urban areas in Western Europe, is afflicted with high particle levels (Putaud et al., 2004). The city is densely populated, characterized by a large volume of vehicular traffic and located in the center of the Po valley, one of the most industrialized regions in Northern Italy with frequently occurring wintertime inversions. Under these conditions, PM can reach elevated levels, frequently exceeding PM₁₀ standards (Lonati et al., 2008). Accurate characterization of particle-induced redox activity in Milan is therefore necessary to properly gauge its potential toxicity.

The chemical composition of PM in Milan has been quite extensively investigated (Lonati et al., 2008; Marcazzan et al., 2001; Vecchi et al., 2004). However, its particle-induced toxicity has only been scarcely explored (Gualtieri et al., 2011; Perrone et al., 2010) and relevant data remains incomplete. In this study, PM_{2.5}-associated redox activity at an urban site in Milan is examined. Fine PM samples were collected for a year-long period then analyzed for their chemical composition and ROS-activity. Results of this study provide a quantitative assessment of PM_{2.5}-induced redox activity in this urban setting and some insights on its key drivers.

Findings can thus be used for implementing more effective and source-specific regulatory strategies in this area.

5.1.2. Methodology

5.1.2.1 Sample Collection

Fine and coarse PM ($PM_{2.5}$ and $PM_{10-2.5}$) samples were collected at about 10 m above ground level in the outside area of Santa Maria Delle Grazie Church in the city center of Milan (+45° 27' 59.51", +9° 10' 14.26"). The sampling campaign lasted from December 2009 to November 2010. During this period, twenty-four-hour size-segregated PM samples were collected on a weekly basis by means of two SioutasTM Personal Cascade Impactor Samplers (SioutasTM PCIS, SKC Inc., Eighty Four, PA, USA (Misra et al., 2002; Singh et al., 2002)). Each PCIS was operated at a flow rate of 9 lpm as well as loaded with 37 and 25 mm filters for $PM_{2.5}$ and $PM_{10-2.5}$ analyses, respectively. However, only the $PM_{2.5}$ fraction is discussed in this chapter, with particular focus on its redox activity and relation to chemical composition. For the purpose of chemical speciation, one PCIS was loaded with Teflon filters (Pall Life Sciences, Ann Arbor, MI) while the other one with quartz microfiber filters (Whatman International Ltd, Maidstone, England). To determine PM mass concentration, the weekly Teflon filters were pre-weighed and post-weighed after equilibration, using a Mettler 5 Microbalance (Mettler Toledo Inc, Columbus, OH, USA) under controlled conditions (relative humidity of 40-45% and temperature of 22-24 °C).

5.1.2.2 Chemical Analyses

To conduct chemical analyses of the $PM_{2.5}$ samples, the Teflon and quartz filters were sectioned into portions. The fractions used for elemental and organic carbon (EC and OC, respectively) determination were grouped into weekly samples and quantified using the NIOSH

Thermal Optical Transmission method (Birch and Cary, 1996). All remaining sections were composited monthly and analyzed for water-soluble OC (WSOC), water-soluble inorganic ions, total metals and organics. WSOC and ionic contents of the samples were measured using a Sievers 900 Total Organic Carbon Analyzer (Stone et al. 2009) and ion chromatography (IC), respectively. The total elemental mass of the filter fractions was measured by means of a high resolution magnetic sector Inductively Coupled Plasma Mass Spectrometry (Thermo-Finnigan Element 2) (Zhang et al., 2008a). A microwave-aided Teflon bomb digestion protocol using a mixture of 1 mL of 16 M nitric acid, 0.25 mL of 12 M hydrochloric acid, and 0.10 mL of hydrofluoric acid was used for this analysis. Moreover, organic speciation was conducted on PM_{2.5} filter composites using gas chromatography mass spectrometry (GC-6980, quadrupole MS-5973, Agilent Technologies). Briefly, the quartz filter composites were spiked with isotopically-labeled standard solutions prior to extraction. Samples were then extracted by dichloromethane and acetone using Soxhlets, followed by rotary evaporation and reduction in volume under high-purity nitrogen. Additional details can be found in Stone et al. (2008).

5.1.2.3 Reactive Oxygen Species (ROS) assay

The macrophage reactive oxygen species (ROS) assay is a fluorogenic cell-based method that assesses ROS production by PM. Prior to the assay, ROS filter fractions were extracted with 1 mL of Milli Q water and filtered through 0.2 µm filters. The experiments were then performed by exposing the rat alveolar cell line (NR8383, American Type Culture Collection) to the aqueous PM suspensions. 2',7'-dichlorodihydrofluorescein diacetate (DCFH-DA), a membrane permeable compound, was used as the fluorescent probe. Upon entering a cell, DCFH-DA is deacetylated, yielding 2',7'-dichlorodihydrofluorescein (DCFH). Non-fluorescent DCFH is then converted by ROS species produced within the cell cytoplasm into the highly fluorescent 2,7-

dichlorofluorescein (DCF), which can be easily monitored using a microplate reader. Further details can be found in Landreman et al. (2008).

5.1.3. Monthly Variation of ROS-Activity

The high, seasonally-varying and chemically-diverse ambient PM_{2.5} levels in this urban environment as well as variety of aerosol sources provided a suitable setting for evaluating the association of PM chemical components with oxidative potential. PM_{2.5} mass concentration and chemical composition were extensively discussed in Chapter 3. Briefly, PM_{2.5} is a major contributor to ambient particle levels in Milan, exhibiting a yearly-average of $34.5 \pm 19.4 \mu\text{g}/\text{m}^3$, in excess of the EU annual mean limit of $25 \mu\text{g}/\text{m}^3$ set for 2015 (Council Directive 2008/50/EC). Specifically, secondary inorganic ions and organic matter ($\text{OC} \times 1.8$ (Turpin and Lim 2001)) were the most dominant fine PM species contributing to $36 \pm 7.1\%$ and $34 \pm 6.3\%$ of its mass on a yearly-based average, respectively. Highest PM_{2.5} concentrations occurred during December-February, when atmospheric dispersion is poorest and combustion-related emissions are high. The current discussion only focuses on PM_{2.5}-induced redox-activity and its association with specific chemical species.

Measured ROS-activity of the monthly PM_{2.5} composites is shown in Figure 5.1a-b on both air volume (μg Zymosan m^{-3} air) and PM mass (μg Zymosan mg^{-1} PM) bases. The volume-based redox activity reflects the redox activity associated with exposure to PM, whereas the mass-based redox activity is a measure of the intrinsic potency of PM.

The air volume-based ROS-activity spanned a 5-fold range, varying from 193 to 920 μg Zymosan/ m^3 with an annual average of $463 \pm 232 \mu\text{g}$ Zymosan/ m^3 . ROS-activity concentrations were higher during December-March, July and October. Peak levels specifically occurred in January ($837 \mu\text{g}$ Zymosan/ m^3) and February ($920 \mu\text{g}$ Zymosan/ m^3), suggesting that population

exposure to redox-active PM_{2.5} species is greatest during these winter months. Lower levels were measured during the remaining months, particularly May (193 $\mu\text{g Zymosan/m}^3$) and June (240 $\mu\text{g Zymosan/m}^3$). With the exception of the ROS-activity peak in July, all maxima coincide with pronounced peaks in PM_{2.5} concentration. The high occurrence in July likely reflects an increased contribution from a specific and seasonally-dependent source of redox-active PM_{2.5} species, possibly secondary organic aerosols (SOA).

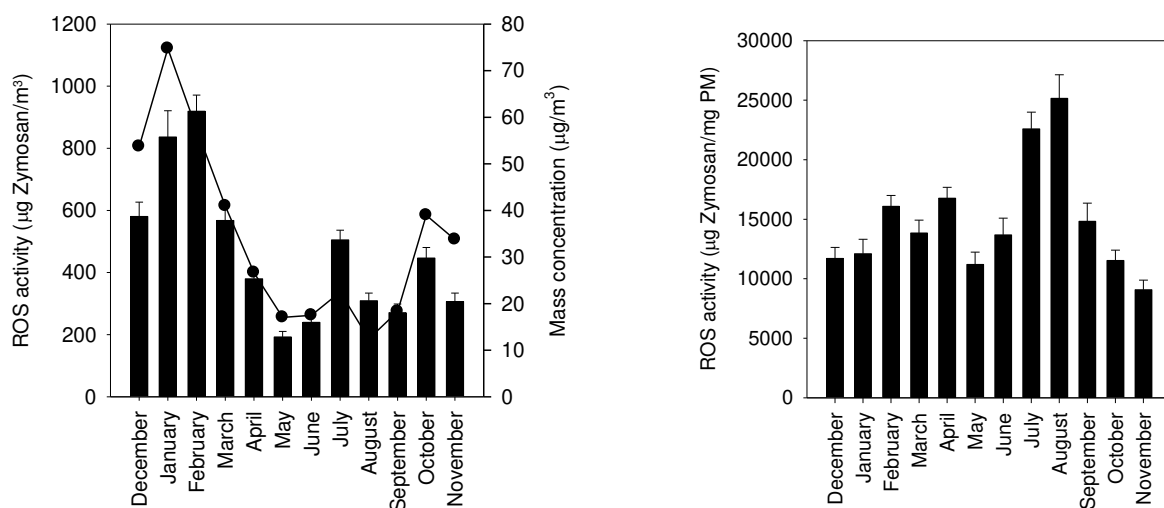


Figure 5.1 Monthly a) mass concentration ($\mu\text{g/m}^3$) (secondary axis) as well as air volume-based ($\mu\text{g Zymosan/m}^3$) and b) PM mass-based (intrinsic) ($\mu\text{g Zymosan/mg PM}$) water-soluble reactive oxygen species (ROS)-activity of ambient PM_{2.5} in Milan. Error bars represent one-sigma propagated uncertainty.

On a per PM mass basis, the measured ROS-activity ranged from a low of 9,080 $\mu\text{g Zymosan/mg PM}$ in November to a high of 25,200 $\mu\text{g Zymosan/mg PM}$ in August. The intra-annual variation averaged (\pm standard deviation) 14,900 \pm 4,760 $\mu\text{g Zymosan/mg PM}$. Monthly ROS-activities were fairly similar during September-June, but peaked at 22,600 and 25,200 $\mu\text{g Zymosan/mg PM}$ in July and August, respectively. Again, these summertime peaks correspond to high specific-activity PM components derived from a seasonally-varying source, potentially SOA. Of particular note is the fact that, compared to other urban areas, the median intrinsic ROS-activity of PM_{2.5} in Milan is about 2- and 7-fold greater than that of fine PM in Lahore,

Pakistan (Shafer et al., 2010) and Denver, USA (Zhang et al., 2008a), respectively. It is also 6.5-14 times the activity of accumulation and quasi-ultrafine mode PM in Long Beach-Los Angeles, USA (Hu et al., 2008).

5.1.4. Association with PM_{2.5} Species

To identify PM_{2.5} chemical components associated with ROS formation in the urban air of Milan, Spearman correlation coefficients (R) were determined between monthly data of ROS-activity and select fine PM species (N=12), as summarized in Table 5.1. WSOC_{nb} represents WSOC that is not associated with biomass burning. Since WSOC is mainly derived from biomass burning and SOA formation processes (Weber et al., 2007), WSOC_{nb} is a likely proxy for secondary organic carbon. It was estimated as the difference between measured WSOC and WSOC from wood-smoke, assuming that the contribution of wood-smoke to OC is 71% water-soluble (Sannigrahi et al., 2006). OC from wood-smoke was determined using OC-to-levoglucosan ratio derived from wood-smoke source profiles (Fine et al., 2004b; Sheesley, 2007).

ROS-activity strongly correlated ($R \geq 0.70$, $p < 0.05$) with S ($R=0.70$), La ($R=0.76$), Ni ($R=0.71$), Cr ($R=0.71$) and Cu ($R=0.76$). Ni, La, Cr and Cu are mainly associated with primary anthropogenic sources, such as vehicular exhaust and fuel oil combustion, as discussed in Chapter 3. Ni, Cr and Cu also have been implicated in ROS formation through redox-cycling or -mediated mechanisms (Valko et al., 2005) These findings are in agreement with previous studies that reported strong correlations between ROS-activity and water-soluble Ni, La and S (Saffari et al., 2013a; Shafer et al., 2010; Verma et al., 2009a). Moreover, Perrone et al. (2010) observed that cell viability reduction is related to Cr, Cu and possibly sulfate in PM₁ and PM_{2.5} samples in Milan. Furthermore, ROS-activity was strongly associated with WSOC_{nb} ($R=0.76$), as

documented by Hu et al. (2008), indicating that secondary organic species are potential drivers of ROS generation. ROS-activity also displayed moderate correlations ($R=0.62-0.69$) with combustion- and vehicular-related components including transition metals Fe, Zn and As as well as water-insoluble organic carbon (WIOC), n-alkanes and PAHs. Hu et al. (2008) also reported an association between ROS-activity and low molecular weight PAHs. ROS-activity also moderately correlated with n-alkanoic acids ($C_{15}-C_{30}$), many of which are formed by photo-oxidation of semi-volatile organic species (Rogge et al., 1993d). All other species (e.g. EC, toluene-, biogenic-derived SOA) exhibited poor or non-significant correlations with ROS generation. It is noteworthy that measured SOA tracers include isoprene, α -pinene, β -caryophyllene and toluene derivatives, but do not include the contributions of other hydrocarbons to SOA formation, which could explain the lack of ROS-activity correlation with toluene- and biogenic-derived SOA, but its high correlation with $WSOC_{nb}$.

Table 5.1 Spearman correlation coefficient (R) between monthly ROS-activity and select species of ambient $PM_{2.5}$ in Milan. Bold indicates significant correlation at a 0.05 level and $R \geq 0.7$. Italic indicates significant correlation at a 0.05 level.

	R
S	0.70
La	0.76
Ni	0.71
As	<i>0.69</i>
Co	<i>0.57</i>
Cu	0.76
Zn	<i>0.64</i>
Cr	0.71
Fe	<i>0.63</i>
WIOC	<i>0.62</i>
WSOC_{nb}	0.76
EC	-0.24
Low MW PAHs	<i>0.64</i>
Medium MW PAHs	<i>0.62</i>
High MW PAHs	<i>0.62</i>
n-alkanes	<i>0.64</i>
Hopanes and steranes	0.35
Levoglucosan	0.34
Biogenic-derived SOA	-0.36
Toluene-derived SOA	0.14
n-alkanoic acids ($C_{15}-C_{30}$)	<i>0.63</i>

These findings indicate that ROS generation is driven by a mixture of species (transition metals and organics), derived from both primary and secondary sources. Overall PM ROS-activity is thus dependent on the relative contributions of their sources to the overall PM concentrations.

5.1.5. Summary and Conclusions

ROS assay results showed that PM_{2.5}-associated redox activity, when expressed per m³ of air volume, is greatest during January (837 µg Zymosan/m³) and February (920 µg Zymosan/m³). Conversely, PM mass-based ROS-activity peaked at 22,600 and 25,200 µg Zymosan/mg PM in July and August, respectively. These maxima likely reflect the contribution of seasonally-dependent and high specific-activity PM components. Additionally, ROS-activity strongly correlated with Ni, La, Cr, Cu and WSOC_{nb}, suggesting that sources of these primary and secondary PM species contribute to ROS induction.

In conclusion, ambient PM_{2.5} in Milan is potentially redox-active. Additional studies, aimed at identifying and determining source contributions implicated in particle-associated redox-activity in this urban environment, should be undertaken. Findings of these investigations can ultimately aid in implementing source-specific regulatory measures for better protection of human health.

5.1.6. Acknowledgements

This research was supported by Southern California Particle Center (SCPC), funded by US EPA (Grant 2145 G GB139) and the University of Southern California (USC) Viterbi School of Engineering. We would like to thank the superintendent of fine arts and culture in Lombardy for his willingness to accept this study. We also wish to acknowledge the support of USC Provost's Ph.D. fellowship. We thank Jeff DeMinter and the staff at the Wisconsin State Laboratory of

Hygiene for their assistance with the chemical measurements. We also wish to thank SIMG-Italian College GPs and ISDE-International Doctors for the Environment for managerial support, Eng. Franco Gasparini, designer of the HVACS for technical help, and the whole management and employees of the Sovrintendenza, particularly Arch. A. Artioli, Arch. G. Stolfi, Arch. Napoleone, Mr. G. Bonnet and Dr. L. Dall'Aglio.

2. Oxidative Potential and Chemical Speciation of Size-Resolved PM at Near-Freeway and Urban Background Sites in the Greater Beirut Area

5.2.1. Introduction

Lebanon, with a growing population and severely limited air pollution controls, is afflicted with elevated PM levels, particularly in its urban areas (Saliba et al., 2010). Lacking an efficient public transportation system (MoE/URC/GEF, 2012) and suffering from inadequate electrical power production on the national grid, its high particle levels can be mainly related to vehicular and diesel generator set emissions. Regional sources could also contribute to its PM concentrations. Being located in the eastern Mediterranean basin, aerosol emissions from industrialized areas of northern and north-eastern Europe are significant particle sources in Lebanon (Saliba et al., 2010; Saliba et al., 2007a).

While the chemical composition of PM in Lebanon has been previously investigated (Massoud et al., 2011; Saliba et al., 2010; Saliba et al., 2007a), its oxidative potential has yet to be explored. Because redox activity is associated with adverse health effects, accurate characterization of PM-associated redox activity at urban and roadside settings can provide impetus for policies to address air quality in Lebanon. In addition, there is a dearth of information on particle toxicity in this region as a whole. To determine PM redox activity in Lebanon, coarse, accumulation ($PM_{2.5-0.25}$, $2.5 \mu\text{m} < d_p < 0.25 \mu\text{m}$) and quasi-ultrafine ($PM_{0.25}$, $d_p < 0.25 \mu\text{m}$) particle samples were collected at near-freeway and urban background sites in the Greater Beirut area. Samples were analyzed for their ability to induce oxidative stress on rat alveolar macrophages based on their ROS content. Their chemical composition was also determined, with particular focus on the effect of metals and trace elements. To the best of the authors' knowledge, this is the first study to evaluate particle-induced toxicity in the Eastern Mediterranean. Findings of this work provide a quantitative assessment of PM-based ROS-

activity in the Greater Beirut area as well as insights on its key drivers and relationship to particle-size. Results can ultimately aid in implementing more informed and targeted control strategies, much-needed but currently lacking, in the area.

5.2.2. Methodology

5.2.2.1 Sampling Sites

The sampling campaign was conducted in the Greater Beirut area at urban background and near-freeway sites, as shown in Figure 5.2.

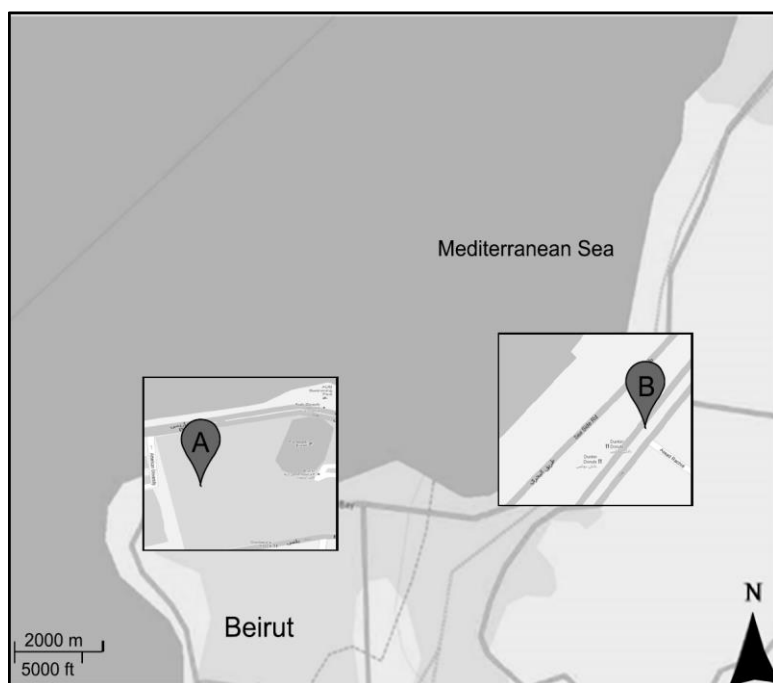


Figure 5.2 Map of the urban background (A) and near-freeway sites (B).

The background site was situated at the American University of Beirut (AUB). This monitoring site, which overlooks the Mediterranean coast from the north/west and AUB campus from the south/east, is mostly surrounded by a dense vegetation cover and pedestrian roads. The nearest street is located about 150 m west of the site. This coastal roadway, which separates the site from the Mediterranean Sea, experiences relatively high traffic activity throughout the day,

especially during peak hours (7-9 a.m. and 4-7 p.m.). Moreover, the sampling site is about 1.5 and 2.5 km away from a leisure yacht club and the commercial port of Beirut, respectively. The second sampling site consisted of 5-lane Jal El Dib freeway, along its southbound segment. The sampling point was directly adjacent to the freeway at about 1 m from its edge and 1.5 m above ground level. The site is therefore heavily influenced by vehicular emissions from the roadway. This freeway, which serves as a main conduit for vehicles traveling from *Mount/North Lebanon* to the capital Beirut, experiences heavy traffic throughout the day, with increased congestion during rush hours (7-11 a.m. and 4-7 p.m.). Additionally, the site is within 0.4 and 3.3 km of the Mediterranean coast and a yacht port/club, respectively. The site is also about 7.5 km from a thermal power plant running on heavy fuel oil, with a sulfur content of 25000-30000 ppm by weight (MoE, 2005).

5.2.2.2 Sample Collection

Sampling was conducted on weekdays during July-August 2012 from 7:00 a.m. to 5 p.m. Samples were concurrently collected at both sites on a weekly basis. Three parallel Sioutas Personal Cascade Impactor Samplers (Sioutas PCIS, SKC Inc., Eighty Four, PA, USA (Misra et al., 2002)), operating at 9 lpm and fitted with PM₁₀ inlets (Chemcomb 3500 speciation sampling cartridge, Thermoelectron Corp., Ohio, USA) were deployed at each location to collect size-resolved particles in the following size ranges: 10-2.5 µm (coarse PM), 2.5-0.25 µm (accumulation PM) and <0.25 µm (quasi-ultrafine PM). For chemical analyses purposes, two PCISs were loaded with Teflon filters (Pall Life Sciences, Ann Arbor, MI) while one PCIS was loaded with quartz microfiber filters (Whatman International Ltd, Maidstone, England). 25 mm filters were used as impaction substrates for PM_{10-2.5} and PM_{2.5-0.25} while 37 mm filters were used as collection media for PM_{0.25}. The collected particle mass was determined by pre- and post-

weighing the Teflon filters using a UMX2 microbalance (Mettler Toledo GmbH, CH-8606 Greifensee, Switzerland), following equilibration under controlled temperature and relative humidity conditions (22–24°C and 40–50%, respectively).

5.2.2.3 Sample Analyses

To perform chemical and oxidative analyses of the samples, each of the collected Teflon and quartz filters was sectioned into two equal portions. Measurements of carbonaceous species and organic compounds were conducted on the quartz substrates, while all other analyses were performed on the Teflon filters. Depending on the analytical mass requirements, measurements were conducted on either individual weekly samples (carbonaceous species, ions, ROS-activity, metals and elements) or composites of the weekly samples (water-soluble organic carbon).

Elemental and organic carbon (EC and OC, respectively) contents of the filters were determined using the NIOSH Thermal Optical Transmission method (Birch and Cary, 1996). The total elemental composition of the filter substrates was measured using a high resolution (magnetic sector) Inductively Coupled Plasma Mass Spectrometry (HR-ICP-MS Thermo-Finnigan Element 2). A mixed acid (1 mL of 16 M nitric acid, 0.25 mL of 12 M hydrochloric acid and 0.1 mL of hydrofluoric acid) microwave-assisted digestion was applied for extraction of total metals and elements (Herner et al., 2006). The water-soluble elemental content of the filters was also quantified using HR-ICP-MS, but following water-extraction and filtration of the samples (Zhang et al., 2008a). Ions and water-soluble organic carbon (WSOC) were respectively determined by ion chromatography and a Sievers 900 Total Organic Carbon Analyzer, after extraction of the samples with high purity water (Schauer et al., 2004; Sullivan et al., 2004).

The redox activity of the samples was measured using a macrophage-based reactive oxygen species (ROS) assay. This assay is a fluorogenic cell-based method that uses 2',7'-

dichlorodihydrofluorescein diacetate (DCFH-DA) as the fluorescent probe. Prior to the assay, substrates were extracted with high purity water and filtered. Rat alveolar macrophage cells (cell line NR8383, American Type Culture Collection) were dispensed into each well of a ninety-six-well plate and exposed to the aqueous extracts for a total time of 2.5 hours at 37 °C under a 6% CO₂ atmosphere. Approximately 15 min before the end of the incubation period, DCFH-DA was added to each prepared sample to achieve a final concentration of 45 μM. DCFH-DA, a membrane permeable compound, is de-acetylated upon entering a cell, yielding 2',7'-dichlorodihydrofluorescein (DCFH). Non-fluorescent DCFH is then converted by ROS species produced within the cell cytoplasm into the highly fluorescent 2,7-dichlorofluorescein (DCF). The fluorescence intensity of each well was hereafter determined (in kinetic mode) at 504 nm excitation and 529 nm emission (515 cutoff) using a m5e microplate reader (Molecular Devices, Inc., Sunnyvale, CA). Further details can be found in Landreman et al. (2008).

5.2.3. Results and Discussion

5.2.3.1 Size-Resolved Particle Mass and Composition

To investigate PM chemical composition, size-resolved particle mass concentrations and mass fractions of bulk PM components (average ±standard error) were determined, as presented in Table 5.3 for each site and particle mode. PM samples were classified into water-insoluble organic matter (WIOM), water-soluble organic matter (WSOM), EC, secondary ions (SI), sea-salt (SS), crustal material (CM) and trace elements (TE).

Table 5.2 Average (\pm standard error) mass concentration and chemical composition of PM_{10-2.5}, PM_{2.5-0.25} and PM_{0.25} at the near-freeway and urban background sites.

	Particle size (μm)	Mass ($\mu\text{g}/\text{m}^3$)	WIOM ((%)	WSOM (%)	EC (%)	SI (%)	SS (%)	CM (%)	TE (%)
Near-freeway	10-2.5	34.0 \pm 1.5	17.5 \pm 3.6	1.6 \pm 0.3	0.7 \pm 0.1	6.0 \pm 1.8	7.3 \pm 2.8	12.2 \pm 3.0	0.5 \pm 0.2
	2.5-0.25	13.8 \pm 0.9	41.7 \pm 8.9	8.8 \pm 0.7	7.7 \pm 1.0	31.3 \pm 7.2	4.1 \pm 2.9	18.6 \pm 2.7	1.8 \pm 0.5
	< 0.25	36.1 \pm 0.9	36.7 \pm 1.2	8.4 \pm 0.9	25.3 \pm 0.9	28.7 \pm 2.3	1.1 \pm 0.8	4.7 \pm 0.6	0.4 \pm 0.05
Background	10-2.5	15.8 \pm 0.9	2.6 \pm 0.7	3.2 \pm 0.7	0.2 \pm 0.1	14.0 \pm 1.9	14.7 \pm 3.1	22.9 \pm 8.1	0.6 \pm 0.3
	2.5-0.25	8.6 \pm 1.0	2.8 \pm 1.3	12.2 \pm 3.0	7.5 \pm 1.2	67.5 \pm 6.2	7.3 \pm 5.2	9.9 \pm 3.6	1.6 \pm 0.4
	< 0.25	14.0 \pm 0.4	8.4 \pm 2.6	21 \pm 1.9	8.9 \pm 0.9	53.5 \pm 11.8	0 \pm 0	2.8 \pm 0.6	0.7 \pm 0.2

WSOM and OM (WSOM+WIOM) were determined by multiplying measured WSOC and OC by a factor of 1.6, respectively (Turpin and Lim, 2001). WIOM was then estimated as the difference between OM and WSOM. SS contribution was determined as the sum of Na^+ concentration and sea-salt fractions of chloride, magnesium, potassium, calcium and sulfate concentrations, assuming standard sea-water composition (Seinfeld and Pandis, 2006) and using Na^+ as a tracer for sea-salt. SI comprises ammonium, nitrate and non-sea-salt sulfate (nss-sulfate), with nss-sulfate estimated by subtracting the sea-salt fraction of sulfate from measured sulfate. The fraction of CM in the PM samples was determined by summing the oxides of crustal metals, Al, K, Fe, Ca, Mg, Ti and Si (Chow et al., 1994; Hueglin et al., 2005; Marcazzan et al., 2001), with Ca and Mg representing their non-sea-salt portions. TE includes other measured elements such as Cu, Zn and Ba.

Total PM (PM_{10}) mass composition was predominated by $\text{PM}_{0.25}$ and $\text{PM}_{10-2.5}$ (each constituting 36-43% of PM_{10}) at both sampling locations. However, particle concentrations were 1.6-2.6 times greater at the near-freeway than background site for all particle-size modes. PM mass levels ranged from 13.8-36.1 and 8.6-15.8 $\mu\text{g}/\text{m}^3$ at the roadside and background locations, respectively. The consistently lower concentrations at the background site illustrate the significant contributions from vehicular emissions and traffic-induced re-suspension to PM levels at the freeway location. Size-resolved PM composition also varied between sites. In $\text{PM}_{0.25}$ and $\text{PM}_{2.5-0.25}$, WIOM was the most dominant component at the near-freeway site (37-42%), with primary vehicular emissions as the most likely sources. On the other hand, SI prevailed at the background site in both of these size modes, contributing to 54-68% of their mass. $\text{PM}_{2.5-0.25}$ - and $\text{PM}_{0.25}$ -WSOM, mainly derived from secondary organic aerosol (SOA) formation processes (Weber et al., 2007), were the next most abundant components at the background site (12-21%),

indicating considerable contributions from secondary sources at this urban site. In $PM_{10-2.5}$, CM was the major PM constituent at the background site ($22.9\pm 8.1\%$), while the next most prominent component at the near-freeway location ($12.2\pm 3\%$). WIOM, with a comparable mass fraction to CM ($17.5\pm 3.6\%$), was predominant in the coarse mode at the roadside location. The formation of $PM_{10-2.5}$ -WIOM could be attributed to the condensation of semi-volatile organic compounds on existing coarse particles or their coagulation with smaller particles (Eiguren-Fernandez et al., 2003; Sioutas et al., 2004). EC, a key tracer for diesel exhaust and fuel oil combustion (Schauer, 2003), significantly contributed to $PM_{0.25}$, particularly at the near-freeway site. It accounted for $25\pm 0.9\%$ of the quasi-ultrafine mass at the roadside site, suggesting an influence from diesel vehicles on road-traffic emissions. Its contribution to the larger particle-size fractions was less substantial, averaging less than 9%. SS mostly contributed to $PM_{10-2.5}$, consistent with expectations, accounting for 7-15% of its mass across sites. TE were the least abundant species, contributing to less than 2% of PM mass across sites and particle-modes. Nonetheless, several of these trace metals (e.g. Co, Mn, Ni) are toxicologically-relevant (Valko et al., 2005), with some of them listed by the U.S. Environmental Protection Agency (EPA) as air toxics (EPA).

5.2.3.2 Metals and Trace Elements

Size-Resolved Concentrations and Crustal Enrichment Factors. The toxicological relevance of several transition metals (e.g. Cu, Cr, Fe) warranted a thorough examination of metals and elements in the PM samples. Average (\pm standard error) mass concentration and crustal enrichment factor (CEF) of select total metals and elements were determined for each particle-mode and sampling site, as displayed in Figures 5.3a-b and 5.4a-b.

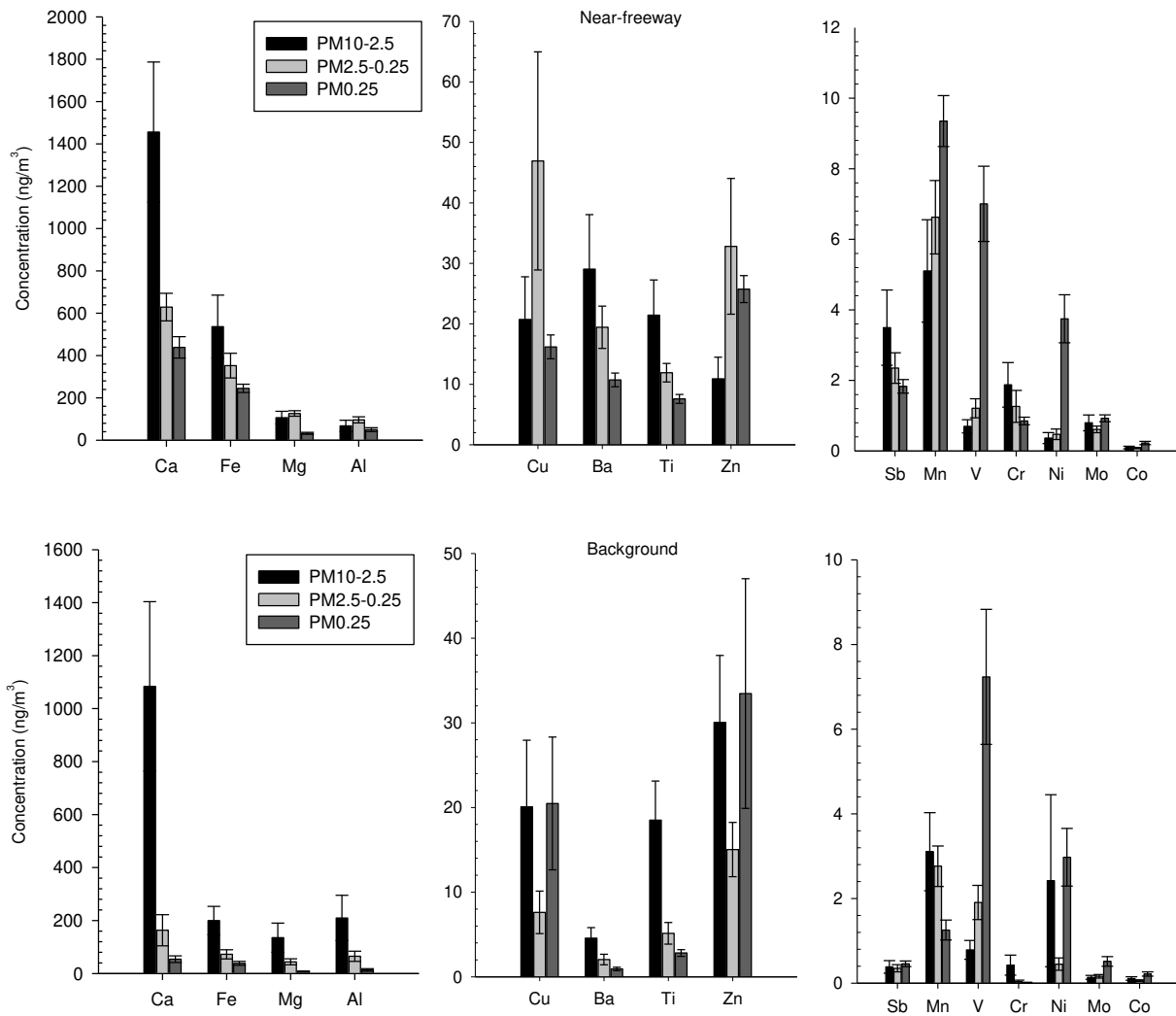


Figure 5.3a-b Average total concentration of metals and elements in $PM_{10-2.5}$, $PM_{2.5-0.25}$ and $PM_{0.25}$ at the a) near-freeway and b) urban background sites. Error bars represent one standard error.

CEFs were estimated in order to assess the relative contributions of anthropogenic and natural sources to the elemental components. For a given element, CEF was estimated as the ratio of its abundance in a PM sample to its average abundance in the upper continental crust after normalization to Al. Al was selected as a reference element and UCC composition was obtained from Taylor and McLennan (1985). Typically, elements with a CEF approaching 1 are of crustal origin whereas elements with a CEF exceeding 10 are considered anthropogenic (Birmili et al.,

2006). We should note that the selection of Al as a reference element could lead to an underestimation of the CEFs if Al was enriched in the samples. To minimize this potential bias, $PM_{2.5-0.25}$ and $PM_{0.25}$ elemental data was combined into $PM_{2.5}$ data in this analysis.

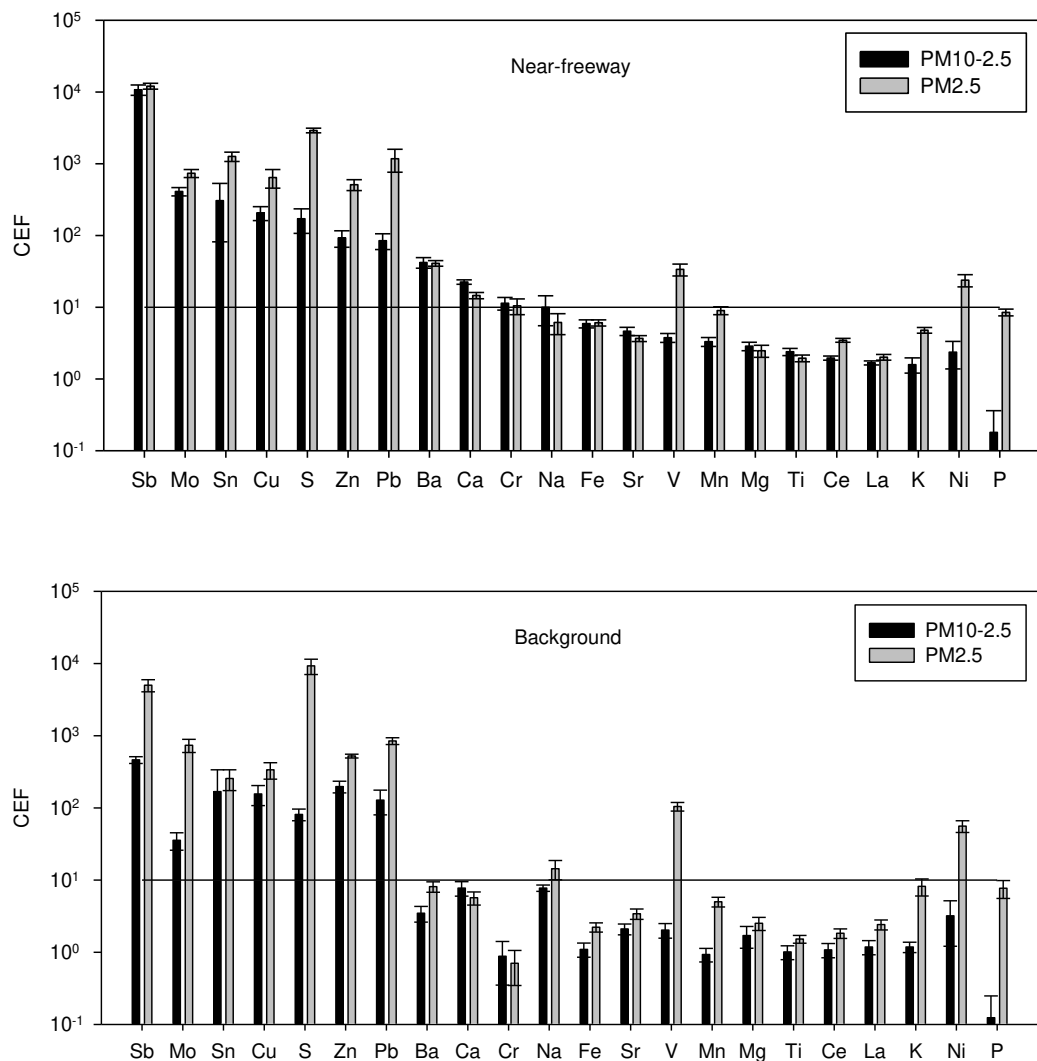


Figure 5.4a-b Average crustal enrichment factors (CEF) in $PM_{10-2.5}$ and $PM_{2.5}$ at the a) near-freeway and b) urban background sites. Error bars represent one standard error.

Size-resolved Ca, Mg, Fe, Al and Ti generally displayed comparable levels and CEFs < 10 at both locations, confirming their soil dust origin. These PM components also showed a gradual increase in concentration with particle-size, reaching a peak in the coarse mode, in accordance with their geochemical origin. Ca was mostly abundant among these elements at both

sampling sites and in all three particle-size fractions, peaking at 1084.2 ± 319.3 and 1455.9 ± 330.5 ng/m^3 in $\text{PM}_{10-2.5}$ at the background and near-freeway locations, respectively. A modest enrichment was also notable for Ca (CEF=15-22) at the roadway site. However, while lube oil emissions contribute to Ca levels (Ntziachristos et al., 2007b) to some extent, the increased enrichment observed for Ca at the roadside could be mainly related to the abundance of calcite and limestone rocks in Lebanon (Abdel-Rahman and Nader, 2002; Kouyoumdjian and Saliba, 2006). Ca crustal fraction may not be adequately represented using the UCC composition from Taylor and McLennan (1985). Furthermore, the strong correlations of Ca with Mg and Ti at the near-freeway site further corroborate its origin in soil dust ($R^2=0.82-0.90$). In contrast, an indication of anthropogenic contamination was generally noted for transition and trace metals. Sb and Ba were overall mostly confined to the coarse fraction and displayed CEFs exceeding 10, which suggests that their sources are anthropogenic, likely brake and tire wear (Sternbeck et al., 2002). These elements also presented greater concentrations (4-11.6 times) and a markedly stronger enrichment at the roadside location, further supporting their traffic-related sources. While both Cu and Zn exhibited a strong enrichment (CEF > 90), indicative of their anthropogenic origin, these elements displayed different partitioning at the sampling sites, suggesting distinct or mixed sources, each producing PM in different size ranges. At the near-freeway location, Cu and Zn were mostly distributed in $\text{PM}_{2.5-0.25}$ (47-56% by mass), similarly to the findings of Lin et al (2005) near a heavily-trafficked road. Lin et al. (2005) reported that Zn and Cu have respective mass median diameters of 1.21 and 1.56 μm , with Zn possibly derived from tire friction or also brake wear in fine PM. In the accumulation mode, Zn strongly correlated with Cu ($R^2=0.92$), but moderately with brake-wear tracer Sb ($R^2=0.61$), implying that Zn and Cu originate from tire wear and brake wear to a lesser extent (Thorpe and Harrison,

2008). On the other hand, at the background location, Cu and Zn were mostly distributed in $PM_{0.25}$ and $PM_{10-2.5}$, accounting for 38-43% of their respective mass, with brake wear as a potential source. While the majority of particles produced by abrasion are in the coarse mode, brake attrition could also contribute to ultrafine particles (Sanders et al., 2003). Cu and Zn have been associated with brake wear in both the coarse and ultrafine PM modes (Hays et al., 2011; Lin et al., 2005). We should, however, note that the rather even distribution of Cu and Zn between the coarse and quasi-ultrafine size ranges could also indicate a multiplicity of sources. Combustion sources, possibly exhaust emissions, may contribute to these elements in $PM_{0.25}$. Ultrafine mode-Zn and $PM_{0.1}$ -Cu have been associated with diesel and gasoline emissions, respectively (Lin et al., 2005). Similarly to Cu and Zn, Mn showed a dissimilar particle-size distribution at the sampling sites. In proximity of the freeway, Mn presented a CEF approaching 10 (9 ± 1.1), with most of its mass (45%) associated with $PM_{0.25}$, thereby suggesting road dust enriched with exhaust combustion emissions, as a possible source for this metal (Lin et al., 2005). At the background location, Mn was less enriched (CEF < 5) and displayed lower levels (0.13-0.61 times) with 82% of its mass distributed relatively evenly between $PM_{2.5-0.25}$ and $PM_{10-2.5}$, which indicates that Mn mainly originates from soil and/or road dust (Manoli et al., 2002). V and Ni were generally more enriched in the fine fraction (CEF = 24-105), with greater partitioning in the quasi-ultrafine mode. These elements, which presented similar $PM_{0.25}$ concentrations at both sampling sites ($p > 0.05$), likely originate from fuel oil combustion (Isakson et al., 2001; Lu et al., 2006) given the proximity of both sites to nearby ports (2.5-3.3 km) and the location of the freeway site within 7.5 km of a thermal power plant. $PM_{2.5}$ - and $PM_{10-2.5}$ -bound Mo displayed a CEF exceeding 10 at both locations. This element, which was mostly confined to the quasi-ultrafine mode (40-63%), exhibited a stronger enrichment and higher

concentrations in proximity of the freeway, confirming its traffic-related source, possibly lube oil combustion (Ntziachristos et al., 2007b). Cr peaked in the coarse mode and was more enriched at the roadway than background location. This element also displayed a CEF approaching 10 in $PM_{10-2.5}$ at the near-freeway location, suggesting its road dust source (Manoli et al., 2002). Co existed in similar amounts at both sites, ranging from a low in $PM_{2.5-0.25}$ (0.06-0.08 ng/m^3) to a high in $PM_{0.25}$ (0.22-0.23 ng/m^3). Despite its trace levels, this element is particularly toxic (Valko et al., 2005) with potential sources as re-suspended soil and possibly industrial sources for the ultrafine mode (Allen et al., 2001; von Schneidmesser et al., 2010).

Water-Solubility. The water solubility of PM is an important physico-chemical property governing its toxicological behavior (Costa and Dreher, 1997). Soluble species exhibit enhanced bioavailability, and may thus be more toxicologically-relevant. Water-soluble metals, in particular, have been implicated as potent initiators of particle-mediated oxidative stress (Ciapetti et al., 1998; Goldsmith et al., 1998). Figure 5.5 shows size-resolved percent water-solubility of select metals and elements, averaged across sites. The solubility of a given PM species was determined as the ratio of its water-soluble to total elemental concentration. Few elements exhibited fractions exceeding 1, which can be attributed to the analytical uncertainties associated with the chemical measurements.

Water-solubility of measured metals and trace elements varied considerably with particle-size and element. It is overall highest in $PM_{0.25}$ and $PM_{2.5-0.25}$ while lowest in $PM_{10-2.5}$. A stronger size-dependency was also observed for Cu, Pb and Cr, with water-solubility peaking in the quasi-ultrafine fraction then decreasing with increasing particle-size. Soil- or road dust-related elements, Al, Ti, Fe and Cr, displayed low water-solubility ($\leq 31\%$), consistent with their geochemical origin. Unlike other crustal elements, Ca was highly water-soluble ($> 70\%$) despite

its mainly soil origin. Ca, which was mostly confined to the coarse mode, is likely present as calcium-carbonate with a significant fraction in the form of calcium nitrate and sulfate, as demonstrated by a previous study conducted in the Beirut area (Kouyoumdjian and Saliba, 2006). Calcium nitrate and sulfate, formed from the reactions of nitric and sulfuric acids with sea-salt or mineral dust (Noble and Prather, 1996), are highly and moderately water-soluble, respectively (Cheung et al., 2012b; Liu et al., 2008). Sea-salt component, Na, displayed a high solubility in all three size fractions, exceeding 78%. S, mainly in the form of soil-associated sulfate in $PM_{10-2.5}$ and ammonium sulfate in $PM_{0.25}$ and $PM_{2.5-0.25}$, was highly water-soluble in all three size fractions (> 81%). Elements, including Zn, Cd, Co, Mn, V, Cu, Ni, Mo, Pb and Sb, displayed peak solubility in the accumulation or quasi-ultrafine modes and were moderately-to-strongly water-soluble in these fractions (>43%). These species are mainly associated with high-temperature combustion processes, such as vehicular exhaust emissions and fuel oil combustion (Isakson et al., 2001; Lin et al., 2005). The water-solubility of these metals was lowest in the coarse mode, ranging between 2 and 59%, which can be attributed to a difference in their geochemical origin and sources across modes. In $PM_{10-2.5}$, these elements are mostly associated with vehicular abrasion or re-suspended road dust (Manoli et al., 2002; Song and Gao, 2011). These results generally agree with those reported for size-fractionated PM in urban areas in the Los Angeles (LA) basin (Hu et al., 2008).

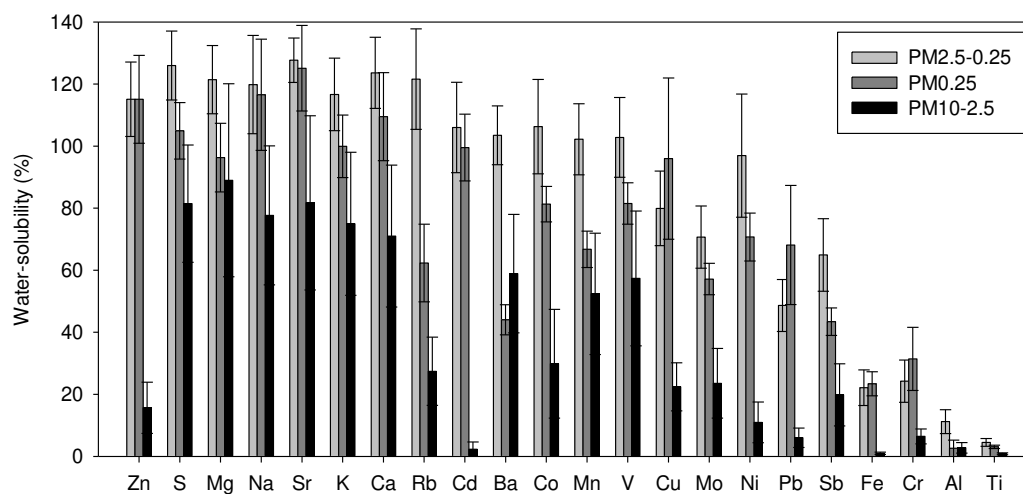


Figure 5.5 Water-solubility of metals and elements in PM_{10-2.5}, PM_{2.5-0.25} and PM_{0.25}, averaged across the sampling sites. Error bars represent one standard error.

Water-Soluble Elemental Composition. The water-soluble elemental composition ($\mu\text{g/g}$ PM) of the size-resolved PM samples is shown in Figure 5.6, with mass fractions averaged across sites. The overall species' distribution in either PM fractions is generally consistent with expectations. Soil-related elements, such as Ti, Ca, Mg, Sr and Al, were least abundant in PM_{0.25}, while mostly prevalent in PM_{10-2.5} or PM_{2.5-0.25}. On the other hand, elements, including Cu, Zn, Mn, V, Ni, Sb, Cr, Mo, As, Co and Cd, were generally largely enriched in the accumulation or quasi-ultrafine modes. In these modes, these elements are mostly derived from high-temperature combustion processes, which emit a large fraction of water-soluble components (Birmili et al., 2006). Moreover, potentially toxic or ROS-active species generally rank high among the considered array of elements. In the accumulation mode, water-soluble Zn and Cu were mostly dominant among the anthropogenic-elements, accounting for 0.19-0.25% of PM_{2.5-0.25}. Their mass fractions also approached those of bulk particle components, Ca, K and Mg, which indicates a significant PM anthropogenic contamination. Additionally, despite their very low

mass fractions (0.01-0.028%), soluble PM_{10-2.5}-Mn as well as PM_{0.25}-V and -Ni are significant contributors to particle mass relative to other trace elements.

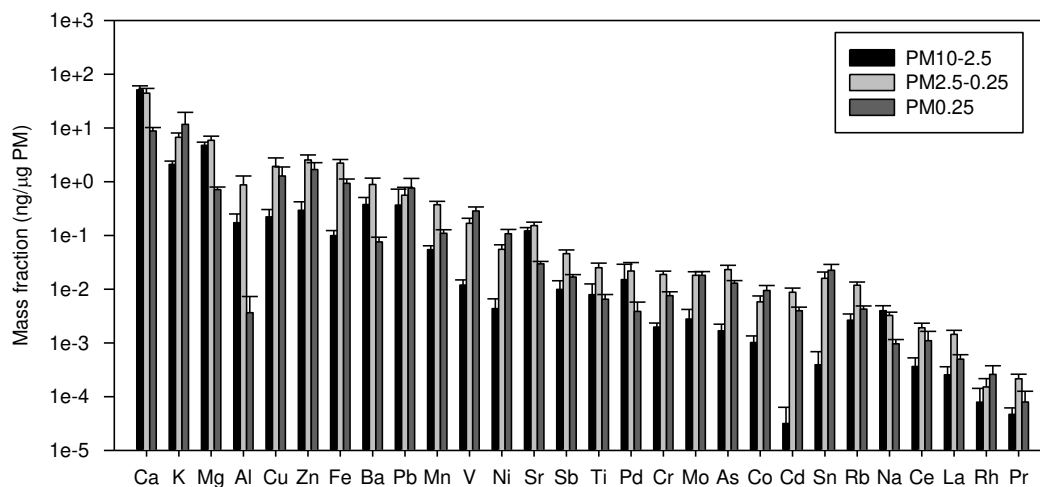


Figure 5.6 Water-soluble elemental composition of PM_{10-2.5}, PM_{2.5-0.25} and PM_{0.25}, averaged across the sampling sites. Error bars represent one standard error.

5.2.3.3 Size-Resolved Reactive Oxygen Species (ROS)-activity

Measured ROS-activity of the size-resolved PM samples is shown in Figure 5.7a-b on both per air volume (μg Zymosan equivalents m^{-3} air) and per PM mass (μg Zymosan equivalents mg^{-1} PM) bases. The air volume-based ROS-activity reflects the redox activity associated with PM exposure, while the PM mass-based ROS-activity is a measure of the intrinsic potency of PM.

The air volume-based ROS-activity was greater (1.5-2.8—fold) at the near-freeway site than background location for all particle-size ranges. This trend, which coincides with higher PM concentrations at the near-freeway site, suggests that exposure to redox-active PM species is greatest at the roadway. The measured ROS-activity also exhibited a particle-size dependency, with lowest activity associated with coarse mode particles at both sampling sites. At the background location, although PM levels reached a minimum in the accumulation mode, the

redox activity varied from a low of 11.7 $\mu\text{g Zymosan}/\text{m}^3$ in $\text{PM}_{10-2.5}$ to a high of 440.0 $\mu\text{g Zymosan}/\text{m}^3$ in $\text{PM}_{2.5-0.25}$. This peak occurrence in the accumulation mode likely reflects the influence of specific and highly redox active PM components. At the roadway site, ROS-activity ranged from a minimum in $\text{PM}_{10-2.5}$ (17.4 $\mu\text{g Zymosan}/\text{m}^3$) to relatively comparable magnitudes in $\text{PM}_{2.5-0.25}$ and $\text{PM}_{0.25}$ (645.6 and 654.9 $\mu\text{g Zymosan}/\text{m}^3$, respectively).

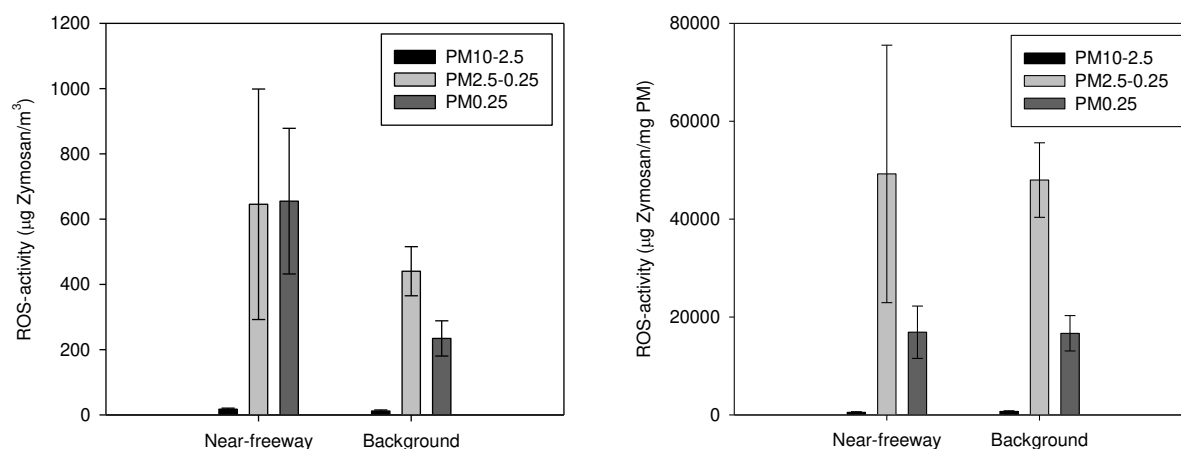


Figure 5.7 Average a) air volume-based ($\mu\text{g Zymosan}/\text{m}^3$) and b) PM mass-based (intrinsic) ($\mu\text{g Zymosan}/\text{mg PM}$) reactive oxygen species (ROS)-activity of $\text{PM}_{10-2.5}$, $\text{PM}_{2.5-0.25}$ and $\text{PM}_{0.25}$ at the near-freeway and urban background sites. Error bars represent one standard error.

On a per PM mass basis, the ROS-activity also exhibited a size-dependent relationship at both sites, ranging from a maximum (49229.6 and 47975.6 $\mu\text{g Zymosan}/\text{mg PM}$) in the accumulation mode to a minimum (528.9 and 698 $\mu\text{g Zymosan}/\text{mg PM}$) in the coarse fraction. This rather large variability (a 69- and 93-fold range) in size-resolved redox activity suggests that ROS-active species have a distinct size-specific distribution, with greater potency associated with $\text{PM}_{2.5-0.25}$ and $\text{PM}_{0.25}$ than the larger $\text{PM}_{10-2.5}$ mode. A strong dependence of ROS on particle size was also documented by Hu et al. for PM in Long Beach/LA (Hu et al., 2008). However, contrary to the volume-based ROS-activity, the size-resolved intrinsic activity (i.e. normalized to

PM mass) was generally comparable at both sampling locations, possibly suggesting a similarity in the sources of putative PM ROS-active species.

5.2.3.4 Association of (ROS)-activity with PM components

To identify PM chemical species (or source tracers) associated with ROS formation in the ambient air of the Greater Beirut area, Spearman correlation coefficients (R) were determined between ROS-activity (μg Zymosan/mg PM) and select PM species (water-soluble metals, EC and OC in ng/ μg PM), as summarized in Table 5.4 for each particle mode. To increase statistical significance, data points from all sites were pooled in this analysis. This was possible given the comparable mass-based ROS activity between sampling locations.

In $\text{PM}_{10-2.5}$, ROS-activity strongly correlated with Mn ($R=0.79$, $p < 0.05$), a component of road dust (Manoli et al., 2002) with moderate water-solubility (52%, one of the highest among all species in coarse PM). A relatively high association was also found between $\text{PM}_{10-2.5}$ -based ROS-activity and Co ($R=0.76$, $p < 0.05$), in agreement with previous findings. Shafer et al. (2010) documented a strong association between water-soluble Mn/Co and ROS-activity in both PM_{10} and $\text{PM}_{2.5}$. In $\text{PM}_{2.5-0.25}$, ROS-activity was strongly correlated with vehicular abrasion element Cu ($R=0.76$, $p < 0.05$), which was more enriched in this size mode (Figure 5.6) and almost entirely water-soluble (Figure 5.5). Cu can act directly to catalyze the formation of ROS via Fenton chemistry (Valko et al., 2005) and has been implicated in ROS formation in $\text{PM}_{2.5}$ in Milan, Italy (Daher et al., 2012). A moderate correlation ($R= 0.66-0.70$, $p < 0.05$) was also noted between $\text{PM}_{2.5-0.25}$ ROS-activity and combustion elements, Ni and Co, consistent with other studies (Hu et al., 2008; Shafer et al., 2010). Both of these metals are associated with redox-cycling or -mediated mechanisms (Valko et al., 2005). In the quasi-ultrafine mode, ROS-activity was robustly associated with V and Ni ($R=0.79$ and 0.73), both elements of residual oil

combustion (Isakson et al., 2001) with greater abundance in $PM_{0.25}$ and high water-solubility (>60%) (Figures 5.5 and 5.6). We should note that these findings are in agreement with several other studies (Hu et al., 2008; Verma et al., 2009a; Verma et al., 2009b), which highlight the impact of heavy fuel oil combustion on particle redox activity. Furthermore, ROS-activity was not correlated with EC in any PM size fraction—a finding that is not unexpected—as EC in isolation does not mechanistically participate in ROS formation. This result is also consistent with earlier investigations (Daher et al., 2012; Saffari et al., 2013a). Lastly, we should emphasize that the lack of an association between ROS-activity and OC does not necessarily imply that OC is not a redox-active agent or does not participate in ROS induction. Previous studies conducted in the LA basin, Denver and Milan documented a moderate association between ROS-activity and WSOC ($R=0.69$ and 0.75 , $p<0.05$) (Daher et al., 2012; Hu et al., 2008; Zhang et al., 2008a). The relationship between ROS-activity and OC in this study, where data from all sites was combined in the regression analysis, could be obscured by the distinct OC chemical composition between the sampling locations. As can be inferred from Table 5.3, OC was mostly water-insoluble at the near-freeway site, while it was predominately water-soluble at the background location. An investigation of size-resolved associations between ROS-activity and WSOC in this study was precluded by the limited number of data points for WSOC ($N<6$). However, a combination of data points for all PM size fractions and sites revealed a significant correlation between ROS-activity and WSOC ($R=0.77$), which implies a potential role for secondary organic compounds in ROS generation.

Table 5.3 Spearman correlation coefficients (R) between ROS-activity (μg Zymosan/mg PM) and select species (ng/ μg PM) in $\text{PM}_{10-2.5}$, $\text{PM}_{2.5-0.25}$ and $\text{PM}_{0.25}$. Bold indicates $R \geq 0.70$ and significant at a 0.05 level.

		$\text{PM}_{10-2.5}$	$\text{PM}_{2.5-0.25}$	$\text{PM}_{0.25}$
Carbonaceous species	OC	-0.52	-0.52	-0.41
	EC	0.05	-0.12	-0.65
Water-soluble metals and elements	V	0.02	0.58	0.79
	Cr	-0.24	0.33	-0.17
	Mn	0.79	0.59	0.13
	Fe	0.50	0.60	0.17
	Co	0.76	0.70	0.08
	Ni	0.29	0.66	0.73
	Cu	0.29	0.76	-0.20
	Zn	-0.04	0.50	-0.30
	As	-0.33	0.59	0.10
	Rb	-0.31	0.50	0.22
	Mo	-0.26	0.49	0.23
	Rh	0.29	0.08	-0.02
	Pd	0.66	-0.28	0.06
	Sb	-0.05	0.29	0.04
	Ba	0.05	0.57	-0.04
Pb	-0.21	-0.22	0.05	
Cd	-	0.60	0.11	

5.2.4. Summary and Conclusions

To determine the oxidative potential of ambient PM in the Greater Beirut area, size-resolved $\text{PM}_{10-2.5}$, $\text{PM}_{2.5-0.25}$ and $\text{PM}_{0.25}$ samples were collected at near-freeway and urban background sites. At both locations, crustal elements, Ca, Mg, Fe, Al and Ti, generally displayed CEFs < 10, indicating their mainly soil dust origin. Conversely, transition metals and trace elements, comprising Cu, Zn, Ba, Mo, V, Ni and Sb, exhibited a stronger enrichment, particularly at the roadway, confirming their anthropogenic sources, such as combustion emissions and vehicular abrasion. These elements as well as Co, many of which are air toxics, were overall largely partitioned in $\text{PM}_{2.5-0.25}$ and $\text{PM}_{0.25}$, with moderate-to-high water-solubility in these modes (>43%). These physico-chemical characteristics may lead to increased adverse biological effects. Notably, road dust tracer Mn and soil-related element Co were highly associated with $\text{PM}_{10-2.5}$ -based ROS-activity. On the other hand, in $\text{PM}_{2.5-0.25}$, vehicular abrasion

element Cu and road dust tracer Co were potential ROS-active species. In $PM_{0.25}$, fuel combustion elements, V and Ni, had the highest correlation with ROS generation. At both sampling sites, ROS-activity reached a minimum in the coarse mode. While size-resolved PM intrinsic ROS-activity was overall comparable at both locations, volume-based ROS-activity was 1.5-2.8 fold greater at the roadway than background location. This trend indicates that exposure to redox-active PM species is greatest near the freeway. Findings of this study call for firm controls on air pollution in the Greater Beirut area. Results also support efforts toward establishing more effective and source-specific regulations for mitigating PM toxicity. Such policies could focus on reducing PM emissions from heavy fuel oil burning (e.g. use of alternative fuel type) and vehicular traffic.

5.2.5. Acknowledgements

This research was supported by the University of Southern California (USC) School of Engineering Fred Champion Endowment as well as the American University of Beirut (AUB) Faculty of Engineering & Architecture and Faculty of Arts and Sciences. We wish to acknowledge the support of USC Provost's Ph.D. fellowship. We also would like to thank Professor James Schauer and Dr. Martin Shafer as well as the staff at Wisconsin State Laboratory of Hygiene for their assistance with the chemical measurements.

3. ROS-Activity: Comparison of Urban Areas

5.3.1. Comparison of Intrinsic ROS-Activity

To put the intrinsic toxicity of ambient PM in Beirut in perspective, the mass-normalized ROS-activity of PM at the urban background sites was compared to that of PM collected from a variety of worldwide urban settings, including Milan, as shown in Figure 5.8. This comparison was possible because the same macrophage-ROS bioassay was applied to PM samples collected in these studies (Cheung et al., 2012b; Daher et al., 2012; Saffari et al., 2013a; Shafer et al., 2010; Verma et al., 2009b). Details about the sampling regimen employed in these studies are provided in Table 5.5. Excluding PM_{2.5} data for LA, the comparison was based on average intrinsic ROS-activity of samples (i.e. PM mass-normalized) collected during similar sampling periods (July-August) in order to maintain consistency. ROS-activity of PM_{2.5} in LA corresponds to that of samples collected in October-November during and after wildfires (Verma et al., 2009b).

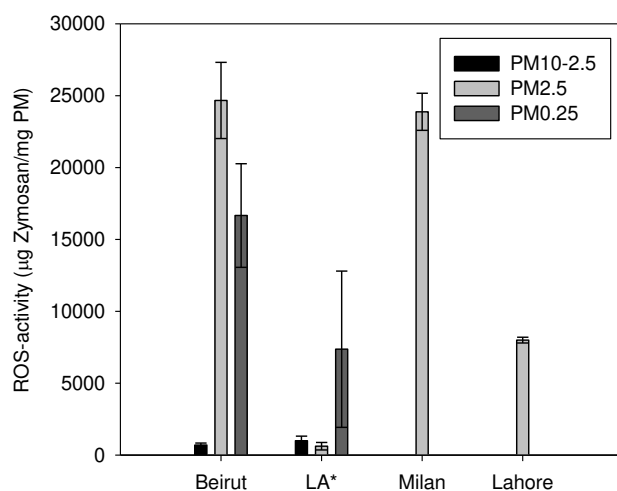


Figure 5.8 Comparison of average intrinsic reactive oxygen species (ROS)-activity (µg Zymosan/mg PM) of PM_{10-2.5}, PM_{2.5} and PM_{0.25} in Beirut (current study) with data from Los Angeles (LA) (Saffari et al., 2013a; Verma et al., 2009b), Milan (Daher et al., 2012) and Lahore (Shafer et al., 2010) during July-August. Error bars represent one standard error. *ROS-activity of ambient PM_{2.5} in LA corresponds to that of samples collected in October-November 2007 during and after wildfires (Verma et al., 2009b).

The mass-based ROS-activity measured in ambient PM_{10-2.5} in Beirut is comparable (0.7 times) to the activity of coarse particles in the LA basin (Cheung et al., 2012b). On the other hand, the intrinsic PM_{0.25}-associated ROS-activity at the background location in Beirut is 2.3-fold greater than that measured at an urban site in LA. While organic matter could play a key role in ROS generation/regulation (Ayres et al., 2008), the observed contrast in ROS-activity is generally consistent with the differences in concentrations and mix of transition metals and trace elements among the two sites. The very strong correlation of ROS-activity with Ni at the urban site in Beirut was not evident at the urban background site in LA. The greater average levels and mass fraction of water-soluble Ni (2.4- and 1.4-fold, respectively) in urban Beirut likely strengthen this correlation. In PM_{2.5}, the intrinsic ROS-activity measured for ambient particles in Beirut is comparable to that reported for PM in Milan-Italy, but several times greater than the activity of PM in urban LA (Verma et al., 2009b) and, impressively, 3.1-fold greater than that of PM in Lahore-Pakistan, one of the most heavily polluted cities globally (Shafer et al., 2010). The difference in ROS values with Lahore is likely due to the dissimilarity in PM sources. PM_{2.5}-induced ROS-activity was related to tracers of re-suspended soil (Ce, Mn) and industrial metallurgical processes (Cd) in Lahore (von Schneidemesser et al., 2010).

5.3.2. Summary and Conclusions

In comparison to other worldwide settings, although the intrinsic redox activity of PM_{10-2.5} in Beirut is comparable to that measured at an urban site in LA, its PM_{0.25}-induced ROS-activity is roughly 2.5-times greater. In addition, the intrinsic ROS-activity of PM_{2.5} in Beirut is fairly comparable to that in Milan, but 3.1-fold greater than that in the heavily polluted city of Lahore where PM_{2.5} levels (~100-400 µg/m³) (Shafer et al., 2010) are orders of magnitude higher than concentrations in Beirut. These results support findings demonstrating that PM-induced

redox activity results from the enhanced toxicity of specific ROS-active species, with water-soluble metals' as important drivers, thereby suggesting that total aerosol mass concentration is a relatively poor metric of aerosol toxicity.

Table 5.4 Summary of studies that examined PM_{0.25}-, PM_{2.5}-, and PM_{2.5-10}-associated oxidative potential using the *in vitro* macrophage-based ROS assay.

Study	Location	Time/period	Size fraction	Species associated with ROS-activity (R>0.7 and p<0.05)
Current	Near-freeway and urban, Beirut	Weekly samples in summer 2012/7 a.m.-5 p.m.	PM _{0.25}	Water-soluble V, Ni
Saffari et al. 2013	Urban, Los Angeles	24-hr time-integrated samples collected once per week during April 2008-March 2009	PM _{0.25}	OC, water-soluble Mn, Zn, Cd
Current	Near-freeway and urban, Beirut	Weekly samples in summer 2012/7 a.m.-5 p.m.	PM _{10-2.5}	Water-soluble Mn, Co
Cheung et al. 2012	Los Angeles basin	Diurnal samples during July-August 2009/7 a.m.-7 p.m.	PM _{10-2.5}	Water-soluble Rh, Cu, Pd, V
Daher et al. 2012	Urban, Milan	24-hr time-integrated samples collected on a weekly basis during December 2009-November 2010	PM _{2.5}	WSOC, total Cu, Ni, S, Cr,
Shafer et al. 2010	Urban, Lahore	Samples collected every 6 th day from January 2007-January 2008	PM _{2.5}	Water-soluble Mn, Cd, Ce
Verma et al. 2009	Urban, Los Angeles	Integrated samples in October–November 2007, during and after wildfires	PM _{2.5}	Water-soluble Cr, Ba, Pb, Fe, Ni, V

Chapter 6 Synthesis, Broader Implications and Recommendations

While an association between mass of particulate matter (PM) and adverse health effects has been observed, the contribution of specific PM components to aerosol toxicity remains unknown. An identification of these critical species requires an accurate characterization of PM. This dissertation focused on investigating the chemical composition, temporal variation, spatial distribution, sources and oxidative properties of size-resolved PM. The association of PM redox activity—quantified using a macrophage-based *in vitro* reactive oxygen species (ROS) assay—with particle-size-resolved and chemically-speciated PM was also examined using linear regression analysis. In doing so, this research supports efforts towards establishing more cost-effective and carefully-targeted PM control strategies for mitigating particle toxicity. Locations of study encompassed distinct areas, ranging from highly-polluted metropolitans to desert-like locations in the Greater Beirut area, Milan and the Los Angeles basin. PM bulk chemical composition was determined by conducting a chemical mass closure. An emphasis was given to the organic aerosol fraction in addition to metals and trace elements. The variation in PM-induced ROS-activity with particle-size, location and monthly scales was also investigated. Monthly variation in primary and secondary PM_{2.5} sources was quantified using the Chemical Mass Balance (CMB) model and fixed tracer-to-OC ratios applied to fine PM collected at an urban site in Milan. Spatial variability in quasi-ultrafine PM (PM_{0.25}) in the complex Los Angeles air shed was evaluated using coefficients of divergence analysis. Results from this research work have important implications on both population exposure assessment and air quality regulations.

6.1 Conclusions and Broader Implications

Findings documented in Chapters 2-5 contribute to the current state of scientific knowledge on 1) the variation in PM-chemical composition and -redox activity with location, season and particle-size, 2) the association between PM toxico-chemical properties and identification of source tracers implicated in the induction of PM oxidative potential, 3) primary and secondary source contributions to fine OC and particle mass in a typical urban setting, and 4) PM intrinsic ROS-activity and its variation across urban environments. Improved characterization of PM composition and relative toxicity could facilitate the implementation of more targeted air quality regulations and could provide data to support epidemiological and toxicological studies.

Emerging toxicological research has shown that ultrafine particles may be more potent than coarse (PM_{10-2.5}) or fine (PM_{2.5}) particulate matter (Cho et al., 2005; Li et al., 2003). However,

unlike PM_{2.5} or PM₁₀, significantly less is known about ultrafine particles. Measurement results from a year-long sampling campaign at 10 distinct areas in the Los Angeles basin, discussed in Chapter 2, provide additional and much-needed insight on the chemical composition and variability of quasi-ultrafine particles (PM_{0.25}). Reported findings showed that the bulk chemical composition and concentration of PM_{0.25} are considerably affected by location and season. Wintertime levels were highest at the source site, while lowest at the desert-like site. Conversely, summertime concentrations peaked at the inland receptor locations. Chemical mass reconstruction revealed that PM_{0.25} in the basin consists of 49-64% organic matter, 3-6.4% elemental carbon, 9-15% secondary ions, 0.7-1.3% trace ions, and 5.7-17% crustal material and trace elements, on a yearly-average basis. Moreover, while quasi-ultrafine mass is relatively spatially homogeneous in the basin, some of its components, mainly elemental carbon, nitrate as well as crustal material and several toxic metals, were unevenly distributed. Data from this study could assist toxicologists in constructing realistic animal exposure studies involving PM_{0.25}. Additionally, the spatial and temporal contrasts of quasi-ultrafine particles should be considered in the design of epidemiological studies in order to accurately assess population exposure to PM in complex urban air sheds, such as the megacity of Los Angeles.

Reducing ambient PM concentrations and associated toxicity requires an accurate characterization of PM chemical species, major sources and temporal trends. Chapter 3 provides an improved understanding of PM composition, levels and monthly variation in Milan, which can be used to inform air quality policy makers. Results also provide significant insight on particle sources in this area. Findings revealed that PM_{2.5} is a major contributor to PM₁₀ levels in Milan, averaging $34.5 \pm 19.4 \mu\text{g}/\text{m}^3$ throughout the year, in excess of the EU annual mean limit of $25 \mu\text{g}/\text{m}^3$. Specifically, secondary inorganic ions and organic matter were the most dominant fine

PM species contributing to $36\pm 7.1\%$ and $34\pm 6.3\%$ of its mass on a yearly-based average, respectively. Highest $PM_{2.5}$ concentrations occurred during December-February and were mainly attributed to poor atmospheric dispersion. On the other hand, $PM_{2.5-10}$ exhibited an annual average of $6.79\pm 1.67 \mu\text{g}/\text{m}^3$, with crustal elements prevailing. Source apportionment results showed that wood-smoke and secondary organic aerosol sources contribute to $4.6\pm 2.6\%$ and $9.8\pm 11\%$ of fine OC on a yearly-based average, respectively. The remaining OC, mostly water-insoluble, is likely associated with petroleum-derived material that is not adequately represented by existing source profiles, mostly for the U.S., used in this study. Unlike the findings of studies conducted in various cities around the world (Sheesley et al., 2004; Stone et al., 2010; Stone et al., 2008; Zheng et al., 2005), this is the first study to demonstrate that significant sources of water-insoluble OC cannot be explained by traditional profiles. This result is of relevance to the atmospheric community and can be used to guide future research studies that need considering that U.S. mobile sources are likely to be similar to vehicles in Milan in the future, given the adaption of comparable diesel emissions control technologies.

Chapter 4 provides a comparative and detailed analysis of size-resolved PM chemical composition at two contrasting locations, including near-freeway and urban background sites, in the Greater Beirut area. Advancing our understanding of PM chemical composition and its relation to particle-size and location is necessary for an accurate assessment of exposure to PM. Size-resolved particle mass levels were 1.3-2.6 times greater at the roadside than background location. A chemical mass closure showed that $PM_{10-2.5}$ was mostly composed of crustal material, contributing to 12-23% of its mass across sites. On the other hand, in $PM_{2.5-0.25}$ and $PM_{0.25}$, organic matter (46-56%) was dominant at the roadside location, while secondary ions (54-68%) were more abundant at the background site. Relative to diesel-impacted I-710 in Southern

California, levels of vehicular tracers (EC, PAHs, hopanes), including air toxics, were substantially greater at the freeway in this study. These results provide insight on commuter exposure to traffic-related PM in the Beirut area and impetus for policies to address air quality in this region, which represents one case study of developing areas. While atmospheric PM has generally been well-examined in developed countries, particle pollution in developing nations is relatively less explored. Furthermore, findings extend our knowledge on PM composition to other worldwide geographical locations and highlight the importance of regional secondary sources in addition to local primary emissions.

Chapter 5 outlines the variation of PM-induced redox activity with location, season, particle-size and chemical composition. PM measurements in Milan and the Greater Beirut area provided suitable settings to examine this association.

In Milan, PM_{2.5}-induced ROS-activity, expressed per m³ of air volume, peaked in January and February, indicating that personal exposure to PM is greatest during these wintertime months. Conversely, PM mass-based ROS-activity reached greatest levels in July and August, suggesting the influence of specific components on oxidant properties of PM. Additionally, a correlation analysis showed that Ni, La, Cr, Cu and WSOC_{nb} are strongly associated with ROS formation, suggesting that sources of these species are potential significant contributors to ROS induction.

In the Greater Beirut area, Mn, Cu, Co, V, Ni and Zn were overall mostly distributed in PM_{2.5-0.25} and PM_{0.25}, with high water-solubility in these modes (> 60%). The increased water-solubility and presence of these metals, many of which are air toxics, in small size ranges constitute an added health risk. Of particular concern are water-soluble elements with strong correlations ($R \geq 0.70$) with ROS-activity. In PM_{2.5-10}, Mn and Co, which are road dust components, were highly associated with ROS-activity. In PM_{2.5-0.25}, Cu -a tracer of vehicular abrasion- and Co -a road

dust element- were highly correlated with ROS generation. In $PM_{0.25}$, V and Ni, originating from fuel oil combustion, had the highest correlations with ROS formation. Additionally, size-resolved ROS-activity, expressed per m^3 of air volume, was 1.5-2.8 times greater at the roadside than background location, indicating that exposure to redox-active PM species may be greatest near the freeway. Furthermore, ROS-activity (on per unit of PM mass) displayed a particle-size dependency, with lowest activity associated with $PM_{10-2.5}$. Relative to other urban settings, the intrinsic (i.e. PM mass-normalized) ROS-activity of ambient $PM_{2.5}$ in Beirut is fairly comparable to that reported in Milan but 3.1-times $PM_{2.5}$ activity in Lahore, despite the considerably higher PM levels in Lahore. This finding is of particular note since it supports the notion that PM redox activity results from the enhanced toxicity of specific ROS-active species rather than total mass. Overall, findings reported in this chapter provide a quantitative assessment of particle-size-resolved ROS-activity and insights on its spatial and temporal behavior, necessary for properly gauging PM toxicity. Results also provide the much-needed information on the association of size-resolved and chemically-speciated PM components with particle oxidative potential, which could help guide emission reduction strategies and formulate air quality regulations.

6.2 Limitations

While this dissertation contributes to the current state of scientific knowledge on size-resolved particle properties (chemical and oxidative), variability (temporal and spatial) and sources, a consideration of the limitations of the presented work is necessary to further advance our knowledge on PM characteristics and related health effects.

Although the reported results (Chapters 2-5) provide valuable insight on PM chemical and oxidative profiles, particle sampling in the documented studies was restricted to ten-hour- or twenty-four-hour-time-integrated measurements due to the time-, resource-, and labor-intensive

nature of the campaigns. Considering PM complexity and variability, more highly-time-resolved measurements (e.g. diurnal, morning Vs. afternoon time episodes) could provide greater insight on the formation mechanisms, source strength emissions and oxidative profile of size-resolved PM and their variation with meteorological parameters (e.g. temperature, wind speed and direction —all of which vary over time scales shorter than 24 hours). The adopted time-integrated approach also imposes limitations on the interpretation of PM spatial variability. The coefficients of divergence analysis, used to determine the spatial heterogeneity of quasi-ultrafine particles ($PM_{0.25}$) in the Los Angeles basin (Chapter 2), was based on twenty-four-hour-time-integrated data. This approach, however, may not reflect the spatial distribution of $PM_{0.25}$ over finer time scales. Previous investigations in eastern and source regions of the Los Angeles basin examined the spatial variability in particle number concentrations on diurnal scales, using hourly data, and found greater spatial heterogeneity during morning commute and late evening hours (Hudda et al., 2010; Krudysz et al., 2009). Such variability, which is relevant to acute exposures assessment, may not be fully captured by this time-integrated approach.

Another point of consideration is the comparative assessment of the intrinsic redox activity of PM collected from a variety of worldwide urban settings, which was presented in Chapter 5. While measures were taken to ensure consistency among studies (i.e. apply same extraction methodology and oxidative assay, restrict comparisons to same sampling season), the sampling protocols were not always identical. For instance, PM collection at the urban site in Beirut was conducted from 7:00 a.m. to 5 p.m. while particle collection at other urban areas (e.g. Milan, Lahore) was based on 24-hour measurements. An ideal analysis would have consisted of identical sampling protocols in all studies. Furthermore, this comparative assessment of particle oxidative potential is based on PM mass-normalized ROS-activities. This analysis, therefore,

does not take into account the exposure levels at each urban environment. It is also important to note that measuring PM oxidative potential using the adopted macrophage cellular assay represents a valuable, but one of many methods, for assessing PM relative toxicity.

Additionally, the chemical and toxicological characterization of urban PM in Beirut (Chapters 4 and 5) was based on measurements of PM collected during summer. While results provide significant and much-needed information on PM properties in this area, a more comprehensive analysis necessitates a consideration of PM temporal behavior (e.g. seasonal variation).

Lastly, while source apportionment results at an urban site in Milan, discussed in Chapter 3, provide insights into wood-smoke and secondary organic aerosol source contributions to fine OC, findings were limited by the lack of source profiles characteristic of the area.

6.3 Recommendations

Findings from this dissertation could be used as a benchmark in future research work. They also support efforts towards implementing more rationally-targeted PM control strategies and designing more carefully-constructed studies for personal exposure assessment.

6.3.1 Health Effects Community

Epidemiological studies typically utilize one or few central monitoring stations to characterize population exposure to PM (Wilson et al., 2005). A year-long measurement of quasi-ultrafine particles ($PM_{0.25}$) at 10 distinctly different sites in the Los Angeles basin, discussed in Chapter 2, showed that the chemical composition and concentration of $PM_{0.25}$ are considerably affected by season and location, specifically. Some of $PM_{0.25}$ components, mainly elemental carbon, nitrate and several toxic metals, were unevenly distributed in the basin. This temporal and spatial complexity, in particular, of quasi-ultrafine particles should be considered in

the design of epidemiological studies in order to accurately assess personal exposure to PM on “inter-community” scales. Moreover, considering that people spend about 85-90% of their time in indoor environments (Klepeis et al., 2001) and that ambient concentrations may not necessarily represent personal exposure levels, particular focus should also be given to investigating the outdoor-to-indoor infiltration characteristics and indoor sources of ultrafine particles. Penetration characteristics of ultrafine particles are dependent on several factors, such as air exchange rates and PM chemical characteristics (including volatility). Volatile particles of outdoor origin can experience substantial changes and may be lost to building walls during indoor penetration (Sioutas et al., 2005). Characterization of urban particle infiltration should account for these factors as well as the large spatial variations exhibited by ultrafine PM near sources (e.g. freeway), which could affect its volatility properties (Sioutas et al., 2005; Zhu et al., 2002). The seasonal variability, spatial behavior and infiltration characteristics of ultrafine particles should thus be carefully considered in the design of epidemiological studies for accurate personal exposure assessment.

The correlation analysis between ROS-activity and size-resolved PM chemical species, presented in Chapter 5, indicated that road dust components may be drivers of ROS-activity in the coarse and accumulation particle modes. Considering this finding, it is recommended that the potential relative toxicity of road dust components is further evaluated using *in-vivo* studies focusing on road dust. These investigations could be accompanied by road simulator experiments to determine the physico-chemical properties of road dust.

6.3.2 Regulatory Community

While current PM regulations are focused on reducing ambient mass levels of PM₁₀ and PM_{2.5}, correlation analysis in Chapter 5 revealed a unique suite of metals (or source tracers)

implicated in ROS formation, in spite of their very low contribution to particle mass (<1%). In $PM_{10-2.5}$, Mn and Co, which are road dust components, were highly associated with ROS-activity. In $PM_{2.5-0.25}$, Cu -a tracer of vehicular abrasion- and Co -a road dust element- were highly correlated with ROS formation. In $PM_{0.25}$, V and Ni, both originating from fuel oil combustion, displayed robust correlations with ROS formation. These findings suggest that current PM regulation policies could prove relatively ineffective if they were to focus on PM properties or emission sources that mostly contribute to particle mass, but mainly consist of low-toxicity species. It is therefore recommended that PM control strategies focus on sources of components that are mostly responsible for PM-related health effects.

6.3.3 Atmospheric Community

A comparative assessment of particle-size-resolved ROS-activity, detailed in Chapter 5, indicated a strong dependence of mass-based ROS-activity on particle-size, with greater potency associated with $PM_{0.25}$ than larger $PM_{10-2.5}$. These results were, however, based on ten-hour-time-integrated data and restricted to one season. To properly gauge the potential toxicity of ultrafine particles, future studies should aim at investigating the diurnal variation (e.g. morning, midday, afternoon, overnight) in the chemical and oxidative profiles of ultrafine particles at distinct locations (e.g. source, urban, rural, receptor) and during different seasons. Previous studies investigating the diurnal variation in ultrafine particles (Fine et al., 2004c; Verma et al., 2009a) were generally restricted to one or two sampling sites and time episodes.

An investigation of redox activity association with $PM_{2.5}$ chemical species in Milan showed that secondary water-soluble organic carbon (WSOC) robustly correlates with ROS-activity ($R= 0.76$, $p<0.05$), as shown in Chapter 5. These results imply an important role for secondary organic aerosol sources in ROS induction. Water-soluble organic matter (WSOM) and

its role in ROS formation, however, remain poorly understood due to its complex structure and susceptibility for atmospheric processing. WSOM is composed of a variety of compounds, such as polyacidic compounds, mono- and di-carboxylic acids (Decesari et al., 2000). Classical single component speciation approaches normally only account for a few percent of WSOM composition (Decesari et al., 2000). Further investigation of the functional and structural characteristics of WSOC is thus warranted in order to identify specific organic compounds (and consequently sources) implicated in ROS formation.

To identify specific agents of PM toxicity, this dissertation focused on associating ROS-activity with individual chemical components. Additional insight on health-relevant PM sources can, however, be gained by integrating source apportionment techniques with redox activity measurements. Multiple linear regression can be applied to build statistical relationships between ROS formation and identified sources, where ROS production can be predicted from a linear combination of source contributions. Findings from such studies can be particularly useful in targeting specific sources responsible for PM-related health effects.

In conclusion, findings of this dissertation support efforts towards establishing more relevant PM metrics. Current mass metrics are not ideal and may be crude surrogates for high-toxicity PM components. Complementary or new metrics should thus be considered in air quality regulations. Measurement of particle oxidative potential constitutes a valuable approach for assessing aerosol toxicity, which can be used in conjunction with chemical fractionation tools to identify important drivers, and therefore potential sources of PM toxicity. Understanding the association between particle oxidative potential and adverse health outcomes, however, requires carefully-constructed studies that integrate source-specific air quality information, population-based epidemiological

data and toxicological analyses. More rationally-targeted and cost effective particle control strategies that specifically address sources of PM components having the most significant effects on public health could ultimately be implemented.

Bibliography

Abdel-Rahman, A.F.M., Nader, F.H., 2002. Characterization of the Lebanese Jurassic-Cretaceous carbonate stratigraphic sequence: a geochemical approach. *Geological Journal* 37, 69-91.

Allen, A.G., Nemitz, E., Shi, J.P., Harrison, R.M., Greenwood, J.C., 2001. Size distributions of trace metals in atmospheric aerosols in the United Kingdom. *Atmospheric Environment* 35, 4581-4591.

Allen, J.O., Hughes, L.S., Salmon, L.G., Mayo, P.R., Robert, J.J., Cass, G.R., 2000. Characterization and Evolution of Primary and Secondary Aerosols During PM_{2.5} and PM₁₀ Episodes in the South Coast Air Basin

Anderson, H.R., 2000. Differential epidemiology of ambient aerosols. *Philosophical Transactions of the Royal Society of London. Series A: Mathematical, Physical and Engineering Sciences* 358, 2771-2785.

Andrews, E., Saxena, P., Musarra, S., Hildemann, L.M., Koutrakis, P., McMurry, P.H., Olmez, I., White, W.H., 2000. Concentration and composition of atmospheric aerosols from the 1995 SEAVS experiment and a review of the closure between chemical and gravimetric measurements. *Journal of the Air & Waste Management Association* (1995) 50, 648-664.

Arey, J., Zielinska, B., Atkinson, R., Winer, A.M., 1988. Formation of nitroarenes during ambient high-volume sampling. *Environmental Science & Technology* 22, 457-462.

Arhami, M., Minguillón, M.C., Polidori, A., Schauer, J.J., Delfino, R.J., Sioutas, C., 2010. Organic compound characterization and source apportionment of indoor and outdoor quasi-ultrafine particulate matter in retirement homes of the Los Angeles Basin. *Indoor Air* 20, 17-30.

Arhami, M., Sillanpää, M., Hu, S., Olson, M.R., Schauer, J.J., Sioutas, C., 2009. Size-Segregated Inorganic and Organic Components of PM in the Communities of the Los Angeles Harbor. *Aerosol Science and Technology* 43, 145-160.

Ayres, J.G., Borm, P., Cassee, F.R., Castranova, V., Donaldson, K., Ghio, A., Harrison, R.M., Hider, R., Kelly, F., Kooter, I.M., Marano, F., Maynard, R.L., Mudway, I., Nel, A., Sioutas, C., Smith, S., Baeza-Squiban, A., Cho, A., Duggan, S., Froines, J., 2008. Evaluating the toxicity of airborne particulate matter and nanoparticles by measuring oxidative stress potential--a workshop report and consensus statement. *Inhalation toxicology* 20, 75-99.

Baalbaki, R., Al-Assaad, K., Mehanna, C.-J., Saliba, N.A., Katurji, M., Roumié, M., 2013. Road versus roadside particle size distribution in a hot Mediterranean summer- Estimation of fleet emission factors. *Journal of the Air & Waste Management Association* 63, 327-335.

Bauer, H., Schueller, E., Weinke, G., Berger, A., Hitzenberger, R., Marr, I.L., Puxbaum, H., 2008. Significant contributions of fungal spores to the organic carbon and to the aerosol mass balance of the urban atmospheric aerosol. *Atmospheric Environment* 42, 5542-5549.

Becker, S., L. A. Dailey, J. M. Soukup, S. C. Grambow, R. B. Devlin, and Y.-C. T. Huang. , 2005. Seasonal Variations in Air Pollution Particle-Induced Inflammatory Mediator Release and Oxidative Stress. . *Environmental Health Perspectives* 113 1032-1038.

Birch, M.E., Cary, R.A., 1996. Elemental Carbon-Based Method for Monitoring Occupational Exposures to Particulate Diesel Exhaust. *Aerosol Science and Technology* 25, 221-241.

Birmili, W., Allen, A.G., Bary, F., Harrison, R.M., 2006. Trace Metal Concentrations and Water Solubility in Size-Fractionated Atmospheric Particles and Influence of Road Traffic. *Environmental Science & Technology* 40, 1144-1153.

Cabada, J., Pandis, S., Subramanian, R., Robinson, A., Polidori, A., Turpin, B., 2004. Estimating the Secondary Organic Aerosol Contribution to PM_{2.5} Using the EC Tracer Method. Special Issue of *Aerosol Science and Technology* on Findings from the Fine Particulate Matter Supersites Program. *Aerosol Science and Technology* 38, 140-155.

Caserini, S., Anna, F., Anna Maria, M., Marco, M., Elisabetta, A., Alfredo, L., Riccardo, D.L., Valeria, Z., 2007. New insight into the role of wood combustion as key PM source in Italy and in Lombardy region. , in: 16th Annual International Emissions Inventory Conference "Emission Inventories: Integration, A., and Communications" (Ed.), Raleigh, North Carolina, May 14–17, 2007.

Cass, G.R., Hughes, L.A., Bhave, P., Kleeman, M.J., Allen, J.O., Salmon, L.G., Cass, G.R., Hughes, L.A., Bhave, P., Kleeman, M.J., Allen, J.O., Salmon, L.G., 2000. The Chemical Composition of Atmospheric Ultrafine Particles. *Philosophical Transactions of the Royal Society of London. Series A: Mathematical, Physical and Engineering Sciences* 358, 2581-2592.

Castro, L.M., Pio, C.A., Harrison, R.M., Smith, D.J.T., 1999. Carbonaceous aerosol in urban and rural European atmospheres: estimation of secondary organic carbon concentrations. *Atmospheric Environment* 33, 2771-2781.

Chalupa, D.C., Morrow, P.E., Oberdorster, G., Utell, M.J., Frampton, M.W., 2004. Ultrafine particle deposition in subjects with asthma. *Environmental Health Perspectives* 112, 879-882.

Chang, M.C., Sioutas, C., Kim, S., Gong, H., Linn, W.S., 2000. Reduction of nitrate losses from filter and impactor samplers by means of concentration enrichment. *Atmospheric Environment* 34, 85-98.

Cheung, K., Daher, N., Kam, W., Shafer, M.M., Ning, Z., Schauer, J.J., Sioutas, C., 2011a. Spatial and temporal variation of chemical composition and mass closure of ambient coarse particulate matter (PM_{10-2.5}) in the Los Angeles area. *Atmospheric Environment* 45, 2651-2662.

Cheung, K., Daher, N., Shafer, M.M., Ning, Z., Schauer, J.J., Sioutas, C., 2011b. Diurnal trends in coarse particulate matter composition in the Los Angeles Basin. *Journal of Environmental Monitoring* 13.

Cheung, K., Olson, M.R., Shelton, B., Schauer, J.J., Sioutas, C., 2012a. Seasonal and spatial variations of individual organic compounds of coarse particulate matter in the Los Angeles Basin. *Atmospheric Environment* 59, 1-10.

Cheung, K., Shafer, M.M., Schauer, J.J., Sioutas, C., 2012b. Diurnal trends in oxidative potential of coarse particulate matter in the Los Angeles Basin and their relation to sources and chemical composition. *Environmental science & technology* 46, 3779-3787.

Cho, A.K., Sioutas, C., Miguel, A.H., Kumagai, Y., Schmitz, D.A., Singh, M., Eiguren-Fernandez, A., Froines, J.R., 2005. Redox activity of airborne particulate matter at different sites in the Los Angeles Basin. *Environmental Research* 99, 40-47.

Chow, J.C., Watson, J.G., Fujita, E.M., Lu, Z., Lawson, D.R., Ashbaugh, L.L., 1994. Temporal and spatial variations of PM_{2.5} and PM₁₀ aerosol in the Southern California air quality study. *Atmospheric Environment* 28, 2061-2080.

Ciapetti, G., Granchi, D., Verri, E., Savarino, L., Cenni, E., Savioli, F., Pizzoferrato, A., 1998. Fluorescent microplate assay for respiratory burst of PMNs challenged in vitro with orthopedic metals. *Journal of Biomedical Materials Research* 41, 455-460.

Costa, D.L., Dreher, K.L., 1997. Bioavailable transition metals in particulate matter mediate cardiopulmonary injury in healthy and compromised animal models. *Environmental Health Perspectives* 105.

D'Alessandro, A., Lucarelli, F., Mandò, P.A., Marcazzan, G., Nava, S., Prati, P., Valli, G., Vecchi, R., Zucchiatti, A., 2003. Hourly elemental composition and sources identification of fine and coarse PM10 particulate matter in four Italian towns. *Journal of Aerosol Science* 34, 243-259.

Daher, N., Ruprecht, A., Invernizzi, G., De Marco, C., Miller-Schulze, J., Heo, J.B., Shafer, M.M., Shelton, B.R., Schauer, J.J., Sioutas, C., 2012. Characterization, sources and redox activity of fine and coarse particulate matter in Milan, Italy. *Atmospheric Environment* 49, 130-141.

Dahl, A., Gharibi, A., Swietlicki, E., Gudmundsson, A., Bohgard, M., Ljungman, A., Blomqvist, G.r., Gustafsson, M., 2006. Traffic-generated emissions of ultrafine particles from pavement-tire interface. *Atmospheric Environment* 40, 1314-1323.

Decesari, S., Facchini, M.C., Fuzzi, S., Tagliavini, E., 2000. Characterization of water-soluble organic compounds in atmospheric aerosol: A new approach. *Journal of Geophysical Research: Atmospheres* 105, 1481-1489.

Delfino, R.J., Gillen, D.L., Tjoa, T., Staimer, N., Polidori, A., Arhami, M., Sioutas, C., Longhurst, J., 2011. Electrocardiographic ST-Segment Depression and Exposure to Traffic-Related Aerosols in Elderly Subjects with Coronary Artery Disease. *Environmental Health Perspectives* 119, 196-202.

Delfino, R.J., Sioutas, C., Malik, S., 2005. Potential Role of Ultrafine Particles in Associations between Airborne Particle Mass and Cardiovascular Health. *Environmental Health Perspectives* 113, 934-946.

Delfino, R.J., Staimer, N., Tjoa, T., Gillen, D.L., Polidori, A., Arhami, M., Kleinman, M.T., Vaziri, N.D., Longhurst, J., Sioutas, C., 2009. Air Pollution Exposures and Circulating Biomarkers of Effect in a Susceptible Population: Clues to Potential Causal Component mixtures and mechanisms. *Environmental Health Perspectives* 117, 1232-1238.

Dinar, E., Anttila, T., Rudich, Y., 2008. CCN Activity and Hygroscopic Growth of Organic Aerosols Following Reactive Uptake of Ammonia. *Environmental Science & Technology* 42, 793-799.

Draxler, R.L., Rolph, G.D., 2003. HYSPLIT (HYbrid Single-Particle Lagrangian Integrated Trajectory) model. NOAA Air Resources Laboratory, Silver Spring, MD.

Eiguren-Fernandez, A., Miguel, A.H., Froines, J.R., Thurairatnam, S., Avol, E.L., 2004. Seasonal and Spatial Variation of Polycyclic Aromatic Hydrocarbons in Vapor-Phase and PM2.5 in Southern California Urban and Rural Communities. *Aerosol Science and Technology* 38, 447-455.

Eiguren-Fernandez, A., Miguel, A.H., Jaques, P., Sioutas, C., 2003. Evaluation of a denuder-MOUDI-PUF sampling system to measure the size distribution of semi-volatile polycyclic aromatic hydrocarbons in the atmosphere. *Aerosol Science and Technology* 37, 201-209.

EPA, United States Environmental Protection Agency. Technology Transfer Network Air Toxics Web Site, <http://www.epa.gov/ttn/atw/188polls.html>.

- EPA, U.S., 2004. EPA Air Quality Criteria for Particulate Matter (Final Report, Oct 2004). U.S. Environmental Protection Agency, Washington, DC, EPA 600/P-99/002aF-bF, 2004.
- Fantel, A.G., 1996. Reactive oxygen species in developmental toxicity: Review and hypothesis. *Teratology* 53, 196-217.
- Fine, P.M., Chakrabarti, B., Krudysz, M., Schauer, J.J., Sioutas, C., 2004a. Diurnal Variations of Individual Organic Compound Constituents of Ultrafine and Accumulation Mode Particulate Matter in the Los Angeles Basin. *Environmental Science & Technology* 38, 1296-1304.
- Fine, P.M., G. R. Cass, Simoneit, B.R.T., 2004b. Chemical Characterization of Fine Particle Emissions from the Fireplace Combustion of Wood Types Grown in the Midwestern and Western United States. *Environmental Engineering Science* 21, 387-409.
- Fine, P.M., Shen, S., Sioutas, C., 2004c. Inferring the Sources of Fine and Ultrafine Particulate Matter at Downwind Receptor Sites in the Los Angeles Basin Using Multiple Continuous Measurements *Aerosol Science and Technology* 38, 182-195.
- Fine, P.M., Sioutas, C., Solomon, P.A., 2008. Secondary Particulate Matter in the United States: Insights from the Particulate Matter Supersites Program and Related Studies. *Journal of the Air & Waste Management Association* 58, 234-253.
- Friedlander, S., 2000. *Dynamics of Agglomerate Formation and Restructuring in Smoke, Dust and Haze*. . Oxford University Press. New York.
- Garg, B.D., Cadle, S.H., Mulawa, P.A., Groblicki, P.J., Laroo, C., Parr, G.A., 2000. Brake Wear Particulate Matter Emissions. *Environmental Science & Technology* 34, 4463-4469.
- Geller, M., Biswas, S., Sioutas, C., 2006. Determination of Particle Effective Density in Urban Environments with a Differential Mobility Analyzer and Aerosol Particle Mass Analyzer. *Aerosol Science and Technology* 40, 709-723.
- Geller, M.D., Fine, P.M., Sioutas, C., 2004. The Relationship between Real-Time and Time-Integrated Coarse (2.5-10 μm), Intermodal (1-2.5 μm), and Fine (<2.5 μm) Particulate Matter in the Los Angeles Basin. *Journal of the Air & Waste Management Association* 54, 1029-1039.
- Geller, M.D., Kim, S., Misra, C., Sioutas, C., Olson, B.A., Marple, V.A., 2002. A Methodology for Measuring Size-Dependent Chemical Composition of Ultrafine Particles. *Aerosol Science and Technology* 36, 748-762.
- Giuliaci, M., 1988. Physical and dynamical climatology of the Po Valley. Regional Meteorological Service, Bologna (in Italian).
- Goldsmith, C.A., Imrich, A., Danaee, H., Ning, Y.Y., Kobzik, L., 1998. Analysis of air pollution particulate-mediated oxidant stress in alveolar macrophages. *Journal of toxicology and environmental health. Part A* 54, 529-545.
- Gualtieri, M., Ovrevik, J., Mollerup, S., Asare, N., Longhin, E., Dahlman, H.-J., Camatini, M., Holme, J.A., 2011. Airborne urban particles (Milan winter-PM_{2.5}) cause mitotic arrest and cell death: Effects on DNA, mitochondria, AhR binding and spindle organization. *Mutation Research* 713, 18-31.
- Gustafsson, M., G. R. Blomqvist, A. Gudmundsson, A. Dahl, E. Swietlicki, M. Bohgard, J. Lindbom, and A. Ljungman, 2008. Properties and toxicological effects of particles from the interaction between tyres, road pavement and winter traction material *Science of The Total Environment* 393, 226-240.
- Halliwell, B., Cross, C.E., 1994. Oxygen-derived species—Their relation to human-disease and environmental-stress. *Environmental Health Perspectives* 102, 5-12.

Hasselriis, F., Licata, A., 1996. Analysis of heavy metal emission data from municipal waste combustion. *Journal of Hazardous Materials* 47, 77-102.

Hays, M.D., Cho, S.-H., Baldauf, R., Schauer, J.J., Shafer, M., 2011. Particle size distributions of metal and non-metal elements in an urban near-highway environment. *Atmospheric Environment* 45, 925-934.

Herner, J.D., Green, P.G., Kleeman, M.J., 2006. Measuring the Trace Elemental Composition of Size-Resolved Airborne Particles. *Environmental Science & Technology* 40, 1925-1933.

Hinds, W.C., 1999. *Aerosol Technology: Properties, Behavior, and Measurement of Airborne Particles*. John Wiley & Sons.

Ho, K., Lee, S., Cao, J., Chow, J., Watson, J., Chan, C., 2006. Seasonal variations and mass closure analysis of particulate matter in Hong Kong. *Science of The Total Environment* 355, 276-287.

Hong, Y.-C., Hwang, S.-S., Kim, J.H., Lee, K.-H., Lee, H.-J., Lee, K.-H., Yu, S.-D., Kim, D.-S., 2007. Metals in Particulate Pollutants Affect Peak Expiratory Flow of Schoolchildren. *Environmental Health Perspectives* 115, 430-434.

Hu, S., Polidori, A., Arhami, M., Shafer, M.M., Schauer, J.J., Cho, A., Sioutas, C., 2008. Redox activity and chemical speciation of size fractionated PM in the communities of the Los Angeles-Long Beach harbor. *Atmospheric Chemistry and Physics* 8, 6439-6451.

Hudda, N., Cheung, K., Moore, K.F., Sioutas, C., 2010. Inter-community variability in total particle number concentrations in the eastern Los Angeles air basin. *Atmos. Chem. Phys.* 10, 11385-11399.

Hueglin, C., Gehrig, R., Baltensperger, U., Gysel, M., Monn, C., Vonmont, H., 2005. Chemical characterisation of PM_{2.5}, PM₁₀ and coarse particles at urban, near-city and rural sites in Switzerland. *Atmospheric Environment* 39, 637-651.

Hughes, L.S., Allen, J.O., Bhave, P., Kleeman, M.J., Cass, G.R., Liu, D.Y., Ferguson, D.P., Morrical, B.D., Prather, K.A., 2000. Evolution of Atmospheric Particles along Trajectories Crossing the Los Angeles Basin. *Environmental Science & Technology* 34, 3058-3068.

Hughes, L.S., Allen, J.O., Kleeman, M.J., Johnson, R.J., Cass, G.R., Gross, D.S., Gard, E.E., Gälli, M.E., Morrical, B.D., Ferguson, D.P., Dienes, T., Noble, C.A., Liu, D.-Y., Silva, P.J., Prather, K.A., 1999. Size and Composition Distribution of Atmospheric Particles in Southern California. *Environmental Science & Technology* 33, 3506-3515.

Hughes, L.S., Allen, J.O., Salmon, L.G., Mayo, P.R., Johnson, R.J., Cass, G.R., 2002. Evolution of Nitrogen Species Air Pollutants along Trajectories Crossing the Los Angeles Area. *Environmental Science & Technology* 36, 3928-3935.

Hughes, L.S., Cass, G.R., Gone, J., Ames, M., Olmez, I., 1998. Physical and Chemical Characterization of Atmospheric Ultrafine Particles in the Los Angeles Area. *Environmental Science & Technology* 32, 1153-1161.

Hwang, I., Hopke, P.K., Pinto, J.P., 2008. Source Apportionment and Spatial Distributions of Coarse Particles During the Regional Air Pollution Study. *Environmental Science & Technology* 42, 3524-3530.

IARC, 1987. *Overall Evaluations of Carcinogenicity: An Updating of IARC Monographs Volumes 1 to 42*. IARC Monographs on the Evaluation of Carcinogenic Risks to Humans, Supplement 7. International Agency for Research on Cancer, Lyon.

Ion, A.C., Vermeylen, R., Kourtchev, I., Cafmeyer, J., Chi, X., Gelencsér, A., Maenhaut, W., Claeys, M., 2005. Polar organic compounds in rural PM_{2.5} aerosols from K-pusztá,

Hungary, during a 2003 summer field campaign: sources and diurnal variations. *Atmospheric Chemistry and Physics Discussions* 5, 1863-1889.

Isakson, J., Persson, T.A., Selin Lindgren, E., 2001. Identification and assessment of ship emissions and their effects in the harbour of Göteborg, Sweden. *Atmospheric Environment* 35, 3659-3666.

Kam, W., Liacos, J.W., Schauer, J.J., Delfino, R.J., Sioutas, C., 2012. Size-segregated composition of particulate matter (PM) in major roadways and surface streets. *Atmospheric Environment* 55, 90-97.

Karageorgos, E.T., Rapsomanikis, S., 2007. Chemical characterization of the inorganic fraction of aerosols and mechanisms of the neutralization of atmospheric acidity in Athens, Greece. *Atmos. Chem. Phys.* 7, 3015-3033.

Kim, E., Larson, T.V., Hopke, P.K., Slaughter, C., Sheppard, L.E., Claiborn, C., 2003. Source identification of PM_{2.5} in an arid Northwest U.S. City by positive matrix factorization. *Atmospheric Research* 66, 291-305.

Kim, S., Shen, S., Sioutas, C., Zhu, Y., Hinds, W.C., 2002. Size Distribution and Diurnal and Seasonal Trends of Ultrafine Particles in Source and Receptor Sites of the Los Angeles Basin. *Journal of the Air & Waste Management Association* 52, 297-307.

Kleindienst, T.E., Jaoui, M., Lewandowski, M., Offenber, J.H., Lewis, C.W., Bhawe, P.V., Edney, E.O., 2007. Estimates of the contributions of biogenic and anthropogenic hydrocarbons to secondary organic aerosol at a southeastern US location. *Atmospheric Environment* 41, 8288-8300.

Klepeis, N.E., Nelson, W.C., Ott, W.R., Robinson, J.P., Tsang, A.M., Switzer, P., Behar, J.V., Hern, S.C., Engelmann, W.H., 2001. The National Human Activity Pattern Survey (NHAPS): a resource for assessing exposure to environmental pollutants. *Journal of exposure analysis and environmental epidemiology* 11, 231-252.

Kouyoumdjian, H., Saliba, N.A., 2006. Mass concentration and ion composition of coarse and fine particles in an urban area in Beirut: effect of calcium carbonate on the absorption of nitric and sulfuric acids and the depletion of chloride. *Atmos. Chem. Phys.* 6, 1865-1877.

Krudysz, M., Moore, K., Geller, M., Sioutas, C., Froines, J., 2009. Intra-community spatial variability of particulate matter size distributions in Southern California/Los Angeles. *Atmos. Chem. Phys.* 9, 1061-1075.

Kuhn, T., Krudysz, M., Zhu, Y., Fine, P., Hinds, W., Froines, J., Sioutas, C., 2005. Volatility of indoor and outdoor ultrafine particulate matter near a freeway. *Journal of Aerosol Science* 36, 291-302.

Kumagai, Y., Arimoto, T., Shinyashiki, M., Shimojo, N., Nakai, Y., Yoshikawa, T., Sagai, M., 1997. Generation of Reactive Oxygen Species during Interaction of Diesel Exhaust Particle Components with NADPH-Cytochrome p450 Reductase and Involvement of the Bioactivation in the DNA Damage. *Free Radical Biology and Medicine* 22, 479-487.

Landreman, A.P., Shafer, M.M., Hemming, J.C., Hannigan, M.P., Schauer, J.J., 2008. A Macrophage-Based Method for the Assessment of the Reactive Oxygen Species (ROS) Activity of Atmospheric Particulate Matter (PM) and Application to Routine (Daily-24 h) Aerosol Monitoring Studies. *Aerosol Science and Technology* 42, 946-957.

LCDR/TEAM, 2000. Beirut urban transport project- Environmental assessment. Volume 2.

Li, N., Sioutas, C., Cho, A., Schmitz, D., Misra, C., Sempf, J., Wang, M., Oberley, T., Froines, J., Nel, A., 2003. Ultrafine particulate pollutants induce oxidative stress and mitochondrial damage. *Environmental Health Perspectives* 111, 455-460.

Liacos, J.W., Kam, W., Delfino, R.J., Schauer, J.J., Sioutas, C., 2012. Characterization of organic, metal and trace element PM_{2.5} species and derivation of freeway-based emission rates in Los Angeles, CA. *The Science of the total environment* 435-436, 159-166.

Limbeck, A., Puxbaum, H., Otter, L., Scholes, M.C., 2001. Semivolatile behavior of dicarboxylic acids and other polar organic species at a rural background site (Nylsvley, RSA). *Atmospheric Environment* 35, 1853-1862.

Lin, C.-C., Chen, S.-J., Huang, K.-L., Hwang, W.-I., Chang-Chien, G.-P., Lin, W.-Y., 2005. Characteristics of Metals in Nano/Ultrafine/Fine/Coarse Particles Collected Beside a Heavily Trafficked Road. *Environmental Science & Technology* 39, 8113-8122.

Liu, Y.J., Zhu, T., Zhao, D.F., Zhang, Z.F., 2008. Investigation of the hygroscopic properties of Ca(NO₃)₂ and internally mixed Ca(NO₃)₂/CaCO₃ particles by micro-Raman spectrometry. *Atmospheric Chemistry and Physics* 8, 7205-7215.

Lonati, G., Giugliano, M., Butelli, P., Romele, L., Tardivo, R., 2005. Major chemical components of PM_{2.5} in Milan (Italy). *Atmospheric Environment* 39, 1925-1934.

Lonati, G., Giugliano, M., Ozgen, S., 2008. Primary and secondary components of PM_{2.5} in Milan (Italy). *Environment International* 34, 665-670.

Lough, G.C., Christensen, C.G., Schauer, J.J., Tortorelli, J., Mani, E., Lawson, D.R., Clark, N.N., Gabele, P.A., 2007. Development of molecular marker source profiles for emissions from on-road gasoline and diesel vehicle fleets. *Journal of the Air & Waste Management Association* (1995) 57, 1190-1199.

Lough, G.C., Schauer, J.J., Park, J.-S., Shafer, M.M., DeMinter, J.T., Weinstein, J.P., 2005. Emissions of Metals Associated with Motor Vehicle Roadways. *Environmental Science & Technology* 39, 826-836.

Lu, G., Brook, J.R., Rami Alfarra, M., Anlauf, K., Richard Leitch, W., Sharma, S., Wang, D., Worsnop, D.R., Phinney, L., 2006. Identification and characterization of inland ship plumes over Vancouver, BC. *Atmospheric Environment* 40, 2767-2782.

Mader, B.T., Pankow, J.F., 2002. Study of the Effects of Particle-Phase Carbon on the Gas/Particle Partitioning of Semivolatile Organic Compounds in the Atmosphere Using Controlled Field Experiments. *Environmental Science & Technology* 36, 5218-5228.

Manchester-Neesvig, J.B., Schauer, J.J., Cass, G.R., 2003. The distribution of particle-phase organic compounds in the atmosphere and their use for source apportionment during the Southern California Children's Health Study. *Journal of the Air & Waste Management Association* (1995) 53, 1065-1079.

Manoli, E., Voutsas, D., Samara, C., 2002. Chemical characterization and source identification/apportionment of fine and coarse air particles in Thessaloniki, Greece. *Atmospheric Environment* 36, 949-961.

Marcazzan, G.M., Ceriani, M., Valli, G., Vecchi, R., 2003. Source apportionment of PM₁₀ and PM_{2.5} in Milan (Italy) using receptor modelling. *The Science of The Total Environment* 317, 137-147.

Marcazzan, G.M., Ceriani, M., Valli, G., Vecchi, R., 2004. Composition, components and sources of fine aerosol fractions using multielemental EDXRF analysis. *X-Ray Spectrometry* 33, 267-272.

- Marcazzan, G.M., Vaccaro, S., Valli, G., Vecchi, R., 2001. Characterisation of PM₁₀ and PM_{2.5} particulate matter in the ambient air of Milan (Italy). *Atmospheric Environment* 35, 4639-4650.
- Massoud, R., Shihadeh, A.L., Roumié, M., Youness, M., Gerard, J., Saliba, N., Zaarour, R., Abboud, M., Farah, W., Saliba, N.A., 2011. Intraurban variability of PM₁₀ and PM_{2.5} in an Eastern Mediterranean city. *Atmospheric Research* 101, 893-901.
- McMurry, P.H., Wang, X., Park, K., Ehara, K., 2002. The Relationship between Mass and Mobility for Atmospheric Particles: A New Technique for Measuring Particle Density. *Aerosol Science and Technology* 36, 227-238.
- Menichini, E., Monfredini, F., Merli, F., 1999. The temporal variability of the profile of carcinogenic polycyclic aromatic hydrocarbons in urban air: a study in a medium traffic area in Rome, 1993-1998. *Atmospheric Environment* 33, 3739-3750.
- Minguillón, M.C., Arhami, M., Schauer, J.J., Sioutas, C., 2008. Seasonal and spatial variations of sources of fine and quasi-ultrafine particulate matter in neighborhoods near the Los Angeles-Long Beach harbor. *Atmospheric Environment* 42, 7317-7328.
- Misra, C., Singh, M., Shen, S., Sioutas, C., Hall, P.M., 2002. Development and evaluation of a personal cascade impactor sampler (PCIS). *Journal of Aerosol Science* 33, 1027-1047.
- MoE, 2005. National environmental action plan, Ministry of Environment, Beirut - Lebanon.
- MoE/UNDP/GEF, 2011. Lebanon's Second National Communication to the UNFCCC, p. 228.
- MoE/URC/GEF, 2012. Lebanon Technology Needs Assessment Report for Climate Change. Chapter 5., Beirut, Lebanon.
- Moore, K., Krudysz, M., Pakbin, P., Hudda, N., Sioutas, C., 2009. Intra-Community Variability in Total Particle Number Concentrations in the San Pedro Harbor Area (Los Angeles, California). *Aerosol Science and Technology* 43, 587-603.
- Moore, K.F., Verma, V., Minguillón, M.C., Sioutas, C., 2010. Inter- and Intra-Community Variability in Continuous Coarse Particulate Matter (PM_{10-2.5}) Concentrations in the Los Angeles Area. *Aerosol Science and Technology* 44, 526-540.
- Morawska, L., Thomas, S., Bofinger, N., Wainwright, D., Neale, D., 1998. Comprehensive characterization of aerosols in a subtropical urban atmosphere: particle size distribution and correlation with gaseous pollutants. *Atmospheric Environment* 32, 2467-2478.
- Morgan, T.E., Davis, D.A., Iwata, N., Tanner, J.A., Snyder, D., Ning, Z., Kam, W., Hsu, Y.-T., Winkler, J.W., Chen, J.-C., Petasis, N.A., Baudry, M., Sioutas, C., Finch, C.E., 2011. Glutamatergic Neurons in Rodent Models Respond to Nanoscale Particulate Urban Air Pollutants in Vivo and in Vitro. *Environmental Health Perspectives* 119, 1003-1009.
- Mozurkewich, M., 1993. The dissociation constant of ammonium nitrate and its dependence on temperature, relative humidity and particle size. *Atmospheric Environment. Part A. General Topics* 27, 261-270.
- Mysliwiec, M.J., Kleeman, M.J., 2002. Source Apportionment of Secondary Airborne Particulate Matter in a Polluted Atmosphere. *Environmental Science & Technology* 36, 5376-5384.
- Nel, A., 2005. Air Pollution-Related Illness: Effects of Particles. *Science* 308, 804-806.

Nel, A.E., Diaz-Sanchez, D., Li, N., 2001. The role of particulate pollutants in pulmonary inflammation and asthma: evidence for the involvement of organic chemicals and oxidative stress. *Current opinion in pulmonary medicine* 7, 20-26.

Nemmar, A., Hoet, P.H.M., Vanquickenborne, B., Dinsdale, D., Thomeer, M., Hoylaerts, M.F., Vanbilloen, H., Mortelmans, L., Nemery, B., 2002. Passage of Inhaled Particles Into the Blood Circulation in Humans. *Circulation* 105, 411-414.

Ning, Z., Geller, M.D., Moore, K.F., Sheesley, R., Schauer, J.J., Sioutas, C., 2007. Daily Variation in Chemical Characteristics of Urban Ultrafine Aerosols and Inference of Their Sources. *Environmental Science & Technology* 41, 6000-6006.

Ning, Z., Polidori, A., Schauer, J.J., Sioutas, C., 2008. Emission factors of PM species based on freeway measurements and comparison with tunnel and dynamometer studies. *Atmospheric Environment* 42, 3099-3114.

Noble, C.A., Prather, K.A., 1996. Real-Time Measurement of Correlated Size and Composition Profiles of Individual Atmospheric Aerosol Particles. *Environmental Science & Technology* 30, 2667-2680.

NRC, 2004. National Research Council. Committee on Research Priorities for Airborne Particulate Matter. *Research Priorities for Airborne Particulate Matter: IV.*, in: *Continuing Research Progress*. The National Academies Press, W., D.C. (Ed.).

Ntziachristos, L., Froines, J.R., Cho, A.K., Sioutas, C., 2007a. Relationship between redox activity and chemical speciation of size-fractionated particulate matter. *Particle fibre and toxicology* 4.

Ntziachristos, L., Ning, Z., Geller, M.D., Sheesley, R.J., Schauer, J.J., Sioutas, C., 2007b. Fine, ultrafine and nanoparticle trace element compositions near a major freeway with a high heavy-duty diesel fraction. *Atmospheric Environment* 41, 5684-5696.

Ntziachristos, L., Ning, Z., Geller, M.D., Sioutas, C., 2007c. Particle Concentration and Characteristics near a Major Freeway with Heavy-Duty Diesel Traffic. *Environmental Science & Technology* 41, 2223-2230.

Oberdörster, G., 2000. Pulmonary effects of inhaled ultrafine particles. *International Archives of Occupational and Environmental Health* 74, 1-8.

Oberdörster, G., Sharp, Z., Atudorei, V., Elder, A., Gelein, R., Lunts, A., Kreyling, W., Cox, C., 2002. Extrapulmonary Translocation of Ultrafine Carbon Particles Following Whole-Body Inhalation Exposure of Rats. *Journal of Toxicology and Environmental Health, Part A* 65, 1531-1543.

Oliveira, C.s., Pio, C., Alves, C.I., Evtyugina, M., Santos, P.c., Gonçães, V.n., Nunes, T., Silvestre, A.J.D., Palmgren, F., Wählén, P., Harrad, S., 2007. Seasonal distribution of polar organic compounds in the urban atmosphere of two large cities from the North and South of Europe. *Atmospheric Environment* 41, 5555-5570.

Oros, D.R., Simoneit, B.R.T., 2000. Identification and emission rates of molecular tracers in coal smoke particulate matter. *Fuel* 79, 515-536.

Pakbin, P., Ning, Z., Shafer, M.M., Schauer, J.J., Sioutas, C., 2010. Seasonal and Spatial Coarse Particle Elemental Concentrations in the Los Angeles Area. *Aerosol Science and Technology* 45, 949-963.

Pakkanen, T.A., Kerminen, V.-M., Korhonen, C.H., Hillamo, R.E., Aarnio, P.i., Koskentalo, T., Maenhaut, W., 2001. Urban and rural ultrafine (PM_{0.1}) particles in the Helsinki area. *Atmospheric Environment* 35, 4593-4607.

Pandis, S.N., Harley, R.A., Cass, G.R., Seinfeld, J.H., 1992. Secondary organic aerosol formation and transport. *Atmospheric Environment. Part A. General Topics* 26, 2269-2282.

Paode, R.D., Shahin, U.M., Sivadechathep, J., Holsen, T.M., Franek, W.J., 1999. Source Apportionment of Dry Deposited and Airborne Coarse Particles Collected in the Chicago Area. *Aerosol Science and Technology* 31, 473-486.

Park, S.S., Kim, Y.J., 2004. PM_{2.5} particles and size-segregated ionic species measured during fall season in three urban sites in Korea. *Atmospheric Environment* 38, 1459-1471.

Penttinen, P., Timonen, K.L., Tiittanen, P., Mirme, A., Ruuskanen, J., Pekkanen, J., 2001. Number concentration and size of particles in urban air: effects on spirometric lung function in adult asthmatic subjects. *Environmental Health Perspectives* 109, 319-323.

Perrone, M.G., Gualtieri, M., Ferrero, L., Porto, C.L., Udisti, R., Bolzacchini, E., Camatini, M., 2010. Seasonal variations in chemical composition and in vitro biological effects of fine PM from Milan. *Chemosphere* 78, 1368-1377.

Peters, A., Dockery, D.W., Muller, J.E., Mittleman, M.A., 2001. Increased particulate air pollution and the triggering of myocardial infarction. *Circulation* 103, 2810-2815.

Peters, A., Wichmann, H.E., Tuch, T., Heinrich, J., Heyder, J., 1997. Respiratory effects are associated with the number of ultrafine particles. *American journal of respiratory and critical care medicine* 155, 1376-1383.

Peters, K.E., Scheuerman, G.L., Lee, C.Y., Moldowan, J.M., Reynolds, R.N., Pena, M.M., 1992. Effects of refinery processes on biological markers. *Energy & Fuels* 6, 560-577.

Pope, C.A., 3rd, Burnett, R.T., Thun, M.J., Calle, E.E., Krewski, D., Ito, K., Thurston, G.D., 2002. Lung cancer, cardiopulmonary mortality, and long-term exposure to fine particulate air pollution. *Journal of the American Medical Association* 287, 1132-1141.

Prahalad, A.K., Soukup, J.M., Inmon, J., Willis, R., Ghio, A.J., Becker, S., Gallagher, J.E., 1999. Ambient Air Particles: Effects on Cellular Oxidant Radical Generation in Relation to Particulate Elemental Chemistry. *Toxicology and Applied Pharmacology* 158, 81-91.

Prophete, C., Maciejczyk, P., Salnikow, K., Gould, T., Larson, T., Koenig, J., Jaques, P., Sioutas, C., Lippmann, M., Cohen, M., 2006. Effects of select PM-associated metals on alveolar macrophage phosphorylated ERK1 and -2 and iNOS expression during ongoing alteration in iron homeostasis. *Journal of toxicology and environmental health. Part A* 69, 935-951.

Putaud, J.-P., Raes, F., Van Dingenen, R., Brüggemann, E., Facchini, M.C., Decesari, S., Fuzzi, S., Gehrig, R., Hüglin, C., Laj, P., Lorbeer, G., Maenhaut, W., Mihalopoulos, N., Müller, K., Querol, X., Rodriguez, S., Schneider, J., Spindler, G., Brink, H.t., Tørseth, K., Wiedensohler, A., 2004. A European aerosol phenomenology--2: chemical characteristics of particulate matter at kerbside, urban, rural and background sites in Europe. *Atmospheric Environment* 38, 2579-2595.

Rinne, H., 2002. Isoprene and monoterpene fluxes measured above Amazonian rainforest and their dependence on light and temperature. *Atmospheric Environment* 36, 2421-2426.

Robarge, W.P., Walker, J.T., McCulloch, R.B., Murray, G., 2002. Atmospheric concentrations of ammonia and ammonium at an agricultural site in the southeast United States. *Atmospheric Environment* 36, 1661-1674.

Robinson, A.L., Donahue, N.M., Shrivastava, M.K., Weitkamp, E.A., Sage, A.M., Grieshop, A.P., Lane, T.E., Pierce, J.R., Pandis, S.N., 2007. Rethinking Organic Aerosols: Semivolatile Emissions and Photochemical Aging. *Science* 315, 1259-1262.

Rogge, W.F., Hildemann L.M., Mazurek M.A., Cass G.R., B.R.T., S., 1997. Sources of fine organic aerosol. 8. Boilers burning no. 2 distillate fuel oil. *Environmental Science & Technology* 31, 2731–2737.

Rogge, W.F., Hildemann, L.M., Mazurek, M.A., Cass, G.R., Simoneit, B.R.T., 1993a. Sources of fine organic aerosol. 2. Noncatalyst and catalyst-equipped automobiles and heavy-duty diesel trucks. *Environmental Science & Technology* 27, 636-651.

Rogge, W.F., Hildemann, L.M., Mazurek, M.A., Cass, G.R., Simoneit, B.R.T., 1993b. Sources of fine organic aerosol. 3. Road dust, tire debris, and organometallic brake lining dust: roads as sources and sinks. *Environmental Science & Technology* 27, 1892-1904.

Rogge, W.F., Hildemann, L.M., Mazurek, M.A., Cass, G.R., Simoneit, B.R.T., 1993c. Sources of fine organic aerosol. 4. Particulate abrasion products from leaf surfaces of urban plants. *Environ. Sci. Technol.* 27 2700-2711.

Rogge, W.F., Hildemann, L.M., Mazurek, M.A., Cass, G.R., Simoneit, B.R.T., 1993. Sources of fine organic aerosol. 5. Natural gas home appliances. *Environmental Science & Technology* 27.

Rogge, W.F., Mazurek, M.A., Hildemann, L.M., Cass, G.R., Simoneit, B.R.T., 1993d. Quantification of urban organic aerosols at a molecular level: Identification, abundance and seasonal variation. *Atmospheric Environment. Part A. General Topics* 27, 1309-1330.

Rutter, A.P., Snyder, D.C., Schauer, J.J., Sheesley, R.J., Olson, M.R., DeMinter, J., 2011. Contributions of resuspended soil and road dust to organic carbon in fine particulate matter in the Midwestern US. *Atmospheric Environment* 45, 514-518.

Saffari, A., Daher, N., Shafer, M.M., Schauer, J.J., Sioutas, C., 2013a. Seasonal and Spatial Variation in Reactive Oxygen Species Activity of quasi-Ultrafine Particles (PM_{0.25}) in the Los Angeles Metropolitan Area and its Association with Chemical Composition *Atmospheric Environment* 79, 566-575.

Saffari, A., Daher, N., Shafer, M.M., Schauer, J.J., Sioutas, C., 2013b. Seasonal and spatial variation of trace elements and metals in quasi-ultrafine (PM_{0.25}) particles in the Los Angeles metropolitan area and characterization of their sources. *Environmental Pollution* 181, 14-23.

Saldiva, P.H.N., Clarke, R.W., Coull, B.A., Stearns, R.C., Lawrence, J., Murthy, G.G.K., Diaz, E., Koutrakis, P., Suh, H., Tsuda, A., Godleski, J.J., 2002. Lung inflammation induced by concentrated ambient air particles is related to particle composition. *American journal of respiratory and critical care medicine* 165, 1610-1617.

Saliba, N.A., El Jam, F., El Tayar, G., Obeid, W., Roumie, M., 2010. Origin and variability of particulate matter (PM₁₀ and PM_{2.5}) mass concentrations over an Eastern Mediterranean city. *Atmospheric Research* 97, 106-114.

Saliba, N.A., Kouyoumdjian, H., Kadamany, G.A., Roumie, M., Mellouki, A., Ravishankara, A.R., 2007a. Short and Long-Term Transport of Crustal and Anthropogenic Inorganic Components of Coarse and Fine Aerosols over Beirut, Lebanon, Regional Climate Variability and its Impacts in The Mediterranean Area. *Springer Netherlands*, pp. 129-142.

Saliba, N.A., Kouyoumdjian, H., Roumié, M., 2007b. Effect of local and long-range transport emissions on the elemental composition of PM_{10-2.5} and PM_{2.5} in Beirut. *Atmospheric Environment* 41, 6497-6509.

Sanders, P.G., Xu, N., Dalka, T.M., Maricq, M.M., 2003. Airborne Brake Wear Debris: Size Distributions, Composition, and a Comparison of Dynamometer and Vehicle Tests. *Environmental Science & Technology* 37, 4060-4069.

Sannigrahi, P., Sullivan, A.P., Weber, R.J., Ingall, E.D., 2006. Characterization of water-soluble organic carbon in urban atmospheric aerosols using solid-state ¹³C NMR spectroscopy. *Environmental Science and Technology* 40, 666-672.

Sardar, S.B., Fine, P.M., Mayo, P.R., Sioutas, C., 2005a. Size-Fractionated Measurements of Ambient Ultrafine Particle Chemical Composition in Los Angeles Using the NanoMOUDI. *Environmental Science & Technology* 39, 932-944.

Sardar, S.B., Fine, P.M., Sioutas, C., 2005b. Seasonal and spatial variability of the size-resolved chemical composition of particulate matter (PM₁₀) in the Los Angeles Basin. *Journal of Geophysical Research* 110, 14 PP.-14 PP.

Schauer, C., Niessner, R., Pöschl, U., 2003. Polycyclic aromatic hydrocarbons in urban air particulate matter: decadal and seasonal trends, chemical degradation, and sampling artifacts. *Environmental Science & Technology* 37, 2861-2868.

Schauer, J.J., 2003. Evaluation of elemental carbon as a marker for diesel particulate matter. *Journal of Exposure Science and Environmental Epidemiology* 13, 443-453.

Schauer, J.J., Kleeman, M.J., Cass, G.R., Simoneit, B.R.T., 2002. Measurement of Emissions from Air Pollution Sources. 5. C₁-C₃₂ Organic Compounds from Gasoline-Powered Motor Vehicles. *Environmental Science & Technology* 36, 1169-1180.

Schauer, J.J., Rodger, B., Kerr, S.C., 2004. Regional haze in Wisconsin: sources and the spatial distribution. *Journal of Environmental Engineering and Science* 3, 213-222.

Schauer, J.J., Rogge, W.F., Hildemann, L.M., Mazurek, M.A., Cass, G.R., Simoneit, B.R.T., 1996. Source apportionment of airborne particulate matter using organic compounds as tracers. *Atmospheric Environment* 30, 3837-3855.

Schnelle-Kreis, J., Sklorz, M., Orasche, J., Stölzel, M., Peters, A., Zimmermann, R., 2007. Semi Volatile Organic Compounds in Ambient PM_{2.5}. Seasonal Trends and Daily Resolved Source Contributions. *Environmental Science & Technology* 41, 3821-3828.

Sciare, J., Bardouki, H., Moulin, C., Mihalopoulos, N., 2003. Aerosol sources and their contribution to the chemical composition of aerosols in the Eastern Mediterranean Sea during summertime. *Atmos. Chem. Phys.* 3, 291-302.

See, S.W., Wang, Y.H., Balasubramanian, R., 2007. Contrasting reactive oxygen species and transition metal concentrations in combustion aerosols. *Environmental Research* 103, 317-324.

Seinfeld, J.H., Pandis, S.N., 2006. *Atmospheric Chemistry and Physics: From Air Pollution to Climate Change*. John Wiley & Sons.

Shafer, M.M., Perkins, D.A., Antkiewicz, D.S., Stone, E.A., Quraishi, T.A., Schauer, J.J., 2010. Reactive oxygen species activity and chemical speciation of size-fractionated atmospheric particulate matter from Lahore, Pakistan: an important role for transition metals. *Journal of Environmental Monitoring* 12, 704-715.

Sheesley, R.J., Schauer, J.J., Bean, E., Kenski, D., 2004. Trends in Secondary Organic Aerosol at a Remote Site in Michigan's Upper Peninsula. *Environmental Science & Technology* 38, 6491-6500.

Sheesley, R.J., Schauer, J.J., Zheng, M., Wang, B., 2007. , 2007. Sensitivity of molecular marker-based CMB models to biomass burning source profiles. *Atmospheric Environment* 41, 9050-9063.

Sillanpää, M., Frey, A., Hillamo, R., Pennanen, A.S., Salonen, R.O., 2005. Organic, elemental and inorganic carbon in particulate matter of six urban environments in Europe. *Atmos. Chem. Phys.* 5, 2869-2879.

Sillanpää, M., Hillamo, R., Saarikoski, S., Frey, A., Pennanen, A., Makkonen, U., Spolnik, Z., Van Grieken, R., Braniš, M., Brunekreef, B., Chalbot, M.-C., Kuhlbusch, T., Sunyer, J., Kerminen, V.-M., Kulmala, M., Salonen, R.O., 2006. Chemical composition and mass closure of particulate matter at six urban sites in Europe. *Atmospheric Environment* 40, Supplement 2, 212-223.

Simoneit, B., 1986. Characterization of organic constituents in aerosols in relation to their origin and transport: a review

International Journal of Environmental Analytical Chemistry 23, 207-237.

Simoneit, B.R.T., 1984. Organic matter of the troposphere-III. Characterization and sources of petroleum and pyrogenic residues in aerosols over the Western United States. *Atmospheric Environment* 18, 51-67.

Simoneit, B.R.T., 1989. Organic-matter of the troposphere. 5. Application of molecular marker analysis to biogenic emissions into the troposphere for source reconciliations. *Journal of Atmospheric Chemistry* 8, 251-275.

Simoneit, B.R.T., Schauer, J.J., Nolte, C.G., Oros, D.R., Elias, V.O., Fraser, M.P., Rogge, W.F., Cass, G.R., 1999. Levoglucosan, a tracer for cellulose in biomass burning and atmospheric particles. *Atmospheric Environment* 33, 173-182.

Singh, M., Jaques, P.A., Sioutas, C., 2002. Size distribution and diurnal characteristics of particle-bound metals in source and receptor sites of the Los Angeles Basin. *Atmospheric Environment* 36, 1675-1689.

Sioutas, C., Delfino, R.J., Singh, M., 2005. Exposure Assessment for Atmospheric Ultrafine Particles (UFPs) and Implications in Epidemiologic Research. *Environmental Health Perspectives* 113, 947-955.

Sioutas, C., Pandis, S., Allen, D.T., Solomon, P.A., 2004. Special issue of *Atmospheric Environment* on findings from EPA's Particulate Matter Supersites Program. *Atmospheric Environment* 38, 3101-3106.

Song, F., Gao, Y., 2011. Size distributions of trace elements associated with ambient particular matter in the affinity of a major highway in the New Jersey-New York metropolitan area. *Atmospheric Environment* 45, 6714-6723.

Sørensen, M., Autrup, H., Møller, P., Hertel, O., Jensen, S.S., Vinzents, P., Knudsen, L.E., Loft, S., 2003. Linking exposure to environmental pollutants with biological effects. *Mutation Research/Reviews in Mutation Research* 544, 255-271.

Squadrito, G.L., Cueto, R., Dellinger, B., Pryor, W.A., 2001. Quinoid redox cycling as a mechanism for sustained free radical generation by inhaled airborne particulate matter. *Free Radical Biology and Medicine* 31, 1132-1138.

Stephanou, E.G., Stratigakis, N., 1993. Oxocarboxylic and .alpha.,.omega.-dicarboxylic acids: photooxidation products of biogenic unsaturated fatty acids present in urban aerosols. *Environmental Science & Technology* 27, 1403-1407.

Sternbeck, J., Sjödin, Å., Andréasson, K., 2002. Metal emissions from road traffic and the influence of resuspension—results from two tunnel studies. *Atmospheric Environment* 36, 4735-4744.

Stone, E., Schauer, J.J., Quraishi, T.A., Mahmood, A., 2010. Chemical characterization and source apportionment of fine and coarse particulate matter in Lahore, Pakistan. *Atmospheric Environment* 44, 1062-1070.

Stone, E.A., Hedman, C.J., Sheesley, R.J., Shafer, M.M., Schauer, J.J., 2009. Investigating the chemical nature of humic-like substances (HULIS) in North American

atmospheric aerosols by liquid chromatography tandem mass spectrometry. *Atmospheric Environment* 43, 4205-4213.

Stone, E.A., Snyder, D.C., Sheesley, R.J., Sullivan, A.P., Weber, R.J., Schauer, J.J., 2008. Source apportionment of fine organic aerosol in Mexico City during the MILAGRO experiment 2006. *Atmos. Chem. Phys.* 8, 1249-1259.

Strader, R., Lurmann, F., Pandis, S.N., 1999. Evaluation of secondary organic aerosol formation in winter. *Atmospheric Environment* 33, 4849-4863.

Sullivan, A.P., Weber, R.J., Clements, A.L., Turner, J.R., Bae, M.S., Schauer, J.J., 2004. A method for on-line measurement of water-soluble organic carbon in ambient aerosol particles: Results from an urban site. *Geophysical Research Letters* 31, L13105.

Taylor, S.R., McLennan, S.M., 1985. *The continental crust: Its composition and evolution.* Blackwell Scientific, Boston, Mass.

Thomaidis, N.S., Bakeas, E.B., Siskos, P.A., 2003. Characterization of lead, cadmium, arsenic and nickel in PM_{2.5} particles in the Athens atmosphere, Greece. *Chemosphere* 52, 959-966.

Thorpe, A., Harrison, R.M., 2008. Sources and properties of non-exhaust particulate matter from road traffic: a review. *The Science of the total environment* 400, 270-282.

Tonne, C., Melly, S., Mittleman, M., Coull, B., Goldberg, R., Schwartz, J., 2007. A Case-Control Analysis of Exposure to Traffic and Acute Myocardial Infarction. *Environmental Health Perspectives* 115, 53-57.

Turner, J.R., Allen, D.T., 2008. Transport of Atmospheric Fine Particulate Matter: Part 2- Findings from Recent Field Programs on the Intraurban Variability in Fine Particulate Matter. *Journal of the Air & Waste Management Association* 58, 196-215.

Turpin, B.J., Huntzicker, J.J., 1995. Identification of secondary organic aerosol episodes and quantitation of primary and secondary organic aerosol concentrations during SCAQS. *Atmospheric Environment* 29, 3527-3544.

Turpin, B.J., Huntzicker, J.J., Larson, S.M., Cass, G.R., 1991. Los Angeles summer midday particulate carbon: primary and secondary aerosol. *Environ. Sci. Technol.* 25, 1788-1793.

Turpin, B.J., Lim, H.-J., 2001. Species Contributions to PM_{2.5} Mass Concentrations: Revisiting Common Assumptions for Estimating Organic Mass. *Aerosol Science and Technology* 35, 602-610.

UNEP/Jordan, 2008. Middle East Fuel Quality Overview. Presented to UNEP Jordan National Post Lead Workshop, Amman.

Valko, M., Morris, H., Cronin, M.T.D., 2005. Metals, toxicity and oxidative stress. *Current medicinal chemistry* 12, 1161-1208.

Vecchi, R., Marcazzan, G., Valli, G., Ceriani, M., Antoniazzi, C., 2004. The role of atmospheric dispersion in the seasonal variation of PM₁ and PM_{2.5} concentration and composition in the urban area of Milan (Italy). *Atmospheric Environment* 38, 4437-4446.

Verma, V., Ning, Z., Cho, A.K., Schauer, J.J., Shafer, M.M., Sioutas, C., 2009a. Redox activity of urban quasi-ultrafine particles from primary and secondary sources. *Atmospheric Environment* 43, 6360-6368.

Verma, V., Polidori, A., Schauer, J.J., Shafer, M.M., Cassee, F.R., Sioutas, C., 2009b. Physicochemical and Toxicological Profiles of Particulate Matter in Los Angeles during the October 2007 Southern California Wildfires. *Environmental Science & Technology* 43, 954-960.

von Schneidmesser, E., Stone, E.A., Quraishi, T.A., Shafer, M.M., Schauer, J.J., 2010. Toxic metals in the atmosphere in Lahore, Pakistan. *Science of The Total Environment* 408, 1640-1648.

Waked, A., Afif, C., 2012. Emissions of air pollutants from road transport in Lebanon and other countries in the Middle East region. *Atmospheric Environment* 61, 446-452.

Watson, J.G., 1984. Overview of receptor model principles. *Air Pollution Control Association* 34, 619.

Weber, R.J., Sullivan, A.P., Peltier, R.E., Russell, A., Yan, B., Zheng, M., de Gouw, J., Warneke, C., Brock, C., Holloway, J.S., Atlas, E.L., Edgerton, E., 2007. A study of secondary organic aerosol formation in the anthropogenic-influenced southeastern United States. *Journal of Geophysical Research: Atmospheres* 112, n/a-n/a.

Westerdahl, D., Fruin, S., Sax, T., Fine, P.M., Sioutas, C., 2005. Mobile platform measurements of ultrafine particles and associated pollutant concentrations on freeways and residential streets in Los Angeles. *Atmospheric Environment* 39, 3597-3610.

Wilson, J.G., Kingham, S., Pearce, J., Sturman, A.P., 2005. A review of intraurban variations in particulate air pollution: Implications for epidemiological research. *Atmospheric Environment* 39, 6444-6462.

Yao, X., Fang, M., Chan, C.K., Ho, K.F., Lee, S.C., 2004. Characterization of dicarboxylic acids in PM_{2.5} in Hong Kong. *Atmospheric Environment* 38, 963-970.

Zhang, Q., Stanier, C.O., Canagaratna, M.R., Jayne, J.T., Worsnop, D.R., Pandis, S.N., Jimenez, J.L., 2004. Insights into the Chemistry of New Particle Formation and Growth Events in Pittsburgh Based on Aerosol Mass Spectrometry. *Environmental Science & Technology* 38, 4797-4809.

Zhang, Y., Schauer, J.J., Shafer, M.M., Hannigan, P.M., Dutton, J.S., 2008a. Source Apportionment of in vitro reactive oxygen species bioassay activity from atmospheric particulate matter. *Environmental Science & Technology* 42, 7502-7509.

Zhang, Y., Schauer, J.J., Zhang, Y., Zeng, L., Wei, Y., Liu, Y., Shao, M., 2008b. Characteristics of particulate carbon emissions from real-world Chinese coal combustion. *Environmental Science & Technology* 42, 5068-5073.

Zheng, M., Fang, M., 2000. Particle-associated Polycyclic Aromatic Hydrocarbons in the Atmosphere of Hong Kong. *Water, Air, & Soil Pollution* 117, 175-189-189-175-189-189.

Zheng, M., Salmon, L.G., Schauer, J.J., Zeng, L., Kiang, C.S., Zhang, Y., Cass, G.R., 2005. Seasonal trends in PM_{2.5} source contributions in Beijing, China. *Atmospheric Environment* 39, 3967-3976.

Zhu, Y., Hinds, W.C., Kim, S., Shen, S., Sioutas, C., 2002. Study of ultrafine particles near a major highway with heavy-duty diesel traffic. *Atmospheric Environment* 36, 4323-4335.

Zhuang, H., Chan, C.K., Fang, M., Wexler, A.S., 1999. Formation of nitrate and non-sea-salt sulfate on coarse particles - The role of aerosol water content and size distribution. *Atmospheric Environment* 33, 4223-4233.

Zielinska, B., Sagebiel, J., McDonald, J.D., Whitney, K., Lawson, D.R., 2004. Emission rates and comparative chemical composition from selected in-use diesel and gasoline-fueled vehicles. *Journal of the Air & Waste Management Association* (1995) 54, 1138-1150.

Zielinska, B., Samy, S., McDonald, J.D., Seagrave, J., 2010. Atmospheric transformation of diesel emissions. Research report (Health Effects Institute), 5-60.